University of Zurich[UZH]

How do existing routing services respond to the needs of mobility-restricted population groups?

GEO 511 Master's Thesis

Author
Annina Ardüser
17-708-587

Supervised by
Dr. Hoda Allahbakhshi

Faculty representative
Prof. Dr. Robert Weibel

28.01.2025
Department of Geography, University of Zurich

Abstract

Creating inclusive cities, a goal established in the United Nations' Sustainable Development Goals (SDGs), seeks to ensure that everyone can fully participate in and contribute to community life, irrespective of their physical abilities. Mobility plays a crucial role in enabling such participation, as it determines access to essential services, social interactions, and economic opportunities. Mobility-impaired individuals encounter significant challenges when navigating urban environments due to physical barriers, inaccessible infrastructure, and inadequate routing services. A lack of readily available accessibility data further contributes to the gap in serving these individuals, as existing routing services often fail to reflect real-world conditions, such as the location of stairs and steps, footpath inclines, or surface conditions. This thesis examined the performance of three existing routing services, namely Google Maps, Open Source Routing Machine (OSRM), and OpenRouteService (ORS), in terms of their ability to assist mobility-impaired individuals in District 1 of Zurich. While Google Maps and Open Source Routing Machine provide pedestrian routing solely for individuals without mobility restrictions, OpenRouteService also offers routes tailored to the needs of wheelchair users. Additionally, the study enhanced the footpath network of District 1 with accessibility-relevant data and applied Dijkstra's Shortest Path algorithm to generate routes for both walking and wheelchair profiles. Routes were generated for 30 origin-destination pairs and evaluated based on route length, complexity (measured by the number of turns), and travel time. The analysis revealed significant disparities between pedestrian and wheelchair routing. Routes designed for wheelchair users were significantly longer, both in terms of distance and travel time, and exhibited greater complexity, with an increased number of turns. While temporary obstacles did not significantly impact the suggested routes' length, travel time, and complexity, they still affected individual routes, leading to considerable detours for mobility-impaired individuals. This study underscores the potential of accessibility-enriched data to address the gap in existing services. By integrating spatial accessibility data into routing algorithms, inclusive and equitable urban mobility can be realised, addressing the growing challenges posed by urbanisation and an increasing global population. Such advancements are crucial for promoting equitable urban mobility and fostering inclusive cities, where all residents can participate in urban communities.

Keywords: spatial accessibility, routing services, accessibility-sensitive routing, wheelchair-accessible routing, geographic information systems

Acknowledgements

First of all, I want to express my heartfelt gratitude to my supervisor, Dr. Hoda Allahbakhsi, for her unwavering support over the past year. Her guidance, advice, and encouragement throughout the course of this thesis made this work possible. Our discussions during regular meetings were crucial in developing this Master's thesis. Her valuable insights helped me shape this thesis and gain a deeper understanding of the importance and impact of spatial accessibility. I sincerely appreciate the time and effort Dr. Hoda Allahbakhsi dedicated to supervising my thesis, and I want to thank her for her constant availability to answer questions and resolve issues. In addition to her supervision, I also thank her for giving me the opportunity to work on the citizen science project "ZuriACT: Zurich Accessible CiTy". I have learned incredibly valuable lessons during these years under her guidance.

Secondly, I am very grateful to Prof. Dr. Robert Weibel for his guidance and valuable feedback on my work, as well as for the opportunity to write my Master's thesis with his Geographic Information Systems group.

Thirdly, I would like to thank my family, friends, and partner for their support, words of encouragement, understanding, and patience during the process of this Master's thesis as well as throughout the years of my studies.

Finally, I would like to thank my fellow students for the numerous hours we spent in the G10 computer room working on our theses. We were all in this together.

Contents

List of Figures

List of Tables

Abbreviations

DEM	Digital Elevation Model
FCA	Floating Catchment Area
GSV	Google Street View
ORS	OpenRouteService
OSM	OpenStreetMap
OSRM	Open Source Routing Machine
POI	Point of Interest
SDGs	Sustainable Development Goals
SPAAR	Dijkstra's Shortest Path Algorithm for Accessible Routing
SVI	Street View Imagery
VGI	Volunteered Geographic Information
ZuriACT	Zurich Accessible CiTy

1 Introduction

1.1 Motivation

The global population is undergoing significant changes, driven by population growth, ageing, urbanisation, and migration (United Nations, 2019). The global population surpassed 8 billion in 2022, with projections suggesting a peak of 10.4 billion by the 2080s (United Nations, 2022, 2024c). Urbanisation is accelerating, with nearly 68% of people expected to live in cities by 2050 (United Nations, 2019). Meanwhile, population ageing is reshaping demographics as life expectancy rises and the share of people aged 65 and older doubles by 2050 (United Nations, 2022, 2024c). This shift is accompanied by an increase in age-related challenges, including mobility restrictions and disabilities (Iburg et al., 2023).

These global population changes have been accompanied by a significant increase in the number of people living with disabilities. According to a 2022 report by the World Health Organization, approximately 1.3 billion people, 16% of the world population, were living with disabilities in 2021. This number increased by over 270 million people in the past decade. These projections and numbers highlight the need for policies and services to address the challenges faced by individuals with disabilities and persons with age-related mobility restrictions (Iburg et al., 2023; United Nations, 2019; World Health Organization, 2022).

To meet future population growth and urbanisation challenges, cities must create inclusive environments that foster accessibility, fair opportunities, and social equality, ensuring that no one is left behind (United Nations, 2018). Numerous definitions of an inclusive city exist, as they are socially constructed and bound to cultural context and languages (Hambleton, 2015). For this thesis, a definition provided by Hambleton (2015, p. 25) and previously also applied by United Nations (2018) will be used:

"The inclusive city is governed by powerful, place-based democratic institutions. All residents are able to participate fully in the society and the economy, and civic leaders strive for just results while caring for the natural environment on which we all depend."

The key to this definition is enabling all city dwellers to participate in social, political and economic life, regardless of their ethnicity, gender, sexual orientation, religion, age or disability (Hambleton, 2015; United Nations, 2018). To create such an inclusive urban environment, the United Nations (2018) introduced six essential elements that should work together. Firstly, an **accessible built environment** ensures that buildings, public spaces, and urban infrastructure are designed to enable people with disabilities to participate actively in society. Secondly, a **positive social environment** is crucial for addressing attitudes, perceptions, and awareness of individuals from different backgrounds, countering stereotypes and promoting inclusion within the community. **Affordability** is the third critical factor in ensuring that the costs of accessibility initiatives do not burden marginalised groups. These costs must be shared between governments and the private sector. Additionally, **geographical availability** ensures that inclusive policies and programmes are evenly distributed across urban areas, allowing as many citizens as possible to benefit from them, regardless of their location. The **quality of political programmes** addressing inclusion is critical. They must be consistent, respectful, and comprehensive, as insincere efforts undermine their purpose and effectiveness. Finally, **meaningful participation** is vital. Empowering target groups to engage in civic, political, and community activities ensures that inclusion efforts are genuine and effective. These elements form the foundation of a truly inclusive city (United Nations, 2018).

The significance of striving for inclusive cities aligns with the Sustainable Development Goals (SDGs) (United Nations, 2024a). The 17 SDGs, comprising 169 targets, form the core of the *2030 Agenda for Sustainable Development*, established by the United Nations and adopted by all member states in 2015. They represent an urgent call to action, bringing together all nations in a global partnership. The defined goals encompass societal objectives, such as improving health and education and reducing inequality, as well as environmental protection efforts, including mitigating climate change and preserving oceans and forests (United Nations, 2024b). In aiming to create sustainable cities and communities, the United Nations established Goal 11 to *"make cities and human settlements inclusive, safe, resilient and sustainable"* (United Nations, 2024a). Moreover, Target 11.7 of the SDGs specifically targets inclusive and accessible public spaces: *"By 2030, provide access to safe, inclusive and accessible, green and public spaces, in particular for women and children, older persons and persons with disabilities"* (United Nations, 2024a). The latest progress assessment of Target 11.7, covering 1'365 cities across 187 countries, highlights disparities in access to open public space. In least-developed countries, fewer than 3 in 10 residents have access to such spaces, compared to 6 to 7 out of 10 people in regions such as North America, Australia, New Zealand, and Europe (United Nations, 2024a). To ensure that the benefits of urbanisation serve all population groups, including older adults with age-related mobility restrictions and people with disabilities, policies need to address accessible public infrastructure such as footpaths, as walking plays a vital role in promoting vibrant and cohesive communities and local trade (Rhoads et al., 2023). In addition to providing essential social functions for cities, walking also positively impacts the environment of a city, reducing air and noise pollution (Rhoads et al., 2023; United Nations, 2019). Furthermore, a lack of walking, as part of a person's physical activity, is associated with lower physical health and higher mental health impairments (Mueller et al., 2015). Accessible infrastructure is necessary to ensure that everyone can benefit from the social, environmental, physical, and mental health advantages, enabling all individuals to actively contribute to the communities within a city (Achuthan et al., 2010; Saha et al., 2019).

Today, numerous obstacles restrict the mobility of older adults dealing with age-related mobility limitations and individuals with special mobility needs, such as wheelchair users, leading to reduced accessibility for these groups (Rahaman et al., 2017). As Cass et al. (2005) observed, travel is essential for constructing and sustaining human networks in social life, professional life, and organisations. The aspect of mobility concerning exclusion was previously highlighted by Kenyon et al. (2002, p. 10), who defined it as follows:

"The process by which people are prevented from participating in the economic, political and social life of the community because of reduced accessibility to opportunities, services and social networks, due in whole or in part to insufficient mobility in a society and environment built around the assumption of high mobility."

Therefore, ensuring that certain population groups are not excluded from society despite their mobility restrictions requires meeting everyone's accessibility needs (Lättman et al., 2016). Allowing all individuals to actively engage in communities fosters inclusivity in cities, positively influencing society beyond population groups with reduced mobility (Kenyon, 2011; Lättman et al., 2016).

1.2 Research Objective

Aiming towards inclusive cities that positively affect society and improve the quality of life, appropriate inclusivity measurements and a robust database on footpath infrastructure (e.g., footpath surface material type, footpath width, etc.) are required but often lacking (Allahbakhshi, 2023; Lättman et al., 2016; Tannert & Schöning, 2018). This deficiency results in incomplete routing suggestions or routes that do not accurately represent real-world conditions in routing services such as Google Maps and those based on OpenStreetMap (OSM) (Allahbakhshi, 2023). However, as motivated above, it is crucial to consider various features that impact accessibility in order to provide digital maps and personalised routing services that cater to the mobility needs of diverse population groups (Beale et al., 2006).

The objective of this Master's thesis is to assess the implementation of accessibility-sensitive pedestrian routing, using Zurich's District 1 as the study area. Historic District 1 is located in the centre of the City of Zurich. With the main train station situated in this district and the presence of numerous public transport lines, such as buses and trams, the area experiences a high volume of commuters (Allahbakhshi, 2023; Zürich Tourismus, 2025). Additionally, various tourist attractions, shopping opportunities, and pedestrian zones are present in the area (Zürich Tourismus, 2025). District 1 is further characterised by its topography (Allahbakhshi, 2023).

A suitable methodology for integrating accessibility information into the footpath network will be applied. I will further evaluate the effectiveness of accessibility-sensitive routing by applying Dijkstra's Shortest Path algorithm to the footpath network containing accessibility information. Additionally, the limitations of existing routing services in accommodating accessibility needs will be identified and highlighted by comparing them against the Dijkstra routing results based on the footpath network enriched with accessibility data. Additionally, I aim to assess the effect of objects temporarily obstructing movement on footpaths on routing results.

The analysis will be limited to District 1 as it will be based on highly detailed accessibility data provided by a data collection campaign conducted in Zurich's District 1. To the best of my knowledge, such detailed databases exist for very few cities worldwide, contributing to the novelty of this study.

With this thesis, I want to contribute to empowering individuals affected by mobility restrictions to use digital navigation services, increasing their autonomy and fostering independence in their daily lives.

1.3 Research Questions

To address the research objective defined in the previous chapter, the following research questions result:

Research Question 1: *How is the footpath network in Zurich's District 1 enhanced with spatial accessibility features?*

Here, several steps are required to ultimately integrate accessibility information into the footpath network of District 1. The steps include clustering and aggregating data points representing mobility obstacles and facilitators, respectively, into meaningful groups, following an approach inspired by Saha et al. (2019). Prior to allocating the accessibility information to the footpaths, the footpaths will be divided into smaller segments, similar to Rahaman et al. (2017). Following this segmentation step, the spatial accessibility features will be assigned to the footpath segments, similar to approaches introduced by Völkel and Weber (2008) or Kasemsuppakorn and Karimi (2009). The allocated spatial accessibility features will facilitate the calculation of a single value per segment, representing the accessibility of the respective segment. Therefore, the accessibility calculations introduced by Li et al. (2022) will be followed, ultimately resulting in a footpath network enhanced with spatial accessibility information.

Research Question 2: *How well do existing routing services respond to the needs of mobility-restricted population groups?*

To answer this question, an approach inspired by the work of Tannert and Schöning (2018) will be adopted: First, 30 meaningful origin-destination pairs will be used to generate routes by Google Maps, Open Source Routing Machine (OSRM), and OpenRouteService (ORS). The resulting routes will then be compared to the routes suggested by Dijkstra's Shortest Path algorithm, applied to the accessibility-enriched footpath network of District 1. Statistical analyses will be performed to compare the route length, travel time, and complexity of the resulting routes.

Research Question 3: *Do temporary obstacles significantly impact routing outcomes for mobility-impaired individuals?*

Certain, non-permanent obstacles will affect the movement of mobility-restricted and disabled persons on footpaths only for a limited amount of time (Georgescu et al., 2024). To assess the impact of such obstacles on routing, two networks will be constructed as a basis for routing. One network will include only permanent accessibility features, such as elements of the built environment (e.g., surface material). The second network will take into account all accessibility features, including those that exist only for a limited duration, such as parked vehicles or construction sites. Dijkstra's Shortest Path algorithm will be applied to both networks to generate routes for 30 origin-destination pairs. The proposed routes will be compared and assessed based on route lengths, travel times, and route complexities.

1.4 Structure of This Thesis

This Master's thesis is organised as follows: after Chapter 1, which introduces the topic, motivation, and research questions, along with the thesis objectives, Chapter 2 situates the thesis within a broader scientific context, highlighting relevant prior work and existing research gaps. Chapter 3 provides a detailed description of the datasets that form the foundation of this study, including accessibility information, federal population data, and geometrical data from municipal and cantonal sources, as well as openly available data on various Points of Interest (POIs). The sources and structures of the various datasets are explained. Chapter 4 outlines the methods employed to explore the research questions, such as allocating accessibility information to the footpaths of District 1 and creating a spatial network containing accessibility data. Following this, the routing approaches are discussed. Finally, the chapter concludes by describing the statistical analyses conducted. Chapter 5 presents the findings, including the method of allocating accessibility information to footpaths, the routing results, and the final statistical analysis outcomes. Chapter 6 reviews the findings, places them within a broader scientific context, and answers the research questions. Finally, Chapter 7 summarises the key findings and their implications.

2 Background

2.1 Accessibility

Aiming towards the introduced inclusive cities, appropriate inclusivity measurements are needed (Lanza et al., 2023). One potential measure is *Spatial Accessibility*, defined as *"the potential of opportunities for interaction"* (Hansen, 1959), since accessibility has been recognised as a factor of individual participation in social networks (Pot et al., 2024). Insufficient access to essential services, social networks, goods, and other opportunities improving quality of life is closely linked to social exclusion, as it can restrict individuals from fully participating in the economic, political, and social aspects of their community (Pot et al., 2024). Thus, accessibility can measure inclusivity, namely the ability to participate in communities' economic, political, and social life considering different transportation systems, spatial opportunities and the individual's abilities to move (Lanza et al., 2023). Spatial accessibility, therefore, describes how easily different locations and services can be reached from a geospatial location through movement in physical space (Allahbakhshi & Ardüser, 2024). It considers the spatial distribution of activities, individuals' physical and mobility capabilities, and their preferences or needs for accessing these destinations (Hansen, 1959). In alignment with the definition of spatial accessibility provided by Hansen (1959), Lanza et al. (2023) stated that accessibility *"is as much about people as it is about place"*, meaning that an accessibility assessment needs to consider both a person's characteristics, including habits, needs, possibilities, and preferences, as well as the spatial-physical context.

Building on this general understanding of accessibility, this thesis distinguishes between two key concepts: spatial accessibility and (barrier-free) accessibility.

- **Spatial Accessibility:** This refers to the ability to reach desired destinations, such as places, services, and social networks (Pot et al., 2024). It is quantified using various measures that evaluate how well people can access these opportunities, as described in Section 2.1.2. This concept focuses on geographic and infrastructural dimensions, such as proximity, connectivity, and travel times, influencing how easily individuals can interact with their surrounding environment (Guagliardo, 2004).
- **(Barrier-free) Accessibility:** This term is used to denote the barrier-free requirements of footpaths, focusing on how inclusive and navigable these paths are for individuals with different mobility needs. This concept emphasises identifying and addressing physical barriers (e.g., uneven surfaces, steep inclines, or obstacles) that hinder movement, particularly for mobility-restricted population groups, such as individuals with disabilities, older adults, or parents with pushchairs (Arora & Deshpande, 2021; Georgescu et al., 2024). This sense of accessibility highlights the importance of designing inclusive infrastructure that minimises barriers and ensures equitable access for all population groups (Saha et al., 2019).

While these two aspects of accessibility address different scales and concerns, they are closely linked. Spatial accessibility depends not only on the availability of destinations but also on the quality and inclusivity of the paths connecting them. For example, a high level of spatial accessibility is meaningless if the physical paths to these destinations are not inclusive or present barriers (Lopes et al., 2019) for certain groups, such as individuals with disabilities, older adults, or those with pushchairs.

By examining both concepts together, this thesis emphasises the need to address barriers within footpath networks as a critical component of enhancing spatial accessibility. An inclusive design that prioritises barrier-free movement ensures that all individuals can participate fully in social, economic, and cultural life (Arora & Deshpande, 2021), reinforcing the importance of accessibility in both senses.

While spatial accessibility focuses on reaching destinations, the inclusivity of travelling itself heavily depends on footpath accessibility. The following section further explores this vital aspect of barrier-free footpath accessibility.

2.1.1 Footpath Accessibility

Considering the positive impact of walking on cities, as introduced in the previous section, which ranges from the provision of essential social functions (Rhoads et al., 2023) to improved physical health and reduced mental health impairments (Achuthan et al., 2010), accessible pedestrian infrastructure is crucial (Saha et al., 2019). Pedestrian infrastructure encompasses footpaths, crosswalks, as well as other legal pedestrian crossings and areas designated for pedestrians, such as trails or pedestrian streets (Rhoads et al., 2023). Several factors can influence the spatial accessibility of footpath infrastructure, including both internal and external elements. Internal factors include, for instance, an individual's physical mobility capability. External factors comprise the built environment, such as the footpath infrastructure, weather conditions on a specific day, or the attractiveness and comfort of urban design (Georgescu et al., 2024). Georgescu et al. (2024) noted that an obstacle for one person on a particular day might not impede the same individual on another day. Furthermore, another person may not be affected by the obstacle at all (Georgescu et al., 2024). Consequently, current street elements within the footpath infrastructure, such as obstacles or the surface condition of footpaths, can either hinder or facilitate the movement of individuals through physical space, depending on an individual's physical capacity (Lid & Solvang, 2016; Ortega et al., 2021).

Street elements that impede the mobility of individuals with mobility restrictions result in inaccessibility, being perceived as *barriers* or *obstacles* (Hammel et al., 2015). Examples of said barriers include stairs, narrow and steep footpaths, or poor footpath surface conditions (Georgescu et al., 2024). However, the impact level of such barriers on an individual's mobility is highly dependent on the physical capabilities of said individual. Furthermore, some street elements are perceived as a barrier by some individuals, whereas the same street element facilitates the movement of other groups (Georgescu et al., 2024). This effect can be illustrated by the street element *curb*. While a high curb hinders the mobility of a wheelchair user as it is challenging to overcome the height difference, it facilitates the movement of visually impaired individuals by indicating the end of the footpath (Han et al., 2020; Harris et al., 2015; Rosenberg et al., 2013). Street elements hindering individuals' movements on footpaths, i.e., barriers, can be distinguished by their permanence. *Temporary obstacles* only restrict movement on footpaths for a limited amount of time, whereas *permanent obstacles* persist over an unlimited time. Temporary obstacles include parked vehicles or construction sites. Permanent obstacles such as poor footpath surface conditions or specific footpath material, like cobblestone, would require an intervention to be removed (Cushley et al., 2022).

Street elements viewed as *facilitators* aid various individuals in navigating physical space. Examples include benches along the footpath that assist older adults in completing longer journeys (Ottoni et al., 2016). Moreover, curb ramps or ramps, in general, serve as facilitators, as they enable persons with mobility impairments to overcome height differences, such as stairs. However, their proper design is essential; otherwise, such street elements may be seen as barriers despite being constructed to promote footpath movement (Harris et al., 2015; Rosenberg et al., 2013).

Given the accessibility aspect of the previously described street elements, I will hereafter refer to them as *spatial accessibility features*. This term includes footpath features that hinder movement (barriers or obstacles) and those that facilitate it (facilitators). By addressing barriers and facilitators in pedestrian infrastructure, footpath accessibility directly influences the broader concept of spatial accessibility, ensuring fair access to various locations for all.

2.1.2 Spatial Accessibility Measures

While the previous section addressed the physical and inclusive aspects of footpath accessibility, this section focuses on commonly used methods to measure spatial accessibility. These measures assess accessibility based on the spatial distribution of services, transportation networks, and population demand. They provide insights into the general accessibility of opportunities within a given area (Guagliardo, 2004).

Numerous studies have assessed the spatial accessibility of different places, activities, and services. For instance, studies range from measuring spatial access to primary healthcare services in Bhutan (Jamtsho et al., 2015) over research analysing the inequality of urban facilities in Tehran using spatial accessibility (Hosseini et al., 2022) to a study applying spatial accessibility measures on schools in Tiruchirappalli (Rekha et al., 2020). Different accessibility measurements are introduced to evaluate how accessible such services, places, or activities are. The following sections provide an overview of some commonly applied approaches to assess spatial accessibility based on the classification provided by Guagliardo (2004).

Spatial accessibility measures are often based on distance to providers or travel time to provider measurements, aligning with their everyday use in routing, as introduced in Section 2.2.1 (Rahaman et al., 2017; Völkel & Weber, 2008).

While spatial accessibility measures offer significant potential to assess access to services, goods, and activities (Lanza et al., 2023), their limitations must be recognised. As Wolff et al. (2022) highlighted, traditional spatial accessibility measures often fail to account for barriers at finer spatial levels, such as physical obstacles or environmental challenges. This oversight can lead to an incomplete understanding of accessibility, particularly for individuals with mobility restrictions. Addressing these gaps is essential to ensure that accessibility measures reflect the needs of diverse populations and align with the principles of inclusive urban planning.

Provider-to-Population Ratios

Provider-to-population ratios, also known as *supply ratios*, are a widely used measure of spatial accessibility as they are intuitive. Ratios are calculated based on predefined geographical units, such as counties, states, statistical areas, or health service areas, depending on the focus of spatial accessibility analysis (Drake et al., 2021; Guagliardo, 2004). To calculate ratios, the numbers of providers in the area of interest are determined and divided by the population in the same area (Guagliardo, 2004; Schonfeld et al., 1972). Schonfeld et al. (1972) illustrated this by assessing the number of physicians required to provide good primary medical care by considering the number of primary physicians and the population, potentially considering only certain age groups or only the individuals affected by specific diseases (Schonfeld et al., 1972).

The advantage of *provider-to-population ratios* lies in their simplicity. They are easy to compute, allow for comparison over different geographical areas, and can help establish minimal supply standards, which in turn aids in identifying underserved areas. However, the ratios are highly sensitive to the area chosen, e.g., the area's size or configuration (Guagliardo, 2004). This well-known phenomenon is referred to as the *Modifiable Areal Unit Problem (MAUP)* and addresses the issue that geographical areal units can be delineated arbitrarily as there are no standard sets of spatial units (Guagliardo, 2004;

Openshaw, 1984). In addition, the ratios based on areas do not account for variations within the areas and are not able to consider border crossing, meaning that an individual from one area may access service providers in another area as it is closer. In addition, *provider-to-population ratios* are unable to consider distance or travel time from individuals to the service provider locations (Guagliardo, 2004).

Travel Impedance to Nearest Provider

Travel impedance to nearest provider, sometimes called *travel cost*, is determined by measuring the travel distance or travel time from an individual's residence to the nearest provider. Depending on data availability, population points, such as a centroid of a county of residence or census tract, can be used instead of an individual home location (Drake et al., 2021; Guagliardo, 2004). The distance can be calculated using different metrics, such as Euclidean distance or travel distance along a transportation network, like roads or rail systems, which makes *travel impedance to nearest provider* an intuitive measurement of spatial accessibility (Guagliardo, 2004).

While *travel impedance to nearest provider* is an accurate spatial accessibility measurement in rural settings, it has considerable limitations in urban areas. In cities, multiple providers are often located at similar distances, complicating the assessment of accessibility based solely on proximity. Additionally, travel impedance measures do not account for the availability or capacity constraints of providers, which can further limit their effectiveness in urban contexts (Drake et al., 2021).

Average Travel Impedance to Provider

To determine *average travel impedance to provider*, distances are measured from one point, i.e., an individual or a population point, to all providers within a defined area, such as a city or a county. These distances are then summed and averaged. This measure accounts for different service providers reachable within an area from the population point (Guagliardo, 2004). However, the approach is insensitive to border crossing, similar to *provider-to-population ratios*. Restricting the measurements to providers within a specific area overlooks providers just outside the boundaries that might be closer to the population point. Furthermore, the measure overemphasises the impact of providers located close to the edges of the area, as it calculates distances from one point to all providers. Someone located close to one edge of the area might not travel across the entire area to access the service located on the opposite side of the area (Guagliardo, 2004).

Gravity Models

Similar to *average travel impedance to provider*, *gravity models* consider all service providers within a "reasonable distance" (Guagliardo, 2004). They aim to take into account the potential interaction between any population point and all providers, reducing the possibility of interaction with increasing distance or travel impedance, resulting in a spatial accessibility measurement for each point (Delamater, 2013; Guagliardo, 2004). As Guagliardo (2004) stated, *gravity models* are sometimes also known as *cumulative opportunity measures* due to the nature of gravity models of taking all alternative providers into account. The most basic *gravity model* for spatial accessibility can be found in Equation 2.1 (Guagliardo, 2004; Wang & Luo, 2005).

$$A_i = \sum_j \frac{S_j}{d_{ij}^{\beta}} \tag{2.1}$$

A_i is the spatial accessibility at population point i. S_j is the service capacity of a service provider at the provider location j. The travel impedance d describes the distance or travel time between the population point i and the provider location j. The gravity decay coefficient β, or travel friction coefficient β, accounts for the travel weight change as travel time or distance changes. With an increase of summed provider capacity (numerator) or a decrease of summed travel impedance (denominator), spatial accessibility increases (Guagliardo, 2004).

The output of *gravity models* varies. When the spatial accessibility for each population point is calculated, i.e., the distance of each population point to each service provider is determined, the *gravity model* results in a continuous surface containing the accessibility value for each population point (Guagliardo, 2004; McGrail & Humphreys, 2009). A_i can also be estimated at multiple representative locations in different cities, allowing for a comparison of the average accessibility variation across the cities (Guagliardo, 2004).

Besides their simplicity in application, such simple *gravity models* cannot model demand. Spatial accessibility at a given distance from two different service providers would be the same when applying such simple *gravity models*, even though the first service provider might serve 1'000 individuals more than the second one (Guagliardo, 2004). This was addressed by adding V_j to the denominator, a population demand adjustment factor (Equation 2.2) (Guagliardo, 2004).

$$A_i = \sum_j \frac{S_j}{d_{ij}^{\beta} * V_j} \tag{2.2}$$

Further challenging is the determination of the distance decay coefficient β, as it is often unknown and varies in its mathematical form, requiring to estimate β empirically (Delamater, 2013; Guagliardo, 2004).

Floating Catchment Area Analysis

To address challenges in spatial accessibility estimations, e.g., service provider data lacking spatial resolution, Luo and Wang (2003) developed the *two-step floating catchment area* method. The *floating catchment area (FCA) analysis* was first developed to assess urban job accessibility (Guagliardo, 2004). The adaptation from Luo and Wang (2003) consists of two steps: First, a *provider-to-population ratio* is calculated for each area centroid. Providers associated with the centroid are divided by the population that can reach the provider location within a specific travel time. The area where individuals can get to the provider location at a given time is called a catchment. The *provider-to-population ratio* is then assigned to the entire catchment, not just the centroid from which it originated. Repeating this process for all area centroids causes irregularly shaped and overlapping catchments (Guagliardo, 2004). In the second step, the focus lies on population points, consisting of residences or census tract centroids. For each population point, a spatial accessibility value is determined by calculating the sum of *provider-to-population ratios* from all overlapping catchments. These summed values are then assigned to the population point, producing spatial accessibility scores for the entire area (Guagliardo, 2004; Luo & Wang, 2003).

Luo and Wang (2003) showed that this method is an improved *gravity model* and effectively addresses challenges like border crossings (Guagliardo, 2004). However, several limitations still exist. The travel time threshold catchment boundaries are discrete, resulting in consistent spatial accessibility scores near boundaries and a sudden drop beyond these boundaries. Additionally, the chosen travel time threshold impacts spatial accessibility variations, with longer times reducing disparities (Guagliardo, 2004).

Several adaptions of *FCA* analyses have been developed (Jörg et al., 2019). Beyond the commonly used *two-step FCA (2SFCA)*, other variations include the *enhanced two-step FCA (E2SFCA)*, *three-step FCA (3SFCA)*, and *modified-Huff-model-3SFCA (MH3SFCA)*. These represent only a subset of the many adaptations developed to address specific requirements in spatial accessibility assessments (Jörg et al., 2019). A study evaluating the spatial accessibility of homecare workers to the older population in Zurich employed various forms of *FCA* methods (Allahbakhshi et al., 2023).

Kernel Density Method

Based on earlier approaches by Guptill (1975), Guagliardo (2004) created density layers of service providers by using the *Gaussian Kernel* method. The density layer consisted of regular grids, where the spatial accessibility of one grid cell is derived from the provider density at the centre point of the grid cell. Each service provider is represented by a cone (kernel) on the continuous density surface, where the kernel volume illustrates the service provider's total capacity. The kernel radius reflects the assumed extent of the provider's practical service area. The spatial accessibility is then determined by a cell's proximity to a service provider's location, i.e., cells close to a provider receive higher accessibility values (Guagliardo, 2004). Cells with overlapping areas, i.e., multiple service providers lie within a reasonable distance, combine the impact of multiple kernels into a cumulative spatial accessibility value. The method further allows for the weighting of different factors (Guagliardo, 2004). For instance, providers with better online reviews or longer opening hours could receive a higher weight.

Guagliardo (2004) combined the provider density layer with the population density layer in a second step. This approach allowed for the calculation of *provider-to-population ratio* values per grid cell, giving valuable insights into the spatial variation of accessibility. Furthermore, the accessibility layer can be overlaid with census area data, aiming for the calculation of average accessibility per census area (Guagliardo, 2004).

2.2 Routing

This chapter focuses on routing systems and their role in addressing accessibility challenges. By linking accessibility principles to routing, it explores how inclusive navigation can enhance participation in urban life.

Accessibility is a concept that encompasses physical, social, and institutional factors shaping individuals' ability to participate in societal activities (Wolff et al., 2022). In the context of routing, this description highlights the need to consider both spatial accessibility and barrier-free physical accessibility, which ensures equitable access for individuals with diverse mobility needs.

By integrating spatial and physical accessibility principles, routing systems contribute to inclusive cities by enabling equitable access to essential services, employment opportunities, and social participation (Kasemsuppakorn & Karimi, 2009). As Wolff et al. (2022) emphasised, addressing physical barriers in the built environment is critical for fostering equitable participation in all aspects of life. Through accessibility-sensitive routing services, individuals with reduced mobility could benefit greatly, leading to the advancement of inclusivity by responding to diverse mobility needs (Völkel & Weber, 2008). The following section describes routing services and their potential to support inclusive navigation.

2.2.1 Routing Services

In the past two decades, digital navigation systems have emerged and were first widely used for car navigation (Völkel & Weber, 2008). Nowadays, mobile phones with Global Positioning System (GPS) sensors also facilitate navigation for cyclists and pedestrians. Navigation services hold great potential as navigation support for mobility-impaired population groups, e.g., older adults with age-related mobility restrictions, mobility-disabled individuals and visually impaired persons (Rahaman et al., 2017; Völkel & Weber, 2008). However, many current routing services fail to suggest routes applicable to mobility-impaired individuals, as routing services used today mostly base route optimisation on shortest-path algorithms, aiming to minimise route length or travel time (Rahaman et al., 2017; Völkel & Weber, 2008). Furthermore, route length or travel time are commonly used metrics in spatial accessibility measures, such as *travel impedance*, *gravity models*, and *floating catchment area analysis*, introduced in Section 2.1.2. However, additional characteristics of a route might be equally important for different population groups, e.g., the accessibility of a particular route. For instance, visually impaired individuals generally seek to avoid large, crowded and therefore noisy intersections, accepting a longer but safer route (Völkel & Weber, 2008). Similarly, older adults with age-related mobility restrictions and mobility-disabled individuals might prefer a more gentle and safer route instead of the shortest one, with individual perceptions of *gentle* and *safe*. Consequently, the requirements of accessible routes vary between persons and are different regarding physical abilities and personal preferences (Rahaman et al., 2017; Völkel & Weber, 2008). The following sections introduce two routing services as examples of services that are not sensitive to users with mobility impairments and describe them in more detail.

Google Maps

Google Maps (https://www.google.com/maps) is Google's routing engine, and, according to a recent publication from Mehta et al. (2019), one of the world's most influential applications, with roughly 64 million users worldwide. In its early years, the application was restricted to navigation. However, today, it contains various features like street view, estimated time of arrival (ETA) and many more (Mehta et al., 2019). Google Maps uses proprietary data and algorithms, limiting the available information about their implementation (Tannert & Schöning, 2018). However, as stated by Mehta et al. (2019), Google Maps employs graph structures in its routing service to determine the shortest path between origin and destination. Moreover, the A* algorithm, flexible and efficient, is assumed to be implemented by Google Maps (Mehta et al., 2019). The location of origins and destinations, which can be people or places, for suggesting routes is based on Global Positioning System (GPS) data. GPS is a technique used to track an object using a satellite system currently in space. Three satellites are required to determine the exact location of an object or a person in the world, i.e., the coordinates of said location on a map (Mehta et al., 2019). Google Maps suggests available routes between origin and destination locations for cars, public transport, walking and cycling (Google, 2024c). Real-time traffic and public transport updates enable accurate estimation of ETAs, making it a powerful routing tool (Google, 2024a).

Open Source Routing Machine

The Open Source Routing Machine (OSRM), available via https://map.project-osrm.org, is a routing engine running on OpenStreetMap (OSM) data (Open Source Routing Machine, 2024a; OpenStreetMap contributors, 2025). In contrast to other routing services, OSRM is a non-commercial routing engine without a limit on the number of requests or restrictions on derived data sets. By providing the OSRM software as an open source, running on open-source data, transparent and reproducible research is possible (Giraud, 2022). OSRM supports three travel modes: walking, cycling and driving (Open Source Routing Machine, 2024b). Routes are calculated using Contraction Hierarchies (Geisberger et al., 2008; Luxen & Vetter, 2011). Contraction Hierarchies is an algorithm for shortest path calculations in large networks. The algorithm is ideal for applications requiring fast and accurate routing and, therefore, suitable for its implementation into OSRM (Luxen & Vetter, 2011).

2.2.2 Accessibility-Sensitive Routing Services

In recent years, several routing services have been developed with algorithms considering footpath accessibility in navigation suggestions (Rahaman et al., 2017; Völkel & Weber, 2008). An early example is RouteCheckr, a routing algorithm developed by Völkel and Weber (2008), which proposes routes based on personalised accessibility criteria, such as safety or inclines. RouteCheckr is based on crowd-sourced data and relies on user accessibility ratings of footpath segments, with more recent ratings being more relevant for route calculation. The routing algorithm then aims to reduce the route's total weight, i.e., the cost assigned to the route (Völkel & Weber, 2008). As proposed by Völkel and Weber (2008), other approaches also rely on the subdivision of footpath network segments for their enrichment with accessibility data. An exciting example is the Contour-based Accessible Path Routing Algorithm (CAPRA) developed by Rahaman et al. (2017), which bases its route calculation on the incline of the suggested routes, what they consider to be the most influential factor affecting the accessibility of a route. Here, contour lines are used to split the segments of the footpath network into smaller segments, and the incline of each segment is derived from the height difference between the network nodes and the length of the respective network edge. The resulting route suggestions between origin and destination are then compared to each other and Google Maps regarding their distance, height difference, and slope to find the most appropriate route by a cost-benefit analysis.

Contrary to the approaches based on further segmentation, Beale et al. (2006) implemented *Dynamic Segmentation* techniques to propose routes to individuals using different wheelchair types. Dynamic segmentation allows footpath accessibility data to be linked indirectly to the network, not affecting the network structure. The network is stored with its geometry, while point or linear features (events) are stored in separate thematic tables with a unique identifier and a position along the geometry, allowing the locating of the features on the geometry (Cadkin, 2002). This enables the assignment of multiple footpath accessibility features to one segment in the network without the need to adjust the network geometry (Beale et al., 2006). By assigning different weights to spatial accessibility features on footpaths, such as ramps, steps, crossings, or narrow pavements, routes are calculated based on the assumption that spatial accessibility features that are not a barrier for a wheelchair user are implicit in the network, whereas barriers impeding the movement on footpaths are explicitly defined as cost. If a spatial accessibility feature prevents a wheelchair user from moving on the footpath at a specific location, routing at this point is not possible (Beale et al., 2006). The implemented routing approach results in several route suggestions, e.g., shortest distance, route with the minimum urban barriers, avoiding slopes with a gradient higher than a certain threshold, and routes with only crossings controlled by pedestrian signals (Beale et al., 2006).

Several studies regarding routing algorithms for wheelchair users published in the past two decades rely on the implementation of the Dijkstra algorithm (Neis, 2015). Edsger W. Dijkstra introduced the Dijkstra algorithm, which detects the shortest path between two nodes in a graph. The algorithm operates by iteratively selecting the unvisited node with the smallest known distance from the source node, updating the distances to its neighbouring nodes, and marking it as visited. This process repeats until the destination node is reached, ensuring that the shortest path is found efficiently without the need to evaluate all possible paths (Dijkstra, 1959).

OpenRouteService

A routing service capable of considering accessibility-relevant information, such as various spatial accessibility features, is OpenRouteService (ORS) (https://maps.openrouteservice.org/). As its name already indicates, it is an open-source routing engine based on open-source data, such as OSM data (Neis & Zipf, 2008; OpenRouteService, 2024c). Elevation data is derived from the SRTM[1] and GMTED[2] datasets (OpenRouteService, 2024c). Different profile categories are supported in ORS, including cycling, walking, driving with a car, driving with a heavy vehicle, and travelling by using a wheelchair. For cycling, walking, and driving with a heavy vehicle, different subcategories are available to further specify the profile (OpenRouteService, 2024b). ORS allows for the adjustment of some profile parameters, resulting in different route options. These parameters enable the restriction of certain features,

[1]Consortium for Spatial Information (CGIAR-CSI). (2025). SRTM 90m Digital Elevation Database v4.1. https://srtm.csi.cgiar.org

[2]U.S. Geological Survey (USGS). (2010). GMTED2010 Global Multi-resolution Terrain Elevation Data. https://www.usgs.gov/coastal-changes-and-impacts/gmted2010

such as the maximum incline or the minimum surface type. Table 2.1 summarises the parameters available for footpath routing, for walking pedestrians and those using a wheelchair, as well as the default value per parameter.

Table 2.1: Pedestrian walking profiles and their parameters in ORS (OpenRouteService, 2024b, 2024c)

Profile	**Parameter**	**Available Values**	**Default Value**
Foot walking	Route preference	Shortest, recommended	Recommended
	Avoid features	Ferries, fords, steps	
	Avoid borders	All, controlled	
	Avoid countries	*List of countries*	
Wheelchair	Route preference	Shortest, recommended	Recommended
	Maximum inclination	3, 6, 10, 15 %	6%
	Maximum curb height	0.03, 0.06, 0.1 m	0.06 m
	Footway minimum width	1-30 m	1 m
	Route smoothness	Impassable, very horrible, horrible, very bad, bad, intermediate, good, excellent	Good
	Minimum surface type	Grass, ground, pebblestone, gravel, fine gravel, compacted, unpaved, wood, metal, cobblestone, unhewn cobblestone, sett, paving stones, concrete lanes, concrete, asphalt, paved	Cobblestone
	Minimum route grade *(based on OSM categorisation)*	Grade 1, Grade 2, Grade 3, Grade 4, Grade 5	Grade 1
	Only surfaces with known quality	TRUE/FALSE	FALSE
	Allow unsuitable	TRUE/FALSE	FALSE
	Avoid features	Ferries, fords, steps	
	Avoid borders	All, controlled	
	Avoid countries	*List of countries*	

ORS generally implements the Contraction Hierarchies algorithm or the C-ALT algorithm to suggest the shortest path between origin and destination. C-ALT is an algorithm with scaling and performance similar to Contraction Hierarchies. Additionally, it enables custom filters to query the routes (OpenRouteService, 2023). As stated in a forum contribution, the applied routing algorithm depends on the profile and the parameters set, such as *avoid_features* (OpenRouteService, 2023).

2.2.3 Route Choice

When given several alternative routes, pedestrians choose a route depending on different factors. The most fundamental impacts on route choice are often assumed to be travel time and route length. However, further influencing factors have been found, such as the safety of routes or how interesting a route is (Sevtsuk & Basu, 2022). Additionally, it has also been shown that the route's complexity impacts the route choices of pedestrians, representing the ease of navigating a route (Sevtsuk & Basu, 2022).

Routing algorithms typically aim to reduce some sort of cost, generally introduced by travel time or route length (Völkel & Weber, 2008), also are also commonly used variables in spatial accessibility assessments, as introduced in Section 2.1.2. However, these measures do not directly serve mobility-impaired individuals, as other criteria might be equally important to this population group (Tannert & Schöning, 2018). In recent years, routing services that are able to consider such criteria have emerged. These routing services most commonly avoid obstacles, such as stairs or objects on the footpath, consider different surface properties, calculate the incline of footpath segments, and determine the height of the curbs to optimise routes suited for wheelchair users (Tannert & Schöning, 2018). Due to the fact that many different footpath features impact the accessibility of routes, measurements to compare different footpath segments are required (Rahaman et al., 2017; Völkel & Weber, 2008). A common approach to route optimisation is the use of cost functions, which are capable of considering different criteria and allowing for compensation from one criterion by another (Völkel & Weber, 2008).

Beale et al. (2006) applied cost functions for different wheelchair types. The assumption underlying their approach was based primarily on considering objects impeding the accessibility of a route, while facilitators were presumed to be part of the network. Thus, only obstacles were modelled in the network. Besides the presence of obstacles, they considered different weights per obstacle category, the weight of an individual, the rolling resistance, the slope, and the segment length. These criteria were combined in an impedance factor, calculated for every network segment between the origin and destination. Based on these impedance factors, the shortest route and the optimal route with the minimum overall impedance were calculated. Users of their routing algorithm were then given a choice between routes (Beale et al., 2006).

Similar to the approach introduced by Beale et al. (2006), the RouteCheckr system developed by Völkel and Weber (2008) determined the optimal path based on a set of criteria. Each criterion was assigned a weight based on predefined values or user ratings. The weighted criteria were then considered in a cost function when the corresponding objects were present on the route. The final cost per route was computed by combining the weighted criteria with the normalised segment length (Völkel & Weber, 2008).

Route Length

Routing services often aim to reduce the overall route length between an origin and a destination location (Völkel & Weber, 2008). Therefore, shortest path routing algorithms are implemented, such as Dijkstra's shortest path algorithm, A*, or the Contraction Hierarchies algorithm. Routing services introduced earlier also rely on the application of such routing algorithms for the suggestion of shortest routes (Luxen & Vetter, 2011; Mehta et al., 2019; OpenRouteService, 2023). The length of a route is determined simply by summing up the lengths of all route segments (Völkel & Weber, 2008).

Travel Time

Travel time is defined as the time needed to get from the route's origin location to the destination location. While most studies on routing focus on constant travel time, this assumption usually does not hold in reality (Gendreau et al., 2015). Given the length of a route from the origin location to the destination location, travel time depends on external and internal factors. While external factors, such as traffic congestion or weather conditions, are not under the travelling individual's control, internal factors can be adjusted by the individual. Thus, the travel time depends internally on whether the travelling person can set the travel speed independently (Gendreau et al., 2015).

Therefore, travel speed is a crucial factor in determining travel times for specific routes, alongside external factors beyond the control of the travelling individual. The factors impacting pedestrian travel speed are introduced in the following section.

Pedestrian Travel Speed

Travel speed is essential in determining the time necessary to complete one route, i.e., the travel time per route. However, travel speed greatly depends on the travel mode of pedestrians, for instance, walking or using a wheelchair, and is affected by different aspects (OpenRouteService, 2024d). A recently published review of pedestrian walking speed analysis by Giannoulaki and Christoforou (2024) organised the aspects influencing walking speed into the five categories summarised in Table 2.2.

Table 2.2: A sample of factors impacting pedestrian walking speed (Giannoulaki & Christoforou, 2024)

Category	**Category Characteristics**
Pedestrian flow characteristics	Pedestrian traffic state, flow, density, and speed
Pedestrian attributes	Age, gender, and physical attributes that affect pedestrian walking speed
Layout configuration	Characteristics of the walking environment: bottlenecks, corridors, incline, surface, land use, temporary or permanent obstacles
Ambient conditions	Noises, season/weather conditions
Pedestrian behavioural patterns	Walking in a group, carrying baggage, or using a mobile phone

Factors impacting pedestrian walking speed can be distinguished in external and internal factors (Giannoulaki & Christoforou, 2024).

Pedestrian flow characteristics, characterised as an external factor, describe the fundamental traffic flow theory. The inverse relationship between travel speed and density has been well-known for some time. Therefore, with increasing pedestrian density, travel speed is reduced (Giannoulaki & Christoforou, 2024).

Pedestrian attributes, i.e., internal factors, include the above-listed characteristics such as age and gender. For instance, most of the research conducted on pedestrian walking speed concluded that females generally walk slower than males under all circumstances and street conditions, including on footpaths (Boles & Hayward, 1978; Giannoulaki & Christoforou, 2024; Mohammed Alhassan & Mashros, 2015). In their review, Giannoulaki and Christoforou (2024) listed 34 studies analysing pedestrian walking speed, with average walking speeds of 1.20 m/s for females and 1.27 m/s for males overall. In addition to gender, age is often reported to have an influence on pedestrian walking speed (Giannoulaki & Christoforou, 2024). Walking speed typically follows an inverted U-shaped curve with age: it increases to a certain peak in early adulthood and then declines (Figure 2.1). This decline observed primarily in older adults is often attributed to health conditions, reduced stamina, and age-related structural changes (Giannoulaki & Christoforou, 2024; Mohamad Ali et al., 2019).

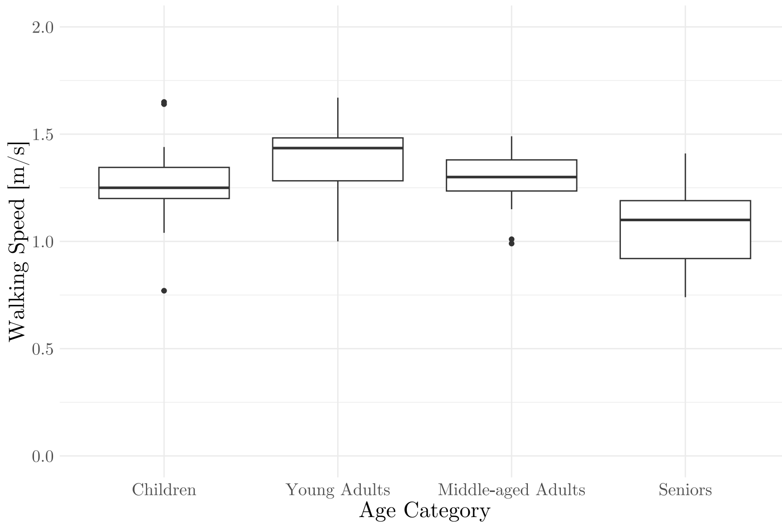

Figure 2.1: Walking speed and age (Giannoulaki & Christoforou, 2024)

The physical condition of individuals is another pedestrian attribute. This also includes personal mobility capacities, such as limited capacities due to mobility restrictions (Georgescu et al., 2024). Such physical conditions were assessed in a study conducted about 25 years ago, where the authors aimed to create data on the travel speeds of disabled people to provide a basis for fire safety engineering. Hence, they experimentally measured the travel speed of individuals from various mobility-impaired population groups (Boyce et al., 1999). A total of 155 disabled participants were involved in different parts of the experiment, such as moving horizontally or on a ramp (Boyce et al., 1999). The found travel speeds are depicted in Figure 2.2. The figure shows that mobility-impaired individuals always travelled at lower speeds than persons without restriction. The travel speed decreases with the growing incline, i.e., from level surfaces to ramps to stairs. Manual wheelchair users posed an exception, as their travel speed increased when moving on a ramp and was highest when moving downward on a ramp.

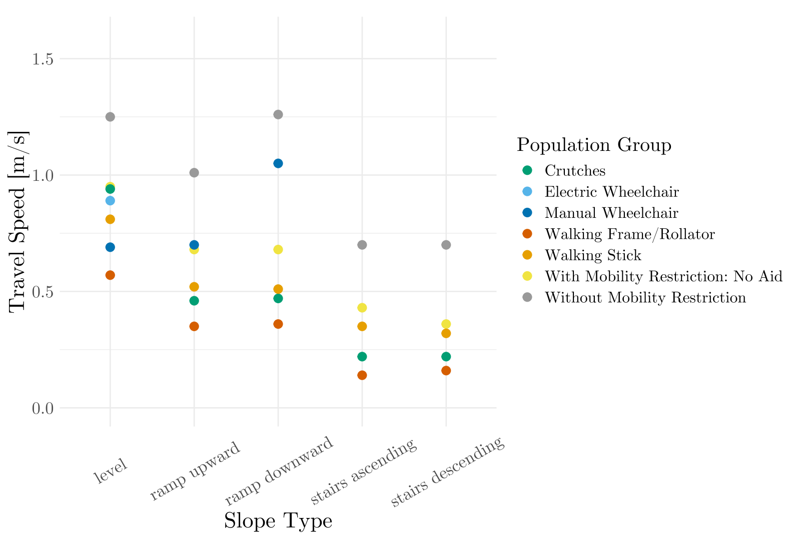

Figure 2.2: Travel speed and mobility restriction (Boyce et al., 1999)

Boyce et al. (1999) included walking speed measurements for individuals without mobility restrictions or disabilities, aiming for comparable travel speed values (Figure 2.2). As wheelchair users are not able to ascend or descend stairs, their travel speed values were not included for these two slope types. Furthermore, Boyce et al. (1999) state in their work that the number of participants decreased considerably for their travel speed assessment in the stairs settings.

An external factor influencing pedestrian walking speeds is the layout configuration of the walking area, including features like surface material, incline, and the presence of both temporary and permanent obstacles (Giannoulaki & Christoforou, 2024). Aghabayk et al. (2021) analysed the impact of footpath slope and pedestrian physical characteristics on walking and jogging speed in their study. They assessed the walking speed of 220 individuals from three different age groups: young (18-34), middle (34-55), and elderly (55+). The measured walking speeds depending on five different footpath slope categories can be found in Figure 2.3: level (0°), gentle uphill/downhill (6%), and steep uphill/downhill (12%). The previously discussed decline in walking speed with increasing age is also visible in the study conducted by Aghabayk et al. (2021).

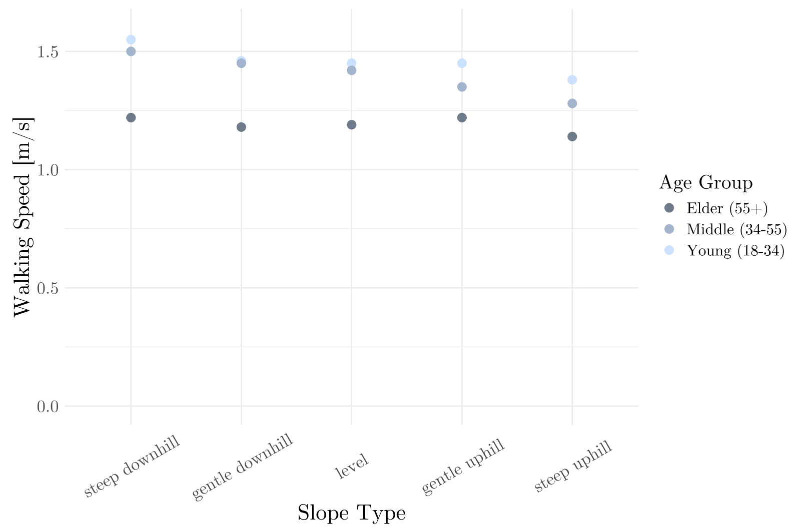

Figure 2.3: Walking speed by age and incline (Aghabayk et al., 2021)

The effect of ambient conditions, such as weather or seasons, on travelling speed is not conclusive. While some studies found lower speeds when pedestrians are faced with ice or snow, leading to a negative effect on pavement conditions, other findings suggested that pedestrians seemed to walk faster to protect themselves from such conditions (Giannoulaki & Christoforou, 2024).

Giannoulaki and Christoforou (2024) reviewed several studies on the impact of pedestrian behavioural patterns. While travelling in a group and using a mobile device reduced travel speed, results for carrying luggage were not conclusive (Caputcu et al., 2016; Giannoulaki & Christoforou, 2024). Giannoulaki and Christoforou (2024) explained the first two behavioural patterns as distractions from travelling, thus resulting in lower walking speeds. For carrying luggage, however, the authors assumed that the type of luggage as well as the person carrying it might impacted the results. For instance, a commuter carrying a briefcase may have travelled faster than a tourist carrying a suitcase (Giannoulaki & Christoforou, 2024).

Route Complexity

Besides travel time and route length, the complexity of a route is assumed to play a crucial role in route choices (Sevtsuk & Basu, 2022). The route complexity is often assessed based on the number of turns necessary to travel from the origin to the destination along a suggested route. If a turn is missed, reaching a destination can be difficult. By minimising the number of turns, the risk of taking a wrong turn is also reduced (Tannert & Schöning, 2018). This approach is handled differently by various routing services. Tannert and Schöning (2018), for instance, found that Google Maps aims for a reduction in the number of turns, although this sometimes involves detours.

The work conducted by Sevtsuk and Basu (2022) showed that the effect of route complexity on route choice was highly dependent on the network geometry. In complex networks, the number of turns was considerably high when travelling from an origin location to a destination location, independent of the route chosen. However, pedestrians tended to choose a simpler route where the network already enabled turn minimisation (Sevtsuk & Basu, 2022).

2.3 Data Availability

To apply routing services with algorithms capable of considering spatial accessibility features, such as the previously mentioned CAPRA or RouteCheckr, data on these features is required (Froehlich et al., 2019). In particular, assessing the spatial accessibility of pedestrian networks depends on data on footpath infrastructure (e.g., footpath surface material type, footpath width, etc.), which is often unavailable (Stefanidis & Bartzokas-Tsiompras, 2024). This lack of readily available footpath accessibility data is, moreover, leading to incomplete routing suggestions or routes not reflecting real-world conditions in routing services such as Google Maps and services based on OSM (Allahbakhshi, 2023). However, taking into account different types of spatial accessibility features for providing digital maps and individualised routing services that can meet the mobility needs of various population groups is essential (Beale et al., 2006). Especially mobility-impaired pedestrians could profit greatly from the use of such routing services, as increased mobility would enable greater autonomy and independence in everyday tasks and activities, raising the possibility of actively participating in communities (Völkel & Weber, 2008). Over the past years, several routing services emerged capable of taking data on spatial accessibility features into account when proposing routes, such as RouteCheckr or OpenRouteService (ORS) (Neis & Zipf, 2008; Völkel & Weber, 2008). However, the lack of data on spatial accessibility features leads to incomplete routing results of such routing services (Rahaman et al., 2017).

Several data collection approaches can be implemented to address the gap regarding the availability of footpath accessibility information. Traditional in-situ data collection methods include the use of sensors, conducting field surveys, or gathering data via mobile apps (Allahbakhshi, 2023). In recent years, the widespread use of the Internet has enabled remote data collection through Street View Imagery (SVI), offering a cost-effective and less time-consuming alternative to conventional field visits (Steinmetz-Wood et al., 2019). Among various platforms providing SVI, Google Street View (GSV) is widely used and serves as the foundation for most remote data collection platforms. This data collection method enables users to remotely and manually assess and document accessibility features by virtually navigating through city streets using SVI (Seekins et al., 2022).

Nevertheless, creating and maintaining an up-to-date geographical database remains an expensive, labour-intensive and time-consuming task, posing considerable challenges for municipalities (Prandi et al., 2014).

Drawing on the technological advances in recent decades and the widespread use of the internet, it has become easier to generate information, share it with others, and edit it from anywhere in the world (Goodchild, 2007). Goodchild (2007) defined the term *Volunteered Geographic Information (VGI)* for this phenomenon specifically regarding spatial knowledge. The author stated that *"anyone with an Internet connection can select an area on the Earth's surface and provide it with a description, including links to other sources"* (Goodchild, 2007, p. 212). A great example of the potential of VGI is OSM, further introduced in Section 3.4. Neis (2015) showed that spatial accessibility data could be derived from OSM and used input for accessibility-sensitive routing. However, a study in progress shows that OSM data may be lacking accessibility-relevant information for routing in the City of Zurich. For instance, only 2.3% of the OSM footpath data include information on steepness or incline (Allahbakhshi, n.d.).

2.4 ZuriACT Project

The introduced data gap has recently been addressed by implementing VGI methods in District 1 of the City of Zurich through the citizen science pilot project "ZuriACT: Zurich Accessible City". The ZuriACT project was a collaboration between the University of Zurich and the City of Zurich that ran from 2023 to 2024, aiming to provide a database on spatial accessibility features of footpaths, i.e., features of the built environment (Allahbakhshi & Ardüser, 2024; University of Zurich, 2024c).

The database can serve as a basis for accurate accessibility assessments, aiding policymakers and urban planners in designing more inclusive and sustainable environments. Furthermore, analysing supplementary accessibility data is critical for bridging scientific gaps in accessibility research, which have persisted due to the scarcity of adequate, comprehensive, and openly available geographic datasets (Allahbakhshi, 2023).

Following the ZuriACT study's scope to include perspectives of mobility-restricted and mobility-disabled persons on spatial accessibility on the footpaths of Zurich, adults (aged 18 and above) with mobility restrictions or mobility disabilities were targeted. The target groups included older adults aged 65 and above, with and without age-related mobility impairments, individuals with situational mobility restrictions, such as parents with pushchairs or caregivers, and mobility-disabled persons, e.g., wheelchair users (Allahbakhshi, 2023). 17 individuals actively participated in the data collection (Allahbakhshi & Ardüser, 2024).

To collect data on spatial accessibility features on the footpaths in District 1 in Zurich, participants used the Project Sidewalk tool (Allahbakhshi & Ardüser, 2024). The digital web tool facilitates remote data collection, enabling individuals with mobility restrictions to evaluate footpath accessibility safely and without exposing themselves to potential risks introduced by inaccessible footpath infrastructure. These are considerable advantages over in-situ measurements, where data collection is labour and time-intensive (Allahbakhshi, 2023; Froehlich et al., 2019).

Within the ZuriACT project, participants built a database containing raw data points on footpath accessibility features in District 1 of Zurich. Further processing and validation of the collected data were necessary to ensure a consistent and comprehensive database (Section 4.1) (Allahbakhshi & Ardüser, 2024).

3 Data

3.1 Spatial Accessibility Features

The spatial accessibility features were collected within the citizen science project ZuriACT. After data collection, the spatial accessibility features were analysed and validated to create a database containing spatial accessibility information reflecting real-world conditions (Allahbakhshi & Ardüser, 2024). Following the data collection period of the ZuriACT project using the Project Sidewalk tool (https://sidewalk-zurich.cs.washington.edu), the infra3D tool (www.infra3d.ch) was used to validate the raw spatial accessibility features and, where necessary, collected further data (Allahbakhshi, 2023; Allahbakhshi & Ardüser, 2024). Project Sidewalk is based on Google Street View (GSV) imagery, whose shortcomings are addressed by infra3D's regularly updated Street View Imagery (SVI) (every two years) with higher resolution and better coverage (Allahbakhshi, 2023; Saha et al., 2019).

Both tools are based on virtually exploring the surroundings along the route, and features are marked by placing a data point on the objects, representing spatial accessibility features, in the SVI (iNovitas AG, 2024; Saha et al., 2019). The geometry of the spatial accessibility features placed on a 3D image is converted into two-dimensional coordinates, i.e., latitude and longitude (Saha et al., 2019).

3.1.1 Point Accessibility Features

The spatial accessibility feature categories available in Project Sidewalk and infra3D are *curb ramp*, *missing curb ramp*, *obstacle in path*, *surface problem*, *crosswalk*, *pedestrian signal*, *occlusion*, and *other*, represented as points in ZuriACT dataset.

The different data points were enriched with different attributes, referred to as tags. Additionally, the data points were attributed with a severity rating of the spatial accessibility feature from 1 *(fully passable)* to 5 *(not passable)* (Table 3.1), as well as the possibility to mark a problem as temporary, if it only exists for a limited amount of time (Saha et al., 2019).

Table 3.1: Severity rating used to describe the impact of an object on footpath accessibility (University of Zurich, 2024a)

Severity Rating	**Meaning**
1	Fully passable
2	Almost fully passable
3	Passable
4	Almost not passable
5	Not passable

Project Sidewalk provides spatially clustered data, where raw data points are already preprocessed and clustered into groups. This clustering process aggregates spatial accessibility features into a single data point, represented by the centroid location of all accessibility features assigned to one cluster. Based on their spatial proximity, the features are grouped by spatial accessibility feature category, e.g., *curb ramp* or *pedestrian signal* (Saha et al., 2019). While using preprocessed data may facilitate the direct implementation of Project Sidewalk data, the data did not fit the purpose of my thesis. At the time of this study, the Project Sidewalk API[1] did not only simplify the spatial accessibility data in terms of its geometry but also aggregated attributes, resulting in the loss of detailed information about single spatial accessibility features. Furthermore, data was validated using infra3D, additionally making the clustered data from the Project Sidewalk API not serviceable for this work. This thesis's clustering and aggregation approaches and their differences from the clustering method implemented by the Project Sidewalk API are described in more detail in Section 4.2.

The following sections describe the point spatial accessibility feature types collected within the ZuriACT project. Figure 3.2 depicts the spatial accessibility feature data points collected in District 1. Besides the characteristics described below, spatial accessibility features can contain further information, namely severity ratings, the information if an object is temporarily influencing footpath accessibility, and manually entered descriptions. All spatial accessibility feature categories contain the above-mentioned information (severity, duration of impact, description), except for the category *occlusion*. Figure 3.1 provides examples for each point accessibility feature category collected within the ZuriACT project. Spatial accessibility features are marked by the label point in the GSV image, where colours are chosen according to the colours used by the Project Sidewalk tool.

Curb Ramp

Short ramps that build up to a curb or cut through a curb are called *curb ramp* features (Figure 3.1a) in the spatial accessibility features dataset (University of Zurich, 2024b). Accessible curb ramps enable individuals with mobility restrictions to cross safely from footpaths to roads and vice versa (University of Washington, Makeability Lab, 2024b). Curb ramps are often present at both ends of crosswalks and pedestrian crossings without crosswalk markings (University of Zurich, 2024a). To enrich the collected curb ramps further, the following tags were available in the dataset (University of Zurich, 2024b): *narrow*, *missing tactile warning*, *steep*, *not enough landing space*, *not level with street*, *surface problem*, *debris/pooled water*, and *points into traffic*.

Missing Curb Ramp

At locations on curbs where ramps would be necessary to cross the street, *missing curb ramp* points (Figure 3.1b) were collected for the spatial accessibility features dataset (University of Zurich, 2024b). Missing curb ramp data points were only included if the curb is not lowered and pedestrians are allowed to cross a street. Tags available for the missing curb ramp feature were *alternate route present*, *no alternate route present*, and *unclear if needed* (University of Washington, Makeability Lab, 2024c).

Obstacle

Objects on footpaths, crosswalks, and pedestrian areas were collected as *obstacle in path* points (Figure 3.1c), *obstacle* here-on, and stored in the dataset on spatial accessibility features (University of Zurich, 2024b). However, objects on footpaths were only classified as *obstacle* when the remaining usable footpath width is less than 1.80 m (Schmidt & Manser, 2024; Schweizerischer Verband

[1] An application programming interface (API) builds on a standardised set of rules that enables different software systems to interact and share data or functionalities seamlessly (Goodwin, 2024). Project Sidewalk provides public access to footpath accessibility data via their API (Saha et al., 2019).

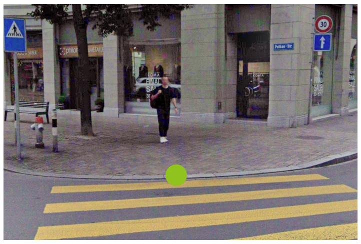

(a) *Curb ramp* feature

(b) *Missing curb ramp* features

(c) *Obstacle* feature

(d) *Surface problem* features

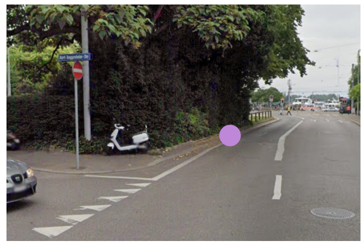

(e) *No sidewalk* feature

(f) *Crosswalk* feature

(g) *Pedestrian signal* feature

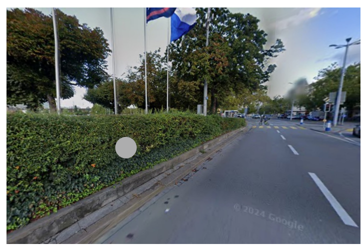

(h) *Occlusion* feature

(i) *Other* feature

Figure 3.1: Collected point spatial accessibility features (University of Washington, Makeability Lab, 2024c)

der Strassen- und Verkehrsfachleute VSS, 2014; University of Washington, Makeability Lab, 2024b). As obstacles can vary greatly, different tags were provided to further distinguish between obstacles: *trash/recycling can*, *litter/garbage*, *fire hydrant*, *pole*, *bollard*, *tree*, *vegetation*, *parked car*, *parked bike*, *parked scooter/motorcycle*, *construction*, *sign*, *garage entrance*, *stairs*, *height difference*, *narrow*, and *outdoor dining area* (University of Washington, Makeability Lab, 2024b).

Surface Problem

Features describing surface problems on footpaths are stored as *surface problem* features (Figure 3.1d) in the spatial accessibility features dataset (University of Zurich, 2024b). These surface problems cause an uncomfortable experience for a mobility-impaired person, up to the point that that person cannot cross the area. Tags available for surface problems are *bumpy*, *uneven/slanted*, *cracks*, *grass*, *narrow*, *brick/cobblestone*, *construction*, *very broken*, *height difference*, *rail/tram track*, *sand/gravel*, *utility panel*, and *debris* (University of Washington, Makeability Lab, 2024c).

No Sidewalk

To indicate missing footpaths along streets, *no sidewalk* points (Figure 3.1e) are contained in the spatial accessibility features dataset (University of Zurich, 2024b). These points can also indicate areas shared by pedestrians and cars, as well as footpaths that end abruptly (University of Washington, Makeability

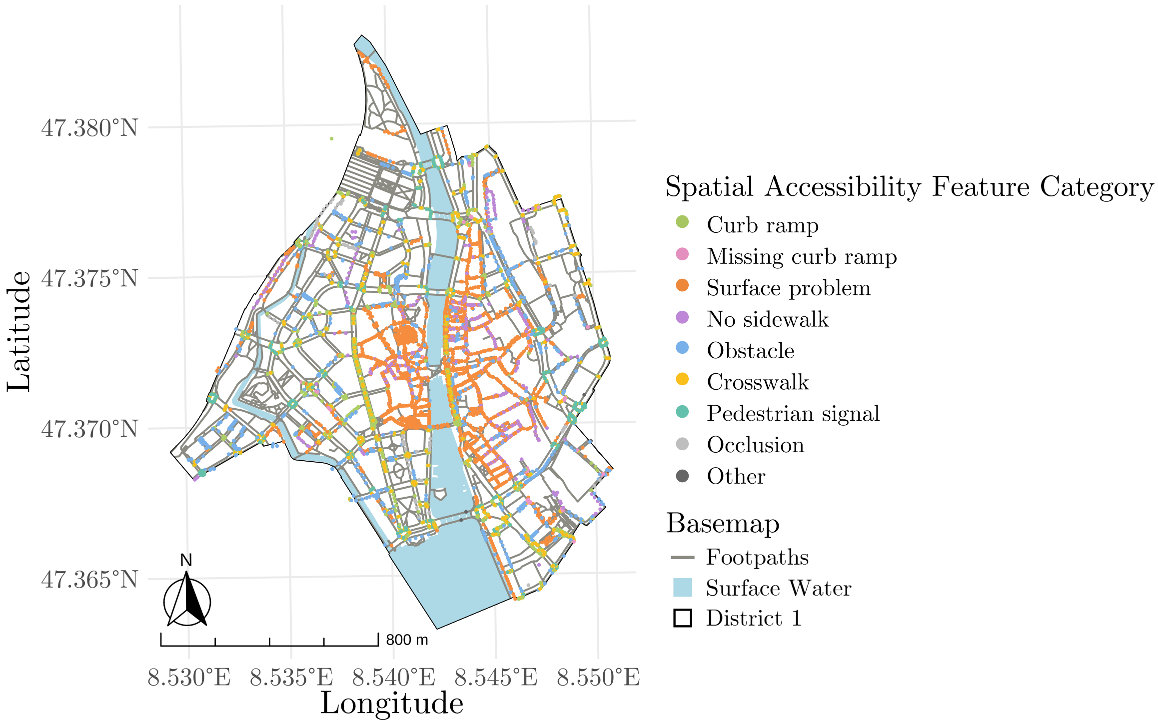

Figure 3.2: Spatial accessibility features

Lab, 2024b; University of Zurich, 2024a). Further description is provided by the tags *ends abruptly*, *gravel/dirt road*, *shared pedestrian/car space*, *pedestrian lane marking*, *street has a sidewalk*, and *street has no sidewalks* (University of Washington, Makeability Lab, 2024c).

Crosswalk

The spatial accessibility features dataset contains the locations of crosswalks as *crosswalk* points (Figure 3.1f) (University of Zurich, 2024b). Crosswalks are legally defined areas to cross streets (University of Zurich, 2024a). Pedestrian crossings without crosswalk marks are not contained in the dataset. Additional information on the crosswalk points in the dataset is provided by the tags *paint fading*, *broken surface*, *uneven surface*, *brick/cobblestone*, *bumpy*, *rail/tram track*, *no pedestrian priority*, *covered walkway* and *very long crossing* (University of Washington, Makeability Lab, 2024b).

Pedestrian Signal

Signals at intersections for pedestrians are also contained in the spatial accessibility features dataset and named *pedestrian signal* (Figure 3.1g) (University of Zurich, 2024b). Pedestrian signals provide a safer way for pedestrians to cross the street. The following tags are included to describe the signal types: *has button* and *button waist height* (University of Washington, Makeability Lab, 2024c; University of Zurich, 2024b).

Occlusion

The dataset contains points marking locations where footpaths cannot be seen, called *occlusion* (Figure 3.1h). Reasons for footpaths not being seen can be various, including objects like cars or vegetation blocking the view and pixelated or blurry images (University of Zurich, 2024a).

Other

As the provided categories might not cover all footpath-relevant accessibility features, *other* points (Figure 3.1i) are available. Two tags, *missing crosswalk* and *no bus stop access*, are provided for *other* features.

3.1.2 Linear Accessibility Features

In addition to the point accessibility feature categories, the three linear features *vertical slope* (Figure 3.3a), *cross slope* (Figure 3.3b), and *width* (Figure 3.3c) are available for linear footpath measurements in infra3D (Figure 3.3) (iNovitas AG, 2024). However, linear features are not employed in this thesis. The decision to exclude the available linear spatial accessibility features is based on the considerable amount of work and time required to preprocess and analyse the dataset, which exceeds the limited time frame of this thesis. Utilising this data would necessitate extensive preprocessing, including interpolation and other adjustments, to ensure its suitability for the intended purpose. Nonetheless, it is assumed that the dataset possesses significant value and potential for future research on footpath accessibility in the City of Zurich.

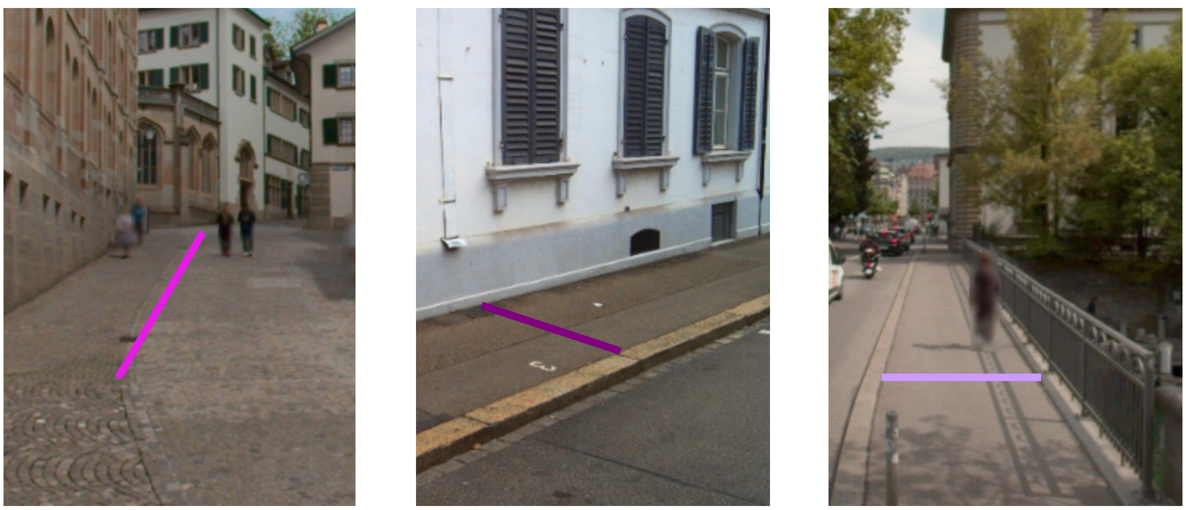

(a) *Vertical slope* feature (b) *Cross slope* feature (c) *Width* feature

Figure 3.3: Collected point spatial accessibility features (iNovitas AG, 2024)

3.2 Surveying Data

3.2.1 Footpath Network

The footpath network used for network enrichment and routing was constructed from the City of Zurich's footpath and cycling network dataset (Stadt Zürich, 2024b). It contains all footpaths and cycling paths in the City of Zurich. The dataset consists of vector LineString data and is provided in the CH1903+/LV95 reference system. The data is regularly updated, with the last update being on 19 October 2022. The dataset includes information such as the road name, whether a cycling path or footpath is present, if there is an extra line for cyclists, or if the cycling path is a one-way street (Stadt Zürich, 2024b).

3.2.2 Districts

District boundaries were used to extract data by location, specifically to remove data not situated in District 1. Consequently, the City of Zurich's district boundaries were employed (Stadt Zürich, 2024c). For the analysis, the most recent version of the district dataset was utilised, which was last updated on 2 October 2023. The dataset consists of polygons representing the city districts and is reported in the CH1903+/LV95 reference system. Additional attributes include the district name and district number (Stadt Zürich, 2024c).

3.2.3 Crosswalk Data

The City of Zurich owns a dataset regarding the location of crosswalks that is not publicly available (Stadt Zürich, 2021a). However, the City provided this data for use within the ZuriACT project. The dataset was last updated in 2021. The dataset is reported as points in the reference system CH1903+/LV95 and contains an identifier used within the administration along with the name of the street being crossed (Stadt Zürich, 2021a).

This dataset was used to supplement the crosswalk data from the ZuriACT project. While the crosswalk data provided by the City of Zurich includes locations not covered by SVI in the Project Sidewalk or the infra3D tool, the ZuriACT dataset offers more comprehensive information. For instance, it contains details about accessibility issues, such as paint fading or lengthy crossings, along with severity ratings that are absent in the City of Zurich's dataset. Furthermore, the ZuriACT crosswalks were gathered using SVI from 2022, rendering them more current than the data supplied by the City of Zurich (Stadt Zürich, 2021a; University of Zurich, 2024b).

3.2.4 Stairs and Height Differences

Data on stairs is based on official surveying data from the City of Zurich and extracted from that dataset (Stadt Zürich, 2024a). However, this led to a dataset that not only contained stairs on footpaths but also stairs leading up to churches and other buildings, as those stairs were all marked as *important* (Stadt Zürich, 2024a). Further preprocessing was necessary to extract only stairs relevant to footpath accessibility, further described in Section 4.1.2.

The stairs data was reported as polygons in the CH1903+/LV95 reference system (Stadt Zürich, 2024a). Similar to the City of Zurich's crosswalk dataset, the stairs dataset retrieved from the official surveying data complements the information on stairs and height differences gathered by the ZuriACT project. Including this data source is particularly important since car-mounted SVI cannot capture data on stairs, which are inherently inaccessible to cars.

3.2.5 Public Transport Tracks

To address surface unevenness caused by rail and tram tracks, the dataset from Kanton Zürich (2024a) on public transport lines in the Canton of Zurich is used. The dataset collected within the ZuriACT project provides spatial accessibility features, namely *crosswalk* and *surface problem*, which indicate the locations of rail and tram tracks. To complete the ZuriACT data, the Canton's public transport lines dataset is used. This dataset contains different data, such as the rail, bus, and tram lines reported in the CH1903+/LV95 reference system. For the purpose of this thesis, only tram lines were of interest as bus lines do not require tracks and rail lines in District 1 run underground, making it impossible for pedestrians to cross them legally (Kanton Zürich, 2024a). In addition to the geometry, the combined dataset of bus and tram lines includes details about the line itself, such as its name and number, a line key, and the direction of the vehicles on the line. To differentiate between bus and tram lines, the field detailing the means of transport is included (Kanton Zürich, 2024a).

3.3 Federal Data

3.3.1 Digital Elevation Model

For reasons explained in Section 3.1.2, no data from ZuriACT was used on vertical slopes, i.e., inclines, in this Master's thesis. Nonetheless, the influence of incline on spatial accessibility has been documented previously (Beale et al., 2006; Rahaman et al., 2017). For instance, Rahaman et al. (2017) identified the gradient of a route as the most influential factor affecting route accessibility in their routing approach. Consequently, I chose to take into account the incline of footpath segments by employing a digital elevation model (DEM) provided by the Federal Office of Topography swisstopo (Bundesamt für Landestopographie swisstopo, 2024), following the method introduced by Pude (2022). The dataset used offered a high spatial resolution of 0.5 m and was reported in the reference system CH1903+/LV95.

3.3.2 Population Raster

To create meaningful routes, it was necessary to establish appropriate origin and destination locations. Origin points were sourced from the Federal Statistical Office's population dataset to reflect the population's home residences Bundesamt für Statistik BFS (2023). Destinations were determined by extracting Points of Interest (POIs) from OSM, as outlined in Section 3.4.2.

To ensure privacy protection, the population dataset provided aggregated population information from the year 2022, represented on a 100 m x 100 m raster and recorded in the CH1903+/LV95 reference system. The dataset included comprehensive demographic details per raster cell, such as total population figures, the number of individuals across various age groups, the number of persons residing in households, as well as information on citizenship and birthplace (Bundesamt für Statistik BFS, 2023). For the purposes of this thesis, the total population per raster cell was the primary variable of interest.

3.4 OpenStreetMap Data

3.4.1 Characteristics of OpenStreetMap

OpenStreetMap (OSM) (www.openstreetmap.org) is a platform established in 2004 that relies solely on contributions of volunteers, a concept known as Volunteered Geographic Information (VGI) (Mooney & Minghini, 2017; OpenStreetMap contributors, 2025). The foundation of VGI lies in the evolution of internet technology. Early internet technologies, often referred to as the static web, were characterised by a one-way content consumption, where users could only view information. In contrast, past advancements introduced interactive platforms that enable individuals to create, share, and edit content through blogs and wikis, commonly known as *Web 2.0*. This shift to user-generated content is fundamental to VGI and, therefore, OSM, facilitating collaborative contributions, exchanges, and edits of spatial data (Goodchild, 2007; Mooney & Minghini, 2017; Roche et al., 2013). Such voluntary or involuntary contributions from citizens have become a viable source of data (Jokar Arsanjani et al., 2015).

With its crowdsourced spatial database, OSM is a prime example of VGI on the internet. Anyone can register as a contributor and supply data to the spatial database (Mooney & Minghini, 2017). This database has become an essential basis for various software systems, applications, tools, and web-based information stores such as wikis (Foody et al., 2017). Correspondingly, the previously introduced routing services OSRM (Section 2.2.1) and ORS (Section 2.2.2) use OSM data as input for their routing algorithms. Furthermore, OSM data has become a valuable data source in research (Foody et al., 2017).

Under the OpenStreetMap licence, access to the database and maps is (almost) free, making it a practical data source (OpenStreetMap Wiki, 2024a). The focus of OSM does not lie on outputs like cartographic outputs or maps but on creating a spatial database containing global cartographic data and information (Mooney & Minghini, 2017). The OSM data model consists of three different types: nodes, ways and relations. Spatial points are represented by nodes with coordinates, usually as latitude and longitude. For polylines, at least two nodes are necessary to create a way. Similarly, a minimum of three nodes are required for a polygon. Relations are logical collections of nodes and ways. OSM requires at least one attribute or tag, named a key/value pair, for each object to characterise the object (Foody et al., 2017). Data contributors can create their own tags, which sometimes leads to confusion and disagreement about the proper use of specific tags. To avoid this, the OSM Map Features pages on the OSM Wiki describe the officially adopted OSM tags (Foody et al., 2017; OpenStreetMap Wiki, 2024c). Wiki pages describe agreed-upon standards and typical application of the tags, promoting consistency within the platform (Foody et al., 2017; Mooney & Minghini, 2017).

Drawing upon the value of the spatial database provided by OSM contributors, this Master's thesis used OSM data to create meaningful routes.

3.4.2 Points of Interest

In conjunction with the origin locations derived from population data, OSM data points served as destination locations. As routes started at population points, reflecting the residences of the population, destinations comprised various points of interest (POIs) from multiple categories (OpenStreetMap contributors, 2024). Table 3.2 displays the tags employed to extract different POIs across several categories within the City of Zurich as spatial points. Categories were created for the purpose of this Master's thesis. Descriptions are based on the explanations provided in the OSM Wiki (OpenStreetMap Wiki, 2024c).

Table 3.2: Extracted POIs from OSM (OpenStreetMap contributors, 2024; OpenStreetMap Wiki, 2024c)

Category	**OSM Tag**	**Description**
Healthcare services	amenity: clinic	Medical centre with more staff than a doctor's office
	amenity: dentist	Place with professional dental surgeon
	amenity: doctors	Place to get medical attention or check up on a physician
	amenity: hospital	Health care institution providing treatment by specialists
	amenity: pharmacy	Shop where pharmacists sell medications
Groceries	amenity: marketplace	Public marketplace where goods and services are traded daily/weekly
	shop: supermarket	Shop for groceries and other goods

Continued on the next page

Category	OSM Tag	Description
Financial and administrative services	amenity: bank	Financial institution where customers can deposit and withdraw money, take loans, invest, and transfer funds
	amenity: post office	Institution that offers services such as sending/collecting letters/parcels or sale of stamps
	amenity: townhall	Often the seat of mayor or a community meeting place
Education	amenity: college	Post-secondary education institution
	amenity: language school	Educational institution to study foreign languages
	amenity: library	Collection of information and services, housed and maintained by a public body, institution, or individual
	amenity: music school	Educational institution specialised in the study, training, and research of music
	amenity: university	Institution for of higher education
Leisure, sports, and entertainment	amenity: bbq	Permanently built place for having a barbecue (BBQ) or grill
	amenity: cinema	Place showing movies, open to the public for a fee
	amenity: community centre	Public locations where members of a community gather for group activities, informal/formal meetings, public information, or events
	leisure: park	Area of open space for recreational use in semi-natural state
	amenity: place of worship	Place of worship, independent of religions or denominations
	amenity: public bath	Location where public bathe together and structures of human-made structures are present
	leisure: sports centre	Facility where sports take place within a enclosed area
	leisure: stadium	Major sports facility with substantial tiered seating

Continued on the next page

Category	OSM Tag	Description
Leisure, sports, and entertainment	amenity: theatre	Location where live performances occur, such as plays, musicals or formal concerts
	tourism: zoo	Place with confined animals on display for public viewing
Food and drinks	amenity: bar	Commercial establishment that sells alcoholic drinks to be consumed on the premises
	amenity: biergarten	Open-air area with benches where beer and other beverages are served
	amenity: cafe	Informal place with sit-down facilities selling beverages and light meals and/or snacks
	amenity: fast food	Place concentrating on very fast counter-only service and take-away food
	amenity: pub	Establishment that sells alcoholic drinks to be consumed on the premises, characterised by traditional appearance
	amenity: restaurant	Formal eating places with sit-down facilities selling full meals served by waiters/waitresses, often licensed to sell alcoholic drinks

Using the tags to download POIs from OSM resulted in a dataset containing 3'205 POIs on 24 October 2024 (Figure 3.4).

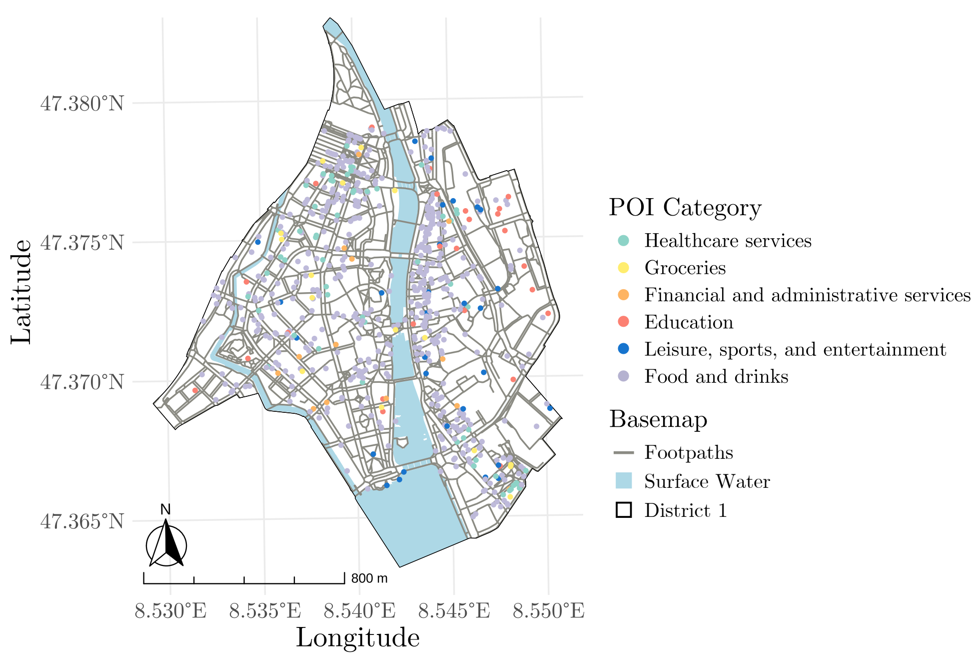

Figure 3.4: POIs extracted from OSM (OpenStreetMap contributors, 2024)

4 Methodology

Using official data as well as crowd-sourced spatial features to add accessibility information to the footpaths of Zurich's District 1 required several preprocessing steps. The steps ultimately served the goal of applying a routing algorithm to the footpath network, namely, Dijkstra's Shortest Path algorithm to the network. The single steps conducted throughout the analysis are displayed in the graph in Figure 4.1. The analysis was conducted using the Software R, version *4.4.0*.

Figure 4.1: Methodology and procedural steps of the analysis

4.1 Data Validation and Preprocessing

Crowd-sourced data hold great potential to enhance the collection of detailed spatial accessibility features, such as relevant information on footpaths (Allahbakhshi, 2023). However, data gathered by citizens necessitates rigorous validation to ensure that the information provided on accessibility mirrors real-world conditions (Wiggins et al., 2011).

4.1.1 Spatial Accessibility Features Validation

As non-experts gathered spatial accessibility data, validating this data was crucial to ensure consistency throughout and confirm that the collected features indeed affected footpath accessibility (Allahbakhshi & Ardüser, 2024). Data validation was conducted as part of the ZuriACT project and this Master's thesis. Five research assistants, including myself, were trained to validate the spatial accessibility features, with each feature reviewed by at least two assistants (Allahbakhshi & Ardüser, 2024).

The validation of the spatial accessibility features in infra3D was conducted by rating the agreement of a collected feature as *agree* for features that were accurately collected, *disagree* for incorrect features, and *not sure* for inconclusive features (Allahbakhshi & Ardüser, 2024; iNovitas AG, 2024; Saha et al., 2019).

For this Master's thesis, spatial accessibility features were filtered by the second validation, which was deemed the agreed-upon validation. This means that the only features included in the further analysis were those where the second validation was *agree*. As the focus of this thesis lies in enriching footpath networks and applying routing services, no additional investigation into the agreement levels of research assistants during validation or similar analyses was performed.

Through data validation, I commonly corrected the following three issues, which could potentially lead to erroneous effects on the routing outcomes:

- Object on footpaths were marked as *obstacles* even though they were not obstructing footpaths, meaning that they did not impact footpath accessibility. Including such objects in the footpath network would lead to erroneous routing results.
- Temporary objects were sometimes not marked as such, meaning that they did not provide the information that the object was only temporarily obstructing the footpath. Examples are construction sites and parked vehicles. Correcting this attribute was required in order to clearly distinguish between temporary and permanent obstacles, which were later used for different routing scenarios.
- In some cases, data points were placed on features not located on footpaths, such as entrance stairs to private buildings. Despite the significance of such accessibility-relevant information, these data points can be incorrectly assigned to the footpath network, leading to inaccurate accessibility assessments and adversely affecting routing results

During the data validation process, missing spatial accessibility features were identified that had either been overlooked or could not be collected due to limited GSV coverage. This led to a final count of 8'909 spatial accessibility features exported from infra3D. After excluding incorrectly collected data points based on the validation process, 8'498 features remained, which were ultimately used in the analysis.

4.1.2 Spatial Accessibility Features Preprocessing

To create a clean dataset, the label data underwent extensive preprocessing in the R. Since the point data downloaded from infra3D consists of individual datasets, one for each spatial accessibility feature type, these datasets are merged into a single dataset containing all data points.

Due to inconsistencies in the data structure between the features previously collected using Project Sidewalk and the data acquired through infra3D, some preprocessing steps were necessary. For instance, obstacles in Project Sidewalk were referred to as *obstacle*, whereas those in infra3D were termed *obstacle**s***. These inconsistent terms generated two distinct spatial accessibility feature datasets that described the same accessibility category. To resolve this, all obstacles created in infra3D were renamed to *obstacle*. Moreover, all datasets were reprojected into the CH1903+/LV95 reference system to ensure consistency. Next, I filtered spatial accessibility features based on the second validation in infra3D, which meant that only data points with a second validation value of *agree* were considered.

Following these steps, the dataset was divided into two subsets to provide a clearer overview. The first subset included all attributes relevant to accessibility, such as the spatial accessibility feature type, the severity of the feature, and the tags assigned to each feature. The second subset comprised the attributes related to the data validation process, including details on who validated a data point and how the label was validated (e.g., *agree*, *disagree*, *not sure*).

Revision of Spatial Accessibility Feature Types

Following data preprocessing, the spatial accessibility feature categories were revised, leading to the generation of additional categories derived from the original dataset: *curb ramp*, *missing curb ramp*, *obstacle*, *surface problem*, *no sidewalk*, *crosswalk*, *pedestrian signal*, *occlusion*, and *other*, which are introduced in Section 3.1.1. Table 4.1 summarises the modifications made to these features. The categories *curb ramp*, *missing curb ramp*, and *pedestrian signal* remained unchanged, as their tags primarily served to provide further descriptions of these categories, not allowing for meaningful subdivision.

In contrast, the *obstacle* category was subdivided into new, more specific categories: *construction*, *parked motorcycle/bike*, *parked car*, and *height difference*. This subdivision was made since the various obstacle types have distinct implications for accessibility. For instance, obstacles such as vegetation or poles might be passable for wheelchair users, while height differences, such as steps or stairs, present significant barriers (Georgescu et al., 2024). Construction sites and parked vehicles were further identified as specific types of obstacles. I decided to differentiate between parked cars and parked motorcycles and bikes due to their differing sizes, which results in varying impacts based on the space they occupy. Some features, however, were not reassigned and remained within the broader *obstacle* category.

The original *surface problem* category was divided into two distinct categories. Features with tags describing the surface material were reassigned to the newly created *surface material type* category. *Surface problem* features with tags indicating issues on footpath surfaces, such as cracks or very broken surfaces, remained in the *surface problem* category. Some tags were used across various spatial accessibility feature categories, requiring the consolidation of overlapping features into single categories. For instance, the *construction* tag appeared in both the *obstacle* and *surface problem* categories, leading to redundancy. All features with the *construction* tag were consolidated into the *construction* category to rectify this. The same applies to the *height difference* tag from the *obstacle* category, the *rail/tram track* tag from the *crosswalk* category, and the *narrow* tag also present in the *obstacle* category. Additionally, features initially categorised as *surface problems* and tagged with *utility panel* were reassigned to the *obstacle* category. A manual inspection revealed that these features were not issues on surfaces but rather large obstacles obstructing the footpath.

Features from the *no sidewalk* category, tagged for shared use by both pedestrians and vehicles, were reassigned to the newly established *shared space* category. Meanwhile, *no sidewalk* features with alternative tags remained classified under *no sidewalk*.

The *crosswalk* features were reassigned to different categories, except for those tagged with *no pedestrian priority*, *paint fading*, and *very long crossing*. *Crosswalk* features marked with the tag *brick/cobblestone* were recategorised into the *surface material type* category, which was created from various surface material types derived from the original *surface problem* tags. As a result, *crosswalk* features with tags denoting *broken surface*, *uneven surface*, and *bumpy*, all indicating surface issues, were placed into the *surface problem* category.

Since the *occlusion* category allowed marking areas where the view of the footpath was obstructed, the locations of these labels indicate areas of uncertainty, meaning that spatial accessibility feature collection was not possible there. While this information is vital for potential supplementary in-situ data collection, it did not provide direct information on footpath accessibility. Instead, it introduced a sort of "accessibility uncertainty", which is, without a doubt, a relevant component but not considered in this Master's thesis. Therefore, the *occlusion* category and its data were discarded.

As the manual inspection of the remaining *other* features did not provide any additional accessibility-relevant information, I removed these features and, therefore, the *other* category.

The revision of the spatial accessibility feature categories increased the number of features from 8'498 to 8'935.

Table 4.1: Spatial accessibility features: original and revised categories

Original Spatial Accessibility Feature Category	**Tag**	**New Spatial Accessibility Feature Category**
Curb ramp	Missing tactile warning	Curb ramp

Continued on the next page

Original Spatial Accessibility Feature Category	**Tag**	**New Spatial Accessibility Feature Category**
Curb ramp	Narrow	Curb ramp
	Not enough landing space	Curb ramp
	Not level with street	Curb ramp
	Points into traffic	Curb ramp
	Debris/pooled water	Curb ramp
	Steep	Curb ramp
	Surface problem	Curb ramp
Missing curb ramp	Alternate route present	Missing curb ramp
	No alternate route	Missing curb ramp
	Unclear if needed	Missing curb ramp
Obstacle	Construction	Construction*
	Fire hydrant	Obstacle
	Litter/garbage	Obstacle
	Trash/recycling can	Obstacle
	Narrow	Obstacle
	Outdoor dining area	Obstacle
	Parked bike	Parked motorcycle/bike*
	Parked car	Parked car*
	Parked scooter/motorcycle	Parked motorcycle/bike*
	Pole	Obstacle
	Bollard	Obstacle
	Sign	Obstacle
	Stairs	Height difference*
	Height difference	Height difference*
	Garage entrance	Obstacle
	Tree	Obstacle
	Vegetation	Obstacle
Surface problem	Brick/cobblestone	Surface material type*
	Bumpy	Surface problem
	Very broken	Surface problem

Continued on the next page

Original Spatial Accessibility Feature Category	**Tag**	**New Spatial Accessibility Feature Category**
Surface problem	Uneven/slanted	Surface problem
	Cracks	Surface problem
	Grass	Surface material type*
	Debris	Surface material type*
	Sand/gravel	Surface material type*
	Height difference	Height difference*
	Construction	Construction*
	Narrow	Obstacle**
	Rail/tram track	Rail/tram track*
	Utility panel	Obstacle**
No sidewalk	Ends abruptly	No sidewalk
	Gravel/dirt road	Shared space*
	Covered walkway	No sidewalk
	Pedestrian lane marking	Shared space*
	Shared pedestrian/car space	Shared space*
	Street has a sidewalk	No sidewalk
	Street has no sidewalks	No sidewalk
Crosswalk	Brick/cobblestone	Surface material type*
	Broken surface	Surface problem**
	Uneven surface	Surface problem**
	Bumpy	Surface problem**
	No pedestrian priority	Crosswalk
	Paint fading	Crosswalk
	Rail/tram track	Rail/tram track*
	Very long crossing	Crosswalk
Pedestrian signal	Button waist height	Pedestrian signal
	Has button	Pedestrian signal
	Hard to reach button	Pedestrian signal
	Tactile-audible buttons	Pedestrian signal
	One button	Pedestrian signal

Continued on the next page

Original Spatial Accessibility Feature Category	**Tag**	**New Spatial Accessibility Feature Category**
Pedestrian signal	Two buttons	Pedestrian signal
Occlusion		*Manual inspection*
Other	Missing crosswalk	*Manual inspection*
	No bus stop access	*Manual inspection*

* Newly created spatial accessibility feature category

** Reassigned to another spatial accessibility feature category

Attribute Revision

Temporary Spatial Accessibility Features

Despite extensive data validation, inconsistent data might still persist in the spatial accessibility features dataset. To address a potential source of such inconsistencies, temporary features were explicitly marked. Since the spatial accessibility features already contained the information on whether a feature was temporarily or permanently affecting footpath accessibility (field *temporary* with possible values *TRUE* for temporary and *FALSE* for permanent features), the value of this field could be modified. By ensuring that the *temporary* field was set to *TRUE*, features that were inherently temporary in nature were indicated as such. The spatial accessibility features from the categories *construction*, *parked car*, and *parked motorcycle/bike* were affected by these actions.

This approach was not applied to all feature categories that might temporarily impact footpath accessibility, as some features were not inherently temporary, such as signs from the *obstacle* category. In these instances, I relied on data collection and validation.

Pedestrian Signal Severity

Since the spatial accessibility feature *pedestrian signal* is not rated for severity in either Project Sidewalk or infra3D (iNovitas AG, 2024; University of Washington, Makeability Lab, 2024c), a manual severity assignment process was necessary. The severity rating was determined based on the tags associated with each pedestrian signal. Signals that had both the *has button* and *button waist height* tags were assigned a severity rating of 1. In instances where no tags were assigned to a pedestrian signal, a default severity rating of 2 was applied. Given that the dataset consistently included either both tags, *has button* and *button waist height*, or neither for each pedestrian signal, no further severity estimation was required.

Spatial Accessibility Feature Enrichment with Alternative Data Sources

Alternative data sources were integrated to address gaps in the spatial accessibility features dataset collected within the ZuriACT project. These included the City of Zurich's stairs and unofficial crosswalk data, as well as the Canton of Zurich's public transport line data. These datasets aimed to enrich the ZuriACT dataset, particularly in areas where SVI coverage is limited and, therefore, data is lacking. Furthermore, such official and validated information served as an excellent data source for this thesis. Nevertheless, utilising ZuriACT data offered unique advantages, such as severity ratings for spatial accessibility features and information on whether their impact on accessibility is temporary or permanent. Preprocessing steps were necessary to merge the Canton and City datasets with the ZuriACT dataset. In particular, the geometries of the alternative datasets were converted to points to ensure compatibility with the ZuriACT dataset. The following sections detail the preprocessing steps undertaken for each dataset. The enrichment with alternative data sources led to a total of 13'850 individual spatial accessibility features.

Crosswalks

As introduced in Section 3.2.3, the *crosswalk* features were enriched with an official crosswalk dataset that is not publicly available, provided by the City of Zurich (Stadt Zürich, 2021a). Using this dataset enabled me to address gaps resulting from the limited SVI coverage. Given that the ZuriACT dataset is more extensive, the City's crosswalk dataset underwent several preprocessing steps. To adapt the City's crosswalks to the ZuriACT *crosswalk* features, all attributes from the City's dataset were removed, except for the point locations of the crosswalks. These simplified crosswalks were subsequently merged with the ZuriACT dataset. Since the City of Zurich's dataset was not attributed with tags or information regarding whether they are permanent or temporary features, those values were manually adjusted to align with the ZuriACT dataset. The crosswalks' *temporary* attribute was set to *FALSE*, thereby assuming that they existed indefinitely. As there were no additional tags or severity ratings available, these attributes remained unadjusted and were, therefore, left blank.

Height Difference

Next, the City of Zurich's stairs dataset was merged with the *height difference* features. As the official stairs dataset consists of polygons representing "important stairs", meaning that stairs not located on footpaths were present in the dataset, only relevant stairs were extracted. I used the *st_intersects* function from the *sf* package to identify which stairs polygons overlapped with footpath segments (Pebesma, 2016). After extracting the identified stairs polygons, the centroid (using the function *st_centroid* from the *sf* package) of each polygon was calculated to create point geometries, aligning with the geometry of the ZuriACT data. Following these steps, the stairs dataset was merged with the ZuriACT *height difference* features. The severity rating for stairs was set to the highest possible severity level, 5, as stairs represent a significant barrier for mobility-impaired individuals (Georgescu et al., 2024). Furthermore, stairs were assumed to be a permanent barrier, meaning that the *temporary* attribute was set to *FALSE*.

Rail and Tram Tracks

A public transport line dataset from the Canton of Zurich was utilised to account for uneven surfaces caused by rail and tram tracks. Since the dataset included line geometries for various modes of transport, I extracted the tram lines in District 1. These lines were then split into smaller segments of 10 m using the function *line_segment* from the *stplanr* package (Lovelace & Ellison, 2019). From these segments, centroids were generated with the *st_centroid* function to convert the line geometries into point geometry, compatible with the ZuriACT data geometry. These processes produced points along the tram tracks at regular 10 m intervals. The point data was subsequently merged with the ZuriACT *rail/tram track* features. In line with the assumptions made for the additional stairs and crosswalk datasets, the tram tracks were deemed permanent by setting the *temporary* attribute to *FALSE*. Moreover, an increased severity of 2 was assumed, as the presence of these features adds unevenness to surfaces.

4.2 Clustering and Aggregation

Following the described data preprocessing, the spatial accessibility features were clustered into groups and subsequently aggregated. These two steps were essential in creating meaningful clusters of spatial accessibility features representing real-world footpath features. Due to the remote data collection, the possibility existed that one feature could be marked from different perspectives (various panoramas) by either the same individual or different individuals. This resulted in multiple data points potentially describing the same spatial accessibility feature (Saha et al., 2019). Therefore, spatial accessibility features were organised into clusters and then aggregated to yield a singular data point for each spatial accessibility feature (Saha et al., 2019).

Figure 4.2 illustrates the essential steps involved in the clustering and aggregation process. The clustering phase included the formulation of distance matrices for each spatial accessibility category, followed by the implementation of a clustering algorithm on these matrices. By employing category-dependent distance thresholds, spatial accessibility features were organised into clusters. New geometries were generated for each cluster, representing the midpoint of each grouping. All spatial accessibility features allocated to a given cluster were then consolidated into this newly created midpoint. The methods and tools utilised during these processes are explained in greater detail in the following sections.

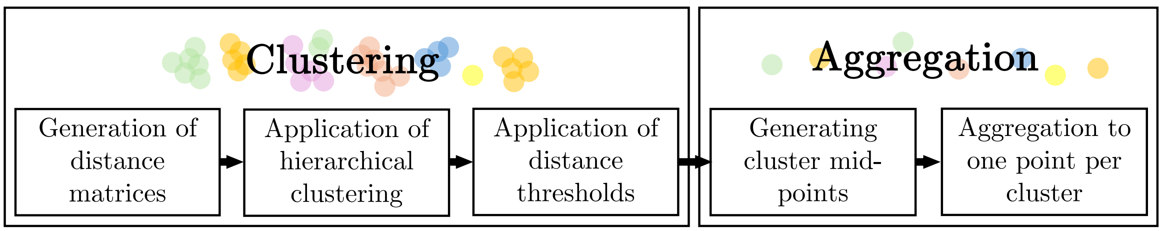

Figure 4.2: Schematic representation of the clustering and aggregation steps

4.2.1 Clustering

To group spatial accessibility features by category, a hierarchical clustering approach was employed, similar to the method used by Saha et al. (2019). The ZuriACT dataset was first divided into subsets based on categories of spatial accessibility features. A pairwise distance matrix for each subset was calculated using the *distm* function from the *geosphere* package (Hijmans et al., 2024), determining the distance between each spatial accessibility feature. The resulting distance matrices were then input into the *hclust* function from the *stats* package (Murtagh, 2024) to perform hierarchical clustering. Initially, each object, i.e., a spatial accessibility feature, was treated as its own cluster. The algorithm then iteratively merged the two most similar clusters at each step, continuing until all objects were combined into a single cluster (Murtagh, 2024). The clustering method *complete* was applied, which uses the maximum distance between points in different clusters to determine similarity. This method is particularly effective for identifying well-separated clusters (Geetha, 2022; Murtagh, 2024). In contrast to the two-step hierarchical clustering algorithm implemented by Saha et al. (2019), which clustered the spatial accessibility feature points first per user and then generally, I did not consider user information to create clusters.

The clustering algorithm was executed for each spatial accessibility feature dataset, resulting in a dendrogram. By applying specific distance thresholds, as described in the following section, these dendrograms were segmented to produce distinct clusters. Figure 4.3 displays the dendrogram for the *no sidewalk* feature, generated by the *hclust* function. The x-axis represents individual spatial accessibility feature points, specifically each *no sidewalk* point collected. The logarithmic y-axis indicates the distance between the individual features. The figure illustrates the application of the *hclust* algorithm, starting with each individual point as a cluster and ending at all points belonging to one cluster. The dashed line displays the distance threshold at which the dendrogram is cut, meaning that all feature points located within a distance lower than the threshold belong to a cluster, whereas features located further away are not assigned to a cluster but instead form a separate cluster.

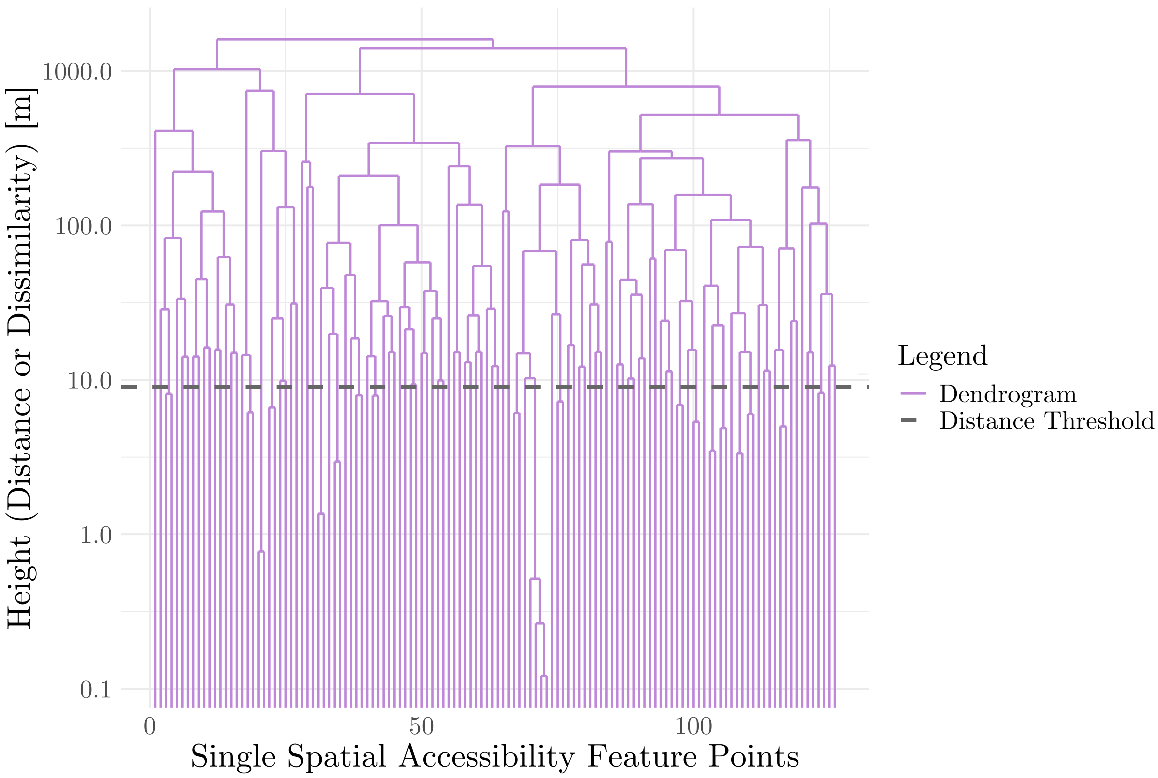

Figure 4.3: Resulting dendrogram of the spatial accessibility feature *no sidewalk*, after the application of the *hclust* function

Distance Thresholds

Distance thresholds were determined to define at which distances spatial accessibility feature points would be considered part of the same cluster or remain as individual clusters. Thus, defining thresholds for each spatial accessibility feature category was crucial. The initial values were based on the clustering approach introduced by Saha et al. (2019), who empirically determined thresholds by iteratively computing clusters at varying distance thresholds ranging from 0 to 50 m. Ultimately, they applied 2 m for *curb ramp* features and 7.5 m for the other feature categories. I selected my threshold values based on the intended length of my segments, beginning with 10 m. The thresholds were then reduced by 1 m per iteration. For feature categories that are naturally located close together, such as two *pedestrian signals* for different directions at an intersection, lower distance thresholds were chosen. The results were evaluated visually, and adjustments were made throughout the network enrichment process. I found that the values ultimately applied, summarised in Table 4.2, represent a good balance between preserving data granularity and minimising information loss.

Table 4.2: Distance thresholds per spatial accessibility feature category, applied for clustering

Spatial Accessibility Feature Category	**Distance Threshold**
Curb ramp	6 m
Missing curb ramp	6 m

Continued on the next page

Spatial Accessibility Feature Category	Distance Threshold
Surface problem	9 m
Surface material type	9 m
No sidewalk	9 m
Obstacle	9 m
Construction	9 m
Height difference	9 m
Parked car	9 m
Parked motorcycle/bike	9 m
Rail/tram track	8 m
Shared space	9 m
Crosswalk	9 m
Pedestrian signal	2 m

4.2.2 Aggregation

Following the clustering process, features assigned to the same cluster were aggregated into a single data point. The approach applied here was built on the methodology introduced by Saha et al. (2019), which was designed for clustering and aggregating Project Sidewalk data available via the API (University of Washington, Makeability Lab, 2024a). However, their aggregation strategy resulted in the loss of accessibility-relevant information, such as tags assigned to the features. Moreover, their aggregation method did not account for the individual who collected the data. Since this information may hold great potential for various applications using spatial accessibility information, such as personalised routing, it is crucial to consider personal perceptions. While this work generalised accessibility-relevant data for a broader group of mobility-impaired individuals, user information, namely anonymised ZuriACT participant information, was retained throughout the data aggregation, which is beneficial for potential future applications.

Data aggregation per cluster was performed using the *summarise* function from the *dplyr* package (Wickham et al., 2024). This function generates one entry for each value of a grouping variable, making it suitable for aggregating clustered data. For each category of spatial accessibility feature, I combined every cluster into a single data point. The description below provides information regarding the calculations for the new attributes found in the clustered and aggregated data:

- **Location:** The new single point location for all feature points assigned to a cluster is determined by averaging the latitude and longitude of each feature point within that cluster.
- **Severity Rating:** The new severity rating was determined as the median severity rating of the spatial accessibility features within a cluster. Unlike the Project Sidewalk approach, which employed the mean, the median was selected to minimise sensitivity to outliers. In instances where the cluster contained an even number of features, the higher severity rating was chosen.
- **Temporary:** The *temporary* field, a binary variable with values of *TRUE* or *FALSE*, was determined based on the most frequently mentioned variable within the cluster, indicating whether a

spatial accessibility feature was temporary or permanent.

- **Tags:** Contrary to the aggregation approach from Project Sidewalk, all tags associated with individual features were retained as a list for each aggregated point.
- **Description:** All descriptions provided by ZuriACT participants were preserved to ensure detailed information about spatial accessibility features was maintained.
- **Group:** The information about the participant groups was summarised in a list maintained for the newly developed spatial accessibility feature point.
- **IDs:** To ensure reproducibility and confirm that the aggregation process worked properly, both the original ID of a spatial accessibility feature and the ID identifying individual clusters were retained in the newly aggregated data point.

Figure 4.4 illustrates how spatial accessibility features were clustered (clusters are indicated by colour) and aggregated into a single feature point (stars) containing all relevant information regarding accessibility. The process is represented for the spatial accessibility feature category *curb ramp*. This example effectively demonstrates how multiple data points describe the same curb ramps. Data clustering and aggregation eliminate this redundancy, ultimately consolidating all data points into one single point per curb ramp.

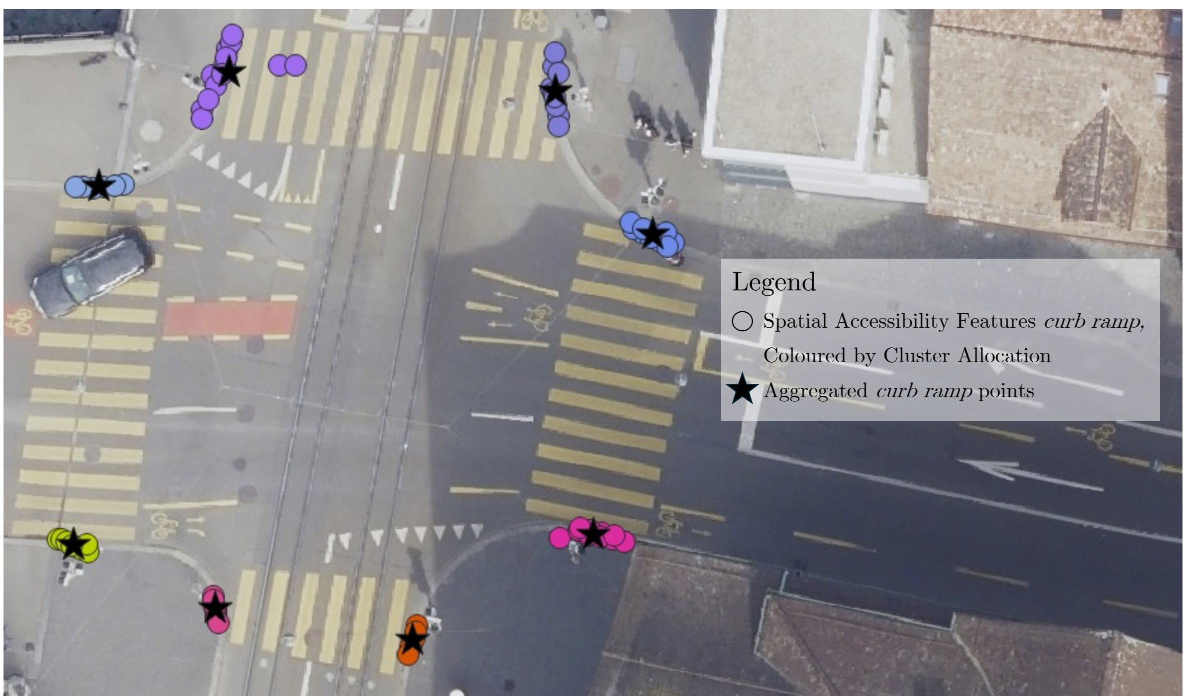

Figure 4.4: Resulting spatial accessibility features *curb ramp* clusters, created by hierarchical clustering, and aggregated *curb ramp* points (Areal image: Kanton Zürich (2020))

4.3 Footpath Network

To apply a routing algorithm, a network was required, as the algorithm generates routes between origins and destinations based on this network (Neis, 2015). Traditionally, a network is represented as a graph $G = (V, E)$, where V denotes a set of vertices or nodes, and E signifies a set of edges that define relationships between these nodes (Rhoads et al., 2023). The adaptation of a real-world transport system network can be straightforward in some instances. For instance, a subway system can be modelled as a spatial network, with stations as nodes and the connections between them depicted as edges (Rhoads et al., 2023). However, road networks tend to be more complex. In a graph representation, nodes correspond to intersections, and edges represent the streets connecting these intersections. Each node effectively serves as a decision point where drivers choose their next direction. This structure, however, implies that only intersections, and not roads, can serve as the starting or ending points of journeys. To overcome this limitation, the network can be inverted, whereby roads are mapped as nodes and intersections as edges. Although this approach addresses the limitation, it is less intuitive (Rhoads et al., 2023). Consequently, Rhoads et al. (2023) state that the translation from a real-world system to a spatial network is a complex process and requires careful adaptation to fit the needs of the application of the spatial network. Figure 4.5 illustrates how footpaths and roads can be mapped as a footpath network and a road network. .

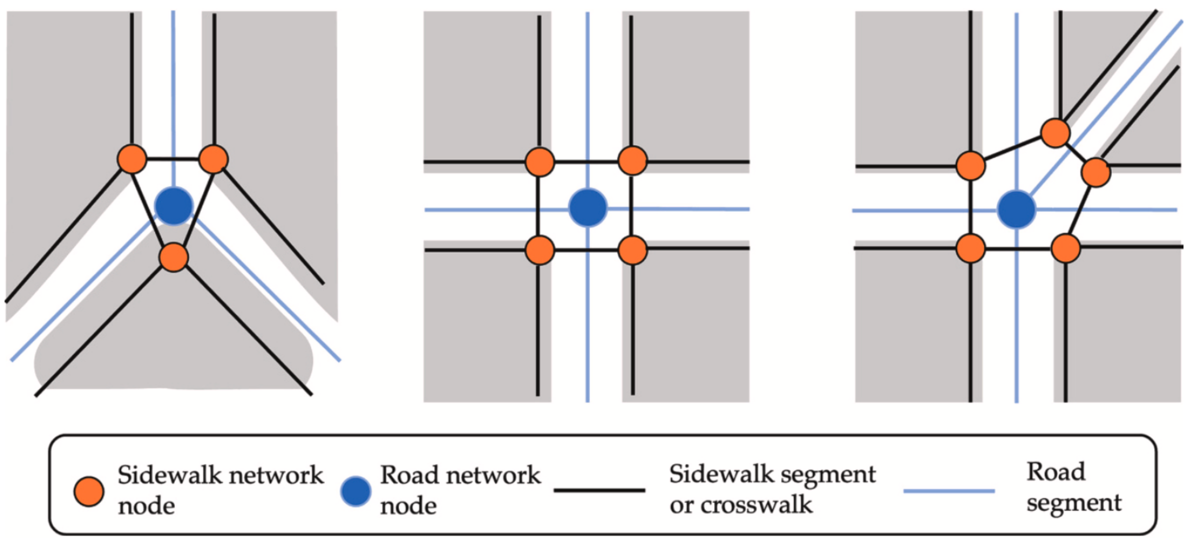

Figure 4.5: Footpath and roads mapped as two networks (Rhoads et al., 2023)

Traditionally, routing algorithms focus on creating the shortest path between origin and destination by minimising the cost of travel time or route length (Sevtsuk & Basu, 2022). However, recent developments emphasise that this parameter alone fails to capture the usability of a route for mobility-impaired individuals. Therefore, additional parameters reflecting route accessibility are necessary. Each of these parameters introduces a specific cost to a route segment (Neis, 2015). Minimising the overall cost of a route involves reducing the number or the negative impact of spatial accessibility features, such as obstacles, ultimately producing the most accessible route option (Neis, 2015).

In this thesis, the network was composed of footpath data for District 1 of the City of Zurich, as further elaborated in 4.3.3. To assess the accessibility of footpath segments, the footpath data was first enriched using the preprocessed spatial accessibility features (Section 4.3.1), followed by the computation of the accessibility-relevant costs introduced by the features (Section 4.3.2). Only after enriching the footpath data and calculating the accessibility costs of individual footpath segments, was the footpath dataset transformed into a footpath network (Section 4.3.3).

4.3.1 Footpath Enrichment with Spatial Accessibility Features

Before transforming the City's footpath dataset into a network, spatial accessibility information was incorporated into the dataset through spatial accessibility features. The following sections outline the steps required to accomplish this task.

Footpath Segmentation

Due to the differing geometries of the data, namely, spatial accessibility features represented as points and the footpath dataset consisting of LineStrings, the footpath dataset required preprocessing prior to data enrichment. Consequently, the footpath lines were split into smaller line segments. A segment length of 10 m was selected, following the methodology of Rahaman et al. (2017). In their study, the authors employed a shortest path algorithm that integrated both length and incline to identify the shortest accessible path, taking elevation changes into account. They overlaid the footpath network with contour lines and divided it at the intersections of the footpath network with the contour lines, thus enabling slope calculations (Rahaman et al., 2017). Rahaman et al. (2017) utilised a fine contour interval of 5 m to capture subtle changes in elevation. To validate their methodology, they applied their shortest path algorithm to a network consisting of 10 m segments, where the slope was computed for each segment. When tested in San Francisco, Lisbon, and Singapore, their study showed that the use of contour lines yielded results comparable to those derived from the 10 m segment network. For District 1 of Zurich, a segment size of 10 m was chosen to detect minor elevation changes. Alternative segment lengths, such as 20 m, were qualitatively evaluated. However, these did not accurately reflect real-world conditions as effectively as the 10 m segments. Given the relatively small study area of District 1, utilising shorter segments proved computationally feasible and provided greater precision in capturing elevation changes.

To divide the footpath lines into smaller segments, the function *line_segment* from the R package *stplanr* was used as it permits the subdivision of sf objects with a LineString geometry into regular segments (Lovelace & Ellison, 2019). The benefit of this function is that the attributes remain intact throughout the segmentation process.

Footpath segmentation was conducted only after the dataset was enriched with the spatial accessibility features *crosswalk*, as explained in the following section, to ensure that the crosswalk information was assigned to the entire crosswalk segment. After enhancing the footpath with *crosswalk* features, the segmentation was carried out before proceeding with further enrichment of spatial accessibility features. The next sections describe the process of enriching the footpath dataset with the spatial accessibility features described in Section 3.1.1.

Crosswalk Features

As previously introduced, *crosswalk* features (Figure 4.6a) were added to the footpath dataset before it was split into smaller segments. This step was taken prior to segmentation to ensure that the *crosswalk* feature was attributed to the entire crossing segment (Figure 4.6b), which could exceed 10 m in length and might otherwise be divided during the segmentation process. In such cases, *crosswak* features would be assigned only to the nearest segment, potentially failing to cover the entire street width (Figure 4.6c).

To attribute the footpath data with the *crosswalk* features, the *crosswalk* points were assigned to the nearest footpath segment using the function *st_nearest_feature* from the R package *sf* (Pebesma, 2016). Additionally, a maximum threshold distance of 3 m was chosen to prevent *crosswalk* features from being incorrectly assigned to a footpath segment that might be nearer than the actual crosswalk but not part of a crosswalk in reality. This threshold of 3 m was established by iteratively enriching the footpath segments with the crosswalk information, starting with 10 m and reducing the threshold

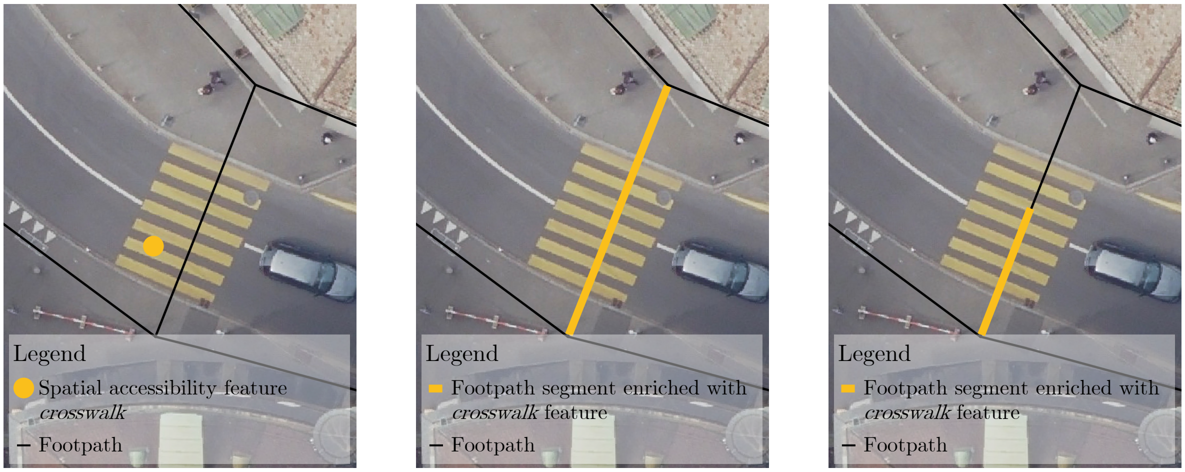

(a) Footpath prior to the allocation with a *crosswalk* feature

(b) Footpath after the allocation with a *crosswalk* feature (prior to segmentation)

(c) Segmented footpath after the allocation with a *crosswalk* feature

Figure 4.6: Footpath enrichment with spatial accessibility feature *crosswalk* (Aerial images: Kanton Zürich (2020))

distance by 1 m per iteration. It has proven to be a suitable compromise between accurately identifying crosswalk segments and incorrectly assigning crosswalk features to footpath segments representing sidewalks. Each footpath segment was ultimately enriched with information on whether it was a *crosswalk* segment or not, i.e., whether a *crosswalk* point was assigned to this footpath segment. In addition to this information, the severity rating and whether a feature was temporary or not were preserved for the subsequent steps.

In addition to the spatial accessibility features *crosswalk* (Figure 4.7a), segments were identified where crossing is possible, though not secured and lacking pedestrian priority. Since the footpath dataset included names for each line, all lines containing the string *Überquerung* (eng. crossing) were recognised (Figure 4.7b), for instance, *Limmatquai Überquerung*. The severity of these segments was assigned a value of 2, given that there was, as previously mentioned, no pedestrian priority. Furthermore, I presumed them to be permanent; thus, *temporary* was marked as *FALSE*. However, this only applied to *Überquerung* segments not previously identified as crosswalks by the *crosswalk* features.

Although spatial accessibility features previously underwent clustering and aggregation steps, there remained a possibility of multiple clustered and aggregated features from the same category being assigned to the same footpath segment. This issue arose from the spatial configuration of clusters and the distance thresholds employed during clustering. These factors could lead to the formation of multiple clusters in a specific area, all of which might share the same nearest footpath segment. Consequently, the aggregated features would be allocated to the same footpath segment. While this issue was more pronounced for other spatial feature categories, it also occurred for *crosswalk* features. To address this, I chose to remove all *crosswalk* features except the one with the highest severity rating, thereby ensuring that the accessibility of a segment was not underestimated. By considering the highest severity, namely the most severe and hence the most inaccessible *crosswalk* rating, I eliminated the possibility of overlooking potentially less accessible features within the same footpath segment.

Alternative Crossing Option

In addition to enhancing crosswalks using the spatial accessibility features (Figure 4.7a) and the names of the footpath lines (Figure 4.7b), a third option for street crossings was examined. This was based on the premise that street crossings are feasible where curbs are lowered and present on both sides of the streets, as indicated by the locations of the spatial accessibility features *curb ramp* (Figure 4.7c).

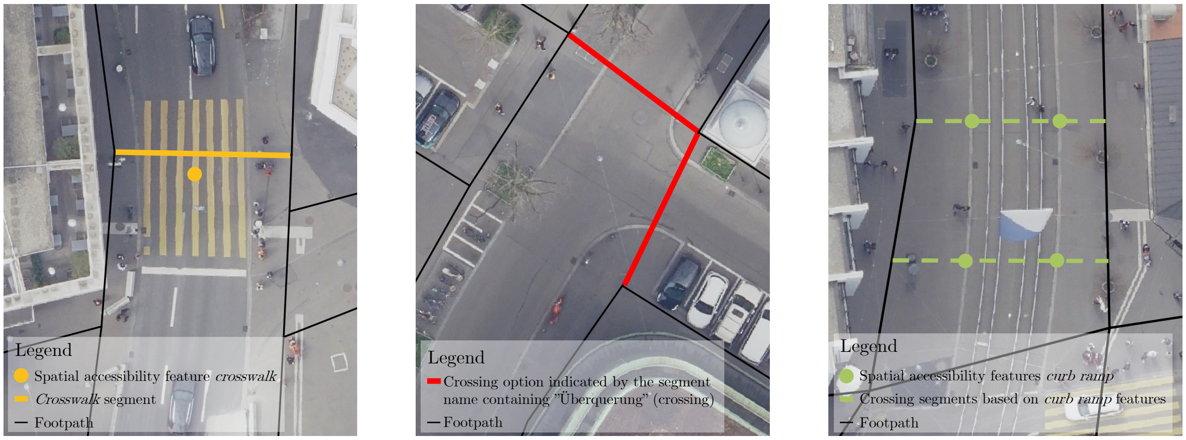

(a) Spatial accessibility feature *crosswalk* allocated to the footpath segment, resulting in a crosswalk segment

(b) Crossing as indicated by the name of the footpath segment containing "Überquerung" (crossing)

(c) Generation of crossing segments based on lowered curbs, indicated by *curb ramp* features

Figure 4.7: Different crossing options (Aerial images: Kanton Zürich (2020))

After identifying footpath segments where the spatial accessibility feature *curb ramp* was present (Figure 4.8) (more on this step in the following section), additional footpath segments were incorporated into the footpath dataset. To generate new segments with lowered curbs, footpath segments with *curb ramp* features were extracted (Figure 4.8c), and segments with *crosswalk* features were temporarily removed from the extracted segments to maintain their geometry and attributes. Only the footpath segments with curb ramps were used for the following steps. *Crosswalk* segments were reintroduced into the footpath dataset after the generation of additional crossing segments.

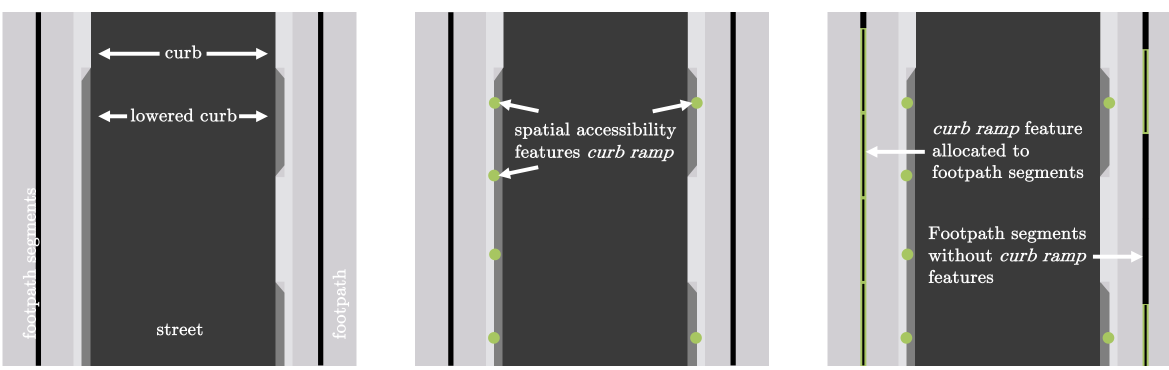

(a) Schematic overview of footpath segments where crossing is possible due to lowered curbs

(b) Spatial accessibility features *curb ramp* indicating the location of lowered curbs

(c) *Curb ramp* features allocation to footpath segments

Figure 4.8: Steps to create additional footpath segments representing crossing options enabled by lowered curbs on both sides of a street (I)

I created a buffer around the footpath segments allocated with *curb ramp* features using the *st_buffer* function from the *sf* package (Pebesma, 2016), simulating slightly more than 50% of the width of a street between the footpaths (Figure 4.9a). The buffer distance of 13 m was determined iteratively, beginning at 20 m and decreasing by 1 m per iteration. The aim was to establish a threshold distance at which the buffers of opposing footpath segments overlapped. This allowed for the identification of non-opposing footpath segments whereby the buffer would not overlap with that of a footpath segment on the opposite side of the street. To support this method, the parameter *end cap style* of the *st_buffer* function was set to *flat*, preventing adjacent footpath segments from lying partially within each other's buffers and thereby creating "false crossings".

While non-overlapping buffers were excluded from the dataset, overlapping buffers were merged using the function *st_union* from the *sf* package (Pebesma, 2016) (Figure 4.9b). The footpath segments with opposing footpath segments were identified by selecting those that intersected with the merged buffers. At that point, I was able to extract footpath segments with lowered curbs on both sides of a street. The subsequent step involved creating lines that connected these segments. To achieve this, I used the City of Zurich's streets (Stadt Zürich, 2023) as an axis upon which perpendicular lines could be constructed, simulating locations where crossings are feasible (Figure 4.9c).

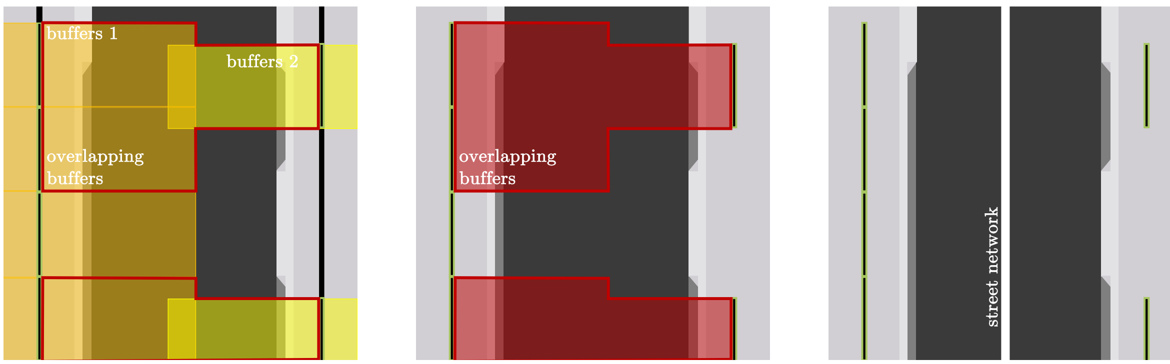

(a) Generation of 13 m-buffers around footpath segments with allocated *curb ramp* feature on both sides of the street (buffer 1 and buffer 2)

(b) Extraction and of overlapping buffers 1 and 2

(c) Addition of street network as a basis to generate new footpath segment representing crossings

Figure 4.9: Steps to create additional footpath segments representing crossing options enabled by lowered curbs on both sides of a street (II)

The street network was assessed carefully since it formed the basis for the creation of new lines. By examining it, streets were manually removed where crossings should not be possible, despite the curbs being lowered on both sides of the street. These situations arose, for instance, where *curb ramp*

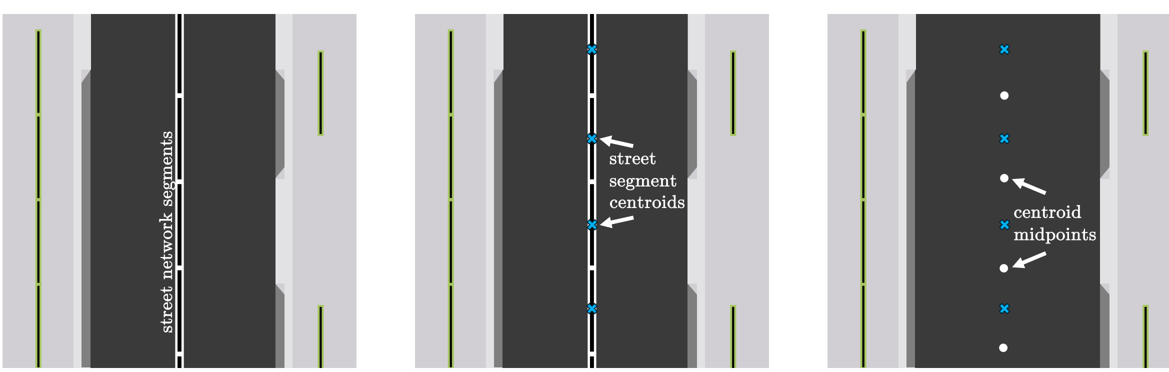

(a) Division of street network into 10 m-segments

(b) Generation of street segments centroids

(c) Midpoints between two consecutive centroids are created

Figure 4.10: Steps to create additional footpath segments representing crossing options enabled by lowered curbs on both sides of a street (III)

features were allocated to sidewalks rather than crossings due to the threshold selection, leading to the erroneous extraction of these sidewalk segments in the initial step. In such instances, crossings were already present, and no additional crossing segment was necessary.

Following these steps, the street lines were further divided into 10 m long segments (Figure 4.10a) using the *stplanr* package's *line_segment* function (Lovelace & Ellison, 2019). A centroid for each segment was then created (Figure 4.10b) through the application of *st_centroid* (Pebesma, 2016). These centroid points acted as origin points for the creation of additional segments, as they were positioned on streets between two footpath segments with lowered curbs. The distances between consecutive centroids were calculated, and midpoints were established at the centre of these consecutive centroids (Figure 4.10c).

Virtual lines connecting consecutive centroids were drawn, and the slope of these virtual lines was determined (Figure 4.11a). Using this slope, two points were created that are perpendicular to the previously generated midpoints, with one on each side of the virtual line connecting the two centroids (Figure 4.11b). An empirical distance of 14 m was selected between the midpoints and the perpendicular points to ensure that the crossings ultimately intersected the footpath lines on either side of the street, allowing the connecting line to span the entire width of the street. The perpendicular points were then connected, simulating the crossing segments (Figure 4.11c).

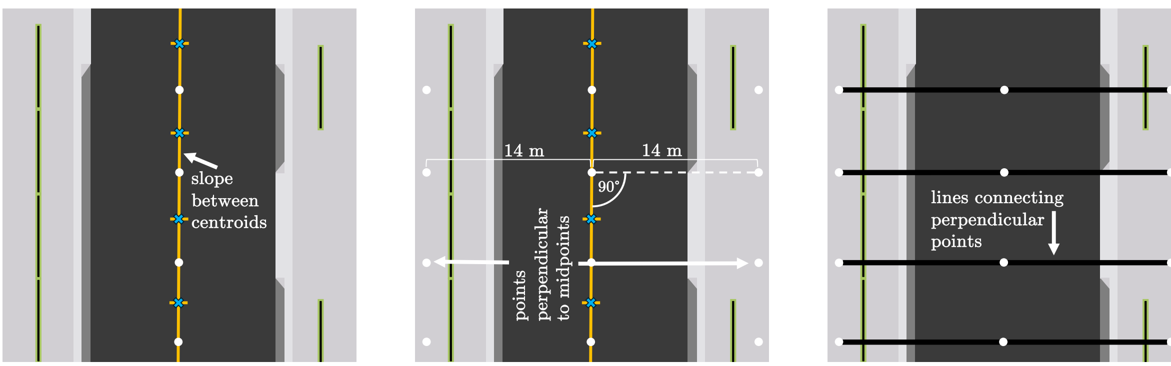

(a) Slope calculation of virtual line connecting two consecutive centroids

(b) Generation of two points perpendicular to the line (based on prior slope calculation) on both sides of the midpoints

(c) Generation of lines connecting the points perpendicular to the midpoints

Figure 4.11: Steps to create additional footpath segments representing crossing options enabled by lowered curbs on both sides of a street (IV)

However, as the length of these lines may exceed the street's width, they were intersected with the merged buffers representing areas between two footpath segments with lowered curbs (Figure 4.12a). This allowed me to cut them at the precise location to ensure proper integration with the footpath network. Since the perpendicular lines were based on midpoints between two centroids, they were sometimes created outside of the buffered areas. These lines were removed, as they did not represent potential crossings. Furthermore, lines not connecting footpath segments with designated *curb ramp* features at both ends were eliminated (Figure 4.12b). Finally, the newly created footpath segments were incorporated into the footpath dataset (Figure 4.12c).

Some overlapping buffer areas were rather small, and no connecting line segment was created there. To address this, I manually added crossing lines at six locations to ensure that my footpath network represented real-world pedestrian crossings.

Following the creation of the crossing's geometry, these newly created lines were assigned accessibility-relevant information. As these crossings are neither part of the official crosswalk dataset nor the official footpath network, I assumed that pedestrians do not have any priority when crossing the streets, sim-

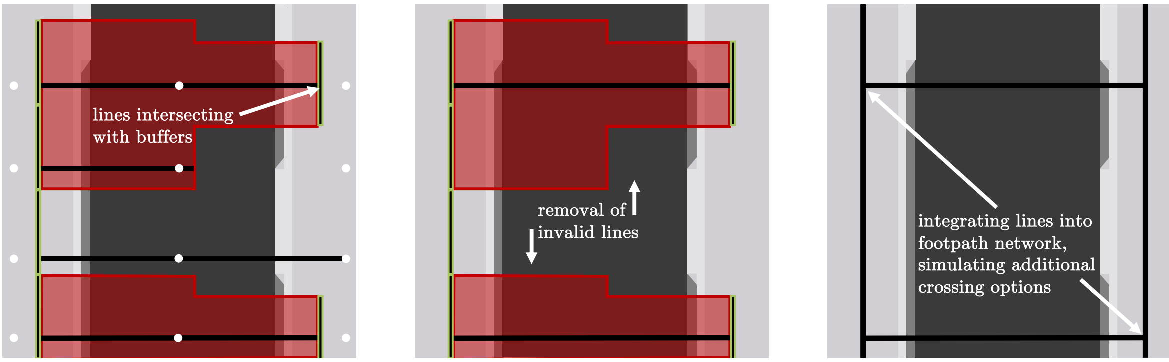

(a) Intersection of connecting lines with overlapping buffer areas

(b) Removal of connecting lines not touching *curb ramp* segments or not located within buffers

(c) Integration of connecting lines into footpath network, representing the option of crossing by lowered curbs

Figure 4.12: Steps to create additional footpath segments representing crossing options enabled by lowered curbs on both sides of a street (V)

ilar to the tag *no pedestrian priority*. In contrast to the crossing segments identified by the name *Überquerung* (Figure 4.7b), the newly generated crossings were not included in the original footpath dataset of the City of Zurich (Stadt Zürich, 2024b). Therefore, a severity of 3 was selected, which is higher than that of the *Überquerung* segments. Furthermore, upon completing the enrichment of the footpath data with crosswalk information, the attribute *temporary* was set to *FALSE* as these crossings did not depend on temporary infrastructure but were solely established at the locations of permanent *curb ramp* objects.

Curb Ramp and *Missing Curb Ramp* Features

Following the *crosswalk* features enrichment and crossing segment generation, the previously allocated *curb ramp* features, which were used to identify segments with lowered curbs, were removed from the footpath dataset. Subsequently, the spatial accessibility features *curb ramp* and *missing curb ramp* were reallocated to the footpath segments to ensure that the spatial accessibility features *curb ramp* were enriched primarily on crosswalks and other crossing segments, as curb ramps typically appear where street crossings are possible (University of Washington, Makeability Lab, 2024b). Therefore, the *curb ramp* and *missing curb ramp* features were initially allocated to footpath segments that formed part of a crossing, i.e., the segments enriched with *crosswalk* features or identified as *crossing* in the previous steps.

If such a segment (or multiple segments) was found within a 5 m distance threshold, the *curb ramp* and *missing curb ramp* features were assigned to the nearest crossing and crosswalk segment using the function *st_nearest_feature* (Pebesma, 2016).

If no crossing segment was found, the curb ramps and missing curb ramps were assigned to the nearest segment within a 7 m distance threshold.

The distance thresholds of 5 and 7 m were selected empirically, beginning with thresholds of 10 m and decreasing them by 1 m in each iteration.

If a street segment was identified as one where curb ramps or missing curb ramps were present, the features were attributed to this segment. If no footpath segment was located within the maximum distance threshold of 7 m for a *curb ramp* and *missing curb ramp*, the feature was not linked to a footpath segment. This approach was adopted to ensure that only features situated on footpaths were considered for their accessibility assessment.

Similar to the spatial accessibility feature *crosswalk*, it is possible that multiple cluster points of *curb ramp* and *missing curb ramp* features were assigned to a single segment. Consequently, the same approach outlined in Section 4.3.1 was adopted: Only the features with the highest severity of the assigned *curb ramp* and *missing curb ramp* features, respectively, were taken into account.

***Pedestrian Signal* Features**

Similar to the strategy employed for *curb ramp* and *missing curb ramp* features, crossing and crosswalk sections were identified as priority segments for the assignment of *pedestrian signal* features.

If such crossing or crosswalk segments were situated within 5 m, the *pedestrian signal* feature was assigned to the nearest one.

However, if no such segment existed, the *pedestrian signal* feature was allocated to the nearest segment within a distance of 7 m.

In case no footpath segment was located within this threshold distance of 7 m, the corresponding *pedestrian signal* features were not assigned to the footpath dataset.

In line with the *crosswalk*, *curb ramp*, and *missing curb ramp* features, only the *pedestrian signal* feature with the highest severity rating was retained in cases where multiple *pedestrian signal* features were assigned to a single footpath segment.

Non-Crossing Spatial Accessibility Features

After enriching the footpath dataset with crossing features, i.e., *crosswalk*, *curb ramp*, *missing curb ramp*, and *pedestrian signal* features, the remaining spatial accessibility features were allocated to the footpaths. These included *surface problem*, *surface material type*, *no sidewalk*, *obstacle*, *construction*, *height difference*, *parked car*, *parked motorcycle/bike*, and *rail/tram track* features.

As these features did not require to be allocated to crosswalk and crossing segments primarily, only one enrichment step was necessary.

If a footpath segment was situated within a distance threshold of 5 m from the location of a spatial accessibility feature, the feature was assigned to the nearest segment. The allocation of a feature to a segment was independent of whether the nearest segment was a standard footpath segment or a previously identified crosswalk or crossing segment. If no segment within the distance threshold was identified, the spatial accessibility feature was not allocated to the footpath dataset.

If multiple spatial accessibility features per category were allocated to the same footpath segment, only the one with the highest severity rating was considered.

The spatial accessibility feature *shared space* was excluded from footpath enrichment due to inconclusive effects on accessibility. This feature was introduced to mark areas where pedestrians and vehicles share the same space, as well as to indicate pedestrian zones. In pedestrian zones in District 1, vehicles are generally prohibited, except for goods handling from 5:00 am to 12:00 pm and certain exemptions such as hotel guests, taxis, and permit holders (Stadt Zürich, 2021b). Shared spaces may adversely affect accessibility for individuals with mobility impairments, as they are not solely reserved for pedestrians, unlike sidewalks. Conversely, pedestrian-only zones may enhance accessibility for these groups by eliminating vehicle presence. Therefore, I argue that pedestrian-only areas, where vehicles are entirely prohibited, should be clearly distinguished from shared areas like pedestrian zones in District 1, where vehicles may be present, and further examination of the actual impact on accessibility is necessary.

Incline

As introduced earlier, footpath incline was determined with the help of a DEM (Pude, 2022) instead of using the spatial accessibility feature *vertical slope* collected within the ZuriACT project (Sections 3.1.2 and 3.3.1).

Therefore, the DEM for District 1 was extracted from the DEM of the City of Zurich. A buffer distance of 100 m was added to the extent of District 1 to ensure that the entire District 1 was covered with raster cells, guaranteeing that there was elevation information everywhere.

The incline calculation using a DEM was based on a trigonometric function, schematically depicted in Figure 4.13 (Warren et al., 2004).

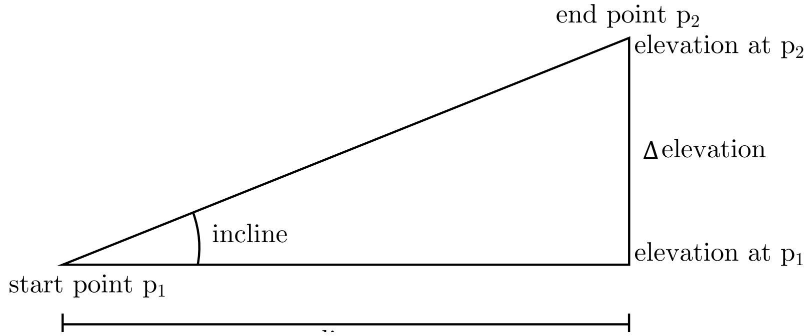

Figure 4.13: Slope calculation using a DEM

First, the locations of the start point p_1 and end point p_2 of each footpath segment were determined. Using the function *st_distance* from the package *sf*, the distance between p_1 and p_2 was calculated ($\Delta distance$) (Pebesma, 2016). To extract the elevation of p_1 and p_2 from the DEM, the *extract* function from the *terra* package (Hijmans, 2020) was applied. The elevation difference ($\Delta elevation$) between p_1 and p_2 was determined as an absolute value due to the fact that, at that point, the direction in which pedestrians travel on a footpath segment was unknown, i.e., uphill from p_1 to p_2 or downhill from p_2 to p_1. Subsequently, when creating the routes from origin to destination, the direction of travel was specified. As incline impacts travel speed, as introduced in Section 2.2.3, incline values were calculated per route to derive travel speed for both uphill and downhill inclines (Section 4.4.3).

Ultimately, the incline was calculated by dividing the elevation difference by the distance difference between p_1 and p_2 (Equation 4.1).

$$slope = \frac{\Delta elevation}{\Delta distance} \tag{4.1}$$

Following the incline calculation, its impact on spatial accessibility was assessed by applying severity ratings based on its value, similar to the severity ratings incorporated for spatial accessibility features. As multiple sources indicate, an incline exceeding 6% is generally deemed inaccessible to wheelchair users (Neis, 2015; Schmidt & Manser, 2024; Schweizerischer Verband der Strassen- und Verkehrsfachleute VSS, 2014). However, Swiss regulations permit inclines of up to 10% for outdoor areas or 12% for covered paths due to spatial and structural constraints (Schweizerischer Verband der Strassen- und Verkehrsfachleute VSS, 2014). Consequently, severity ratings from 1 to 3 were distributed proportionally to slopes from 0 to 6% and 4 was assigned to the incline range from 6 to 12% to consider Swiss regulations. An incline greater than 12% was considered inaccessible, thus, a severity rating of 5 was assigned to these footpath segments (Table 4.3).

Manual post-processing of the severity assignment was required as footpath segments on bridges or along the rivers Limmat, Sihl, or Schanzengraben were assigned an unrealistically high severity rating. Presumably, this was necessary due to incline calculations based on a DEM with a spatial resolution of 0.5 m, which caused inaccuracies when footpath segments were located near a significant height difference within a small horizontal distance, such as bridges over rivers. Footpath segment inclines were identified and confirmed using Google Street View, and severity ratings were assigned based on the ratings of neighbouring footpath segments.

Table 4.3: Severity rating assignment based on footpath segments' absolute incline values

Incline	**Severity Rating**
0% to $<$ 2%	1
2% to $<$ 4%	2
4% to $<$ 6%	3
6% to $\leq$ 12%	4
$>$ 12%	5

4.3.2 Footpath Cost

Current routing services often aim to reduce travel time or route length, seeking the fastest or shortest route (Rahaman et al., 2017). However, solely considering travel time or route length does not adequately address the needs of mobility-restricted population groups; the suggested routes fail to take accessibility along the route into account, which can be a crucial factor in route choice. Furthermore, route accessibility is complex because many factors influence a route's accessibility (Rahaman et al., 2017), including various barriers and facilitators identified by Georgescu et al. (2024). The work conducted by Beale et al. (2006) and Völkel and Weber (2008) introduced methods to incorporate alternative measurements and parameters beyond travel time and route length, as detailed in Section 2.2.3. Consequently, diverse strategies are needed to identify a route that optimises a set of criteria, allowing one criterion to be compensated by another. To create routes that are optimised for multiple criteria, cost functions can be employed to find the best balance between different parameters (Völkel & Weber, 2008).

The cost of travelling on a specific footpath segment is detailed in the following section. The cost for each segment was computed, facilitating comparisons of individual segments as well as different paths made up of multiple footpath segments (Völkel & Weber, 2008).

Access Score

Concluding the footpath enrichment, a score was calculated to represent the accessibility of a single footpath segment, i.e., the weight or cost of travelling through that segment. Therefore, the approach introduced by Hara (2016) was adopted. In his work, Hara (2016) developed an *Access Score* to quantitatively measure the accessibility of a specific street segment or neighbourhood. This method was further applied to crowd-sourced data collected using the Project Sidewalk tool by Li et al. (2022), aiming to assess footpath equity in Seattle, thus proving its suitability for the study at hand. The approach is based on the assumption that the number of footpath accessibility features influences the overall accessibility. In other words, footpath segments with a greater number of spatial accessibility features that negatively affect movement result in lower accessibility, and vice versa (Li et al., 2022). The introduced *Access Score* ranges from [0,1], where 1 signifies high accessibility (*accessible*) and 0 signifies low accessibility (*inaccessible*) for a footpath segment (Hara, 2016; Li et al., 2022). Similar to Hara (2016), Li et al. (2022) counted the number of spatial accessibility features on each footpath segment, constructing the *accessibility feature vector (x_a)*.

In addition to the method proposed by Hara (2016), Li et al. (2022) also considered the severity rating of each spatial accessibility feature, called *significance vector (ws)*, where severity ratings from 1-5 were scaled to values between 0.2-1. Hereby, spatial accessibility features positively affecting spatial accessibility were treated differently than those negatively affecting it. To further preserve the positive and negative impacts of the spatial accessibility features, the values of the *significance vector (ws)* were assigned a polarity (+/—) (Hara, 2016; Li et al., 2022). Table 4.4 summarises the scaled severity and polarity of the object.

Table 4.4: Scaled severity ratings for features with positive and negative impacts

Original Severity Rating	**Negative Features**	**Positive Features**
1	-0.2	1
2	-0.4	0.8
3	-0.6	0.6
4	-0.8	0.4
5	-1	0.2

The *Access Score* of a footpath segment is derived from the dot product of the *significance vector (ws)*, which includes the polarity of the spatial accessibility feature (positive impact versus negative impact on accessibility), and the *accessibility feature vector (x_a)* is calculated. Theoretically, this could yield a value between $(-\infty, \infty)$. To mitigate this issue, Hara (2016) suggested applying a sigmoid function to map it to the range of (0,1). Therefore, the *Access Score* for each footpath segment was calculated as follows:

$$\text{Access Score}_{\text{footpath segment}} = \frac{1}{1 + e^{-(ws \cdot x_a)}} \tag{4.2}$$

In this thesis, the *Access Score*, introduced by Hara (2016) and extended by Li et al. (2022) (Equation 4.2), was utilised to determine the accessibility of a footpath segment, i.e., the routing cost of travelling through a specific segment. However, the approach was further adjusted to facilitate routing navigation for population groups with mobility impairments. Aiming to avoid footpath segments where spatial accessibility features hindered mobility to the extent that a segment became impassable, spatial accessibility features with a severity rating of 5 (*not passable*) directly corresponded to an impassable footpath segment, meaning that the *Access Score* for such footpath segments was set to 0.0.

The *Access Score* was computed twice: the first *Access Score* calculation considered all spatial accessibility features, resulting in *Access Score$_{all}$*. The second *Access Score* considered only permanent features, denoted as *Access Score$_{permanent}$*, with temporary spatial accessibility features being excluded. The computation of these two access scores enabled the analysis of the impact of temporary features on route suggestions for the mobility-impaired population group.

In addition to the *Access Score* calculated for each footpath segment, a *Neighbourhood Access Score* was also determined to identify neighbourhoods with poor accessibility. This approach was based on the score introduced by Li et al. (2022) and facilitates the calculation of the *Neighbourhood Access Score* as follows:

$$\text{Access Score}_{\text{neighbourhood}} = \sum \frac{\text{Access Score}_{\text{segment}} * \text{Footpath length}_{\text{segment}}}{\text{Footpath length}_{\text{neighbourhood}}} \tag{4.3}$$

The *Neighbourhood Access Score* was calculated twice: first, by considering the *Access Score$_{all}$* based on all spatial accessibility features (both temporary and permanent), and second, using the *Access Score$_{permanent}$*, which relies solely on permanent spatial accessibility features.

4.3.3 Footpath Network Building

Following the footpath enrichment, the footpath dataset was ultimately converted into a network to apply Dijkstra's Shortest Path algorithm. As introduced in Section 4.3, the footpath dataset consisting of LineStrings, required translation into a graph G consisting of vertices/nodes V and edges E (Rhoads et al., 2023).

To translate the footpath data into a spatial network, I applied the *as_sfnetwork* function from the *sfnetworks* package in R (van der Meer et al., 2024). The *sfnetworks* package is a powerful tool, connecting the *sf* package for spatial data science with the functionalities of the *tidygraph* package for network analysis (van der Meer et al., 2024). As the spatial network is embedded in a geographical space, its nodes and edges can be represented as geographic features. Most commonly, nodes are represented as points and edges as LineStrings. Furthermore, the *sfnetworks* package offers various functions, also enabling routing, which is of special interest for this thesis.

The network was created as an undirected network using the *as_sfnetwork* function, meaning that travelling in both directions is possible. The LineStrings of the footpath dataset were converted into edges, and nodes were created between these LineStrings, connecting the single edges. The calculated *Access Score* was preserved as an attribute assigned to the edges of the network, representing the cost induced by travelling through the specific edge in a route.

Following the network creation, I analysed the network structure to ensure the correct translation from the footpath dataset to the footpath network. As the *Access Score* was attributed to the edges, I did not assign an additional weight to the network, such as the length of the edges, thus resulting in an unweighted network. Furthermore, the created network was not planar, as overlying edges were present. This is reasonable, given that overlaying edges represented tunnels and underpasses on footpaths in my network. When checking the connectivity of the network, several parts were identified that were not part of the main network, as shown in Figure 4.14.

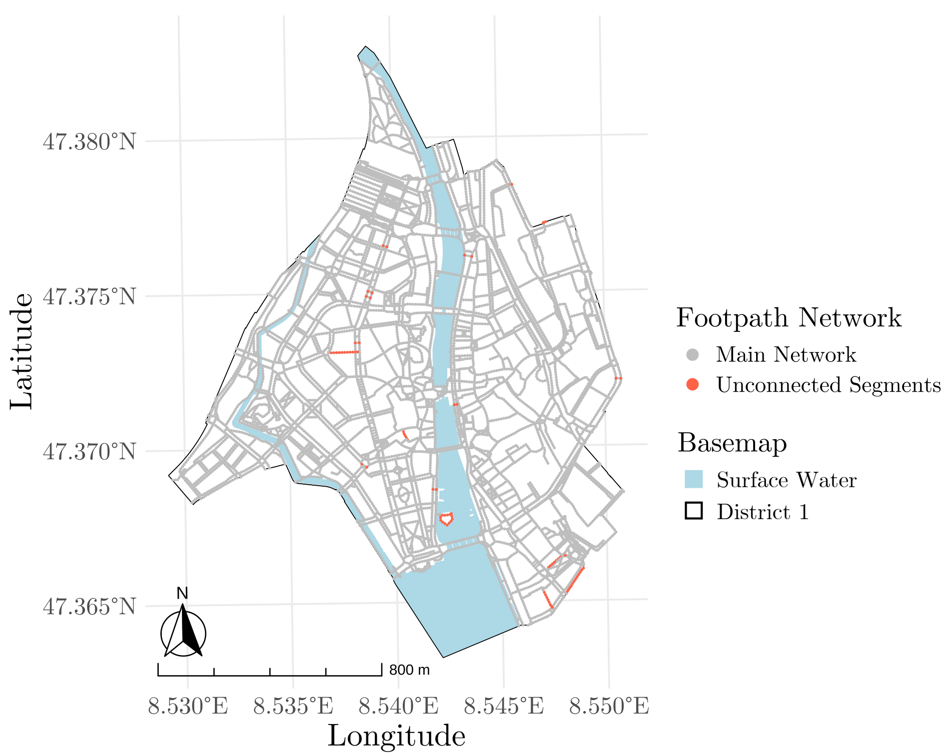

Figure 4.14: Footpath network with disconnected segments

To prevent an unconnected network made up of several parts, these components were reintegrated into the main network, as they could result in incomplete routes, that is, routes ending abruptly at unconnected nodes. Therefore, all edges linked to an unconnected node were extracted (Figure 4.15a). After some minor manual cleaning, such as removing duplicate nodes, the unconnected edges were utilised to split the edges at intersection points, where the unconnected nodes are located on edges (Figure 4.15b). To ensure that the unconnected nodes were precisely positioned at the newly created start or end points of an edge, they were snapped to these points (Figure 4.15b). After the slight relocation of nodes, they were reintegrated into the network (Figure 4.15c).

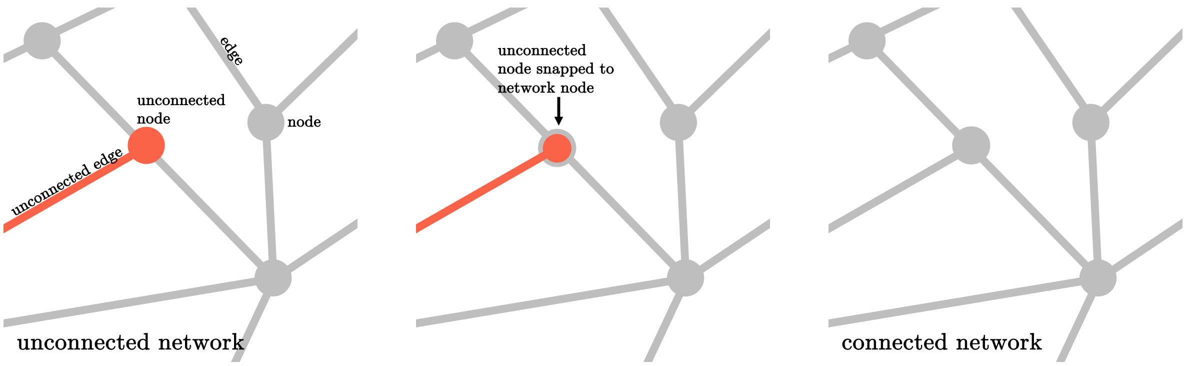

(a) Unconnected network segments

(b) Intersection of unconnected nodes and network edges, creating new network nodes; unconnected nodes were then snapped to newly created network node

(c) Relocated, unconnected network nodes are reintegrated into the footpath network

Figure 4.15: Reintegration of unconnected network segments into main network

As two distinct *Access Scores* were calculated at the footpath level, three separate networks emerged from the footpath dataset instead of attributing a single network to the *Access Score* outcomes. Two networks incorporated the results of the *Access Score* calculations, $\textit{Access Score}_{permanent}$ and $\textit{Access Score}_{all}$. The third network excluded the spatial accessibility features, as it served as the basis for routing individuals without mobility restrictions and, consequently, without specific accessibility requirements. The methodology for creating all three networks was consistent.

4.4 Routing

The following sections detail the creation of routes based on 30 predefined origin-destination pairs (Section 4.4.1). Three routing services were utilised to generate routes between these pairs, namely Google Maps, Open Source Routing Machine (OSRM), and OpenRouteService (ORS) (Section 4.4.2). Following these procedures, Dijkstra's Shortest Path algorithm was implemented on the footpath networks enriched with accessibility information (Section 4.4.2). In aiming for route comparison, three distinct metrics for each route were established: route length, travel time, and route complexity (Section 4.4.3).

4.4.1 Origin-Destination Pairs

The routes suggested by the routing services were based on origin and destination points paired to create meaningful origin-destination pairs.

Origin points were derived from the federal population dataset (Bundesamt für Statistik BFS, 2023), indicating starting locations for routes where people reside. The point dataset arranges these points in a regular grid format of 100 m grid cells. Of these population points, 106 were identified in District 1. The dataset containing the points located in District 1 was utilised to randomly select 30 population points using the *sample_n* function, which is part of the *dplyr* package in R (Wickham et al., 2024). Before the random selection, I manually excluded population points situated at unrealistic origin locations, such as those on the rivers Limmat and Schanzengraben. These population points can be found on such surfaces due to the regular grid layout of the population data, ensuring data protection.

Destination points were extracted from the Points of Interest (POIs) dataset created using OpenStreetMap (OSM) data (OpenStreetMap contributors, 2024). The process of creating the POI dataset is detailed in Section 3.4.2. The POIs were grouped into the categories outlined in Table 3.2. Following the categorisation of the POIs, 30 were randomly selected using the *sample_n* function. To ensure equal representation of all POI categories, 5 POIs from each of the 6 groups were selected, resulting in a total of 30 POIs. As some POIs were significantly more common in certain categories, such as *amenity: bank*, I manually removed a few prior to the random selection.

After the random selection of origins (population points) and destinations (POIs), the origin points were randomly paired with destination points. This was accomplished by assigning each point in both datasets a number between 1 and 30. The paired origin and destination points were then joined and saved as a single dataset, which served as input for the routing step, where 30 routes per routing service were created, one for each pair.

4.4.2 Routing Services

Google Maps

Google's Directions API was employed to create routes between the specified origin-destination pairs. The routes were proposed based on each origin-destination pair submitted to the Directions API (Google, 2024b). Walking was selected as the mode of transportation. Unfortunately, the Directions API does not currently provide wheelchair-accessible routing at the time of this analysis. The Directions API returned the route in a JSON format, including travel time, route length, and the number of turns (Google, 2024b).

Utilising the Directions API from R was straightforward. Firstly, a for-loop was implemented to iterate through each origin-destination pair and store every route in the same list. To request the route via the Directions API, a URL was constructed:

```
url <- paste0(
  'https://maps.googleapis.com/maps/api/directions/json?',
  'origin=', origin_point,
  '&destination=', destination_point,
  '&mode=walking',
  '&key=', api_key
)
```

While the variables *origin_point* and *destination_point* were adjusted by iterating through all 30 origin-destination pairs, the *api_key* remained the same for each request.

As the coordinates of the routes were encoded by the Directions API, a function to decode these routes was necessary. The R *googlePolylines* package provides the *decode* function to convert the encoded route coordinates into latitude and longitude (Cooley et al., 2024).

Finally, the 30 routes stored in a list were transformed into a DataFrame for further analysis.

Open Source Routing Machine

The Open Source Routing Machine (OSRM) is a real-time routing service based on openly available OSM data (Luxen & Vetter, 2011). The OSRM was applied to the previously created origin-destination pair using the R package *osrm*. The *osrm* package calculates routes based on the OSM road network and enables the computation of routes, isochrones, trips, and travel distance matrices (Giraud, 2022). The function *osrmRoute* was employed to compute the routes by iterating through the origin-destination pairs. The variable *osrm.profile* was set to *foot* to return pedestrian routes (Giraud, 2022). In addition to the routes' geometry, routes were attributed with travel times and route lengths.

Similar to the routes created with the Google Directions API, the OSRM routes were ultimately stored as a DataFrame to facilitate the subsequent analysis.

OpenRouteService

Although OpenRouteService (ORS) also provides an API to calculate directions between origin and destination locations (OpenRouteService, 2024a), I decided to manually input the 30 routes into the ORS online routing tool (https://maps.openrouteservice.org/) to control the parameter settings for wheelchair-accessible routes (Table 2.1). As some parameter combinations for wheelchair-accessible routes pertaining to specific origin-destination pairs yielded no route suggestions, the parameters were adjusted manually to generate routes suitable for the wheelchair profile. For the initial route calculations, the default parameters were employed, except for the curb height. ORS uses a default value of 0.06 m, whereas Swiss guidelines recommend a maximum curb height of 0.03 m (Schmidt & Manser, 2024). Table 4.5 summarises the adjusted parameters for wheelchair-accessible routing and indicates which routes had the adjusted parameter values applied instead of the default values. Parameters not mentioned here were not altered, meaning their default values were used as specified in Table 2.1. Furthermore, *steps* were activated for the *avoid features* restriction for wheelchair routing. In contrast to the wheelchair profile, no restrictive parameters were established for the walking profile.

Table 4.5: Applied parameters for wheelchair-accessible routing in ORS, deviating from default values

Route Number	**Parameter**	**Default Value**	**Applied Value**
All routes, if not indicated otherwise	Maximum curb height	0.06 m	0.03 m
All routes	Avoid features		Steps
Route 3	Route smoothness	Good	Intermediate
Route 4	Route smoothness	Good	Intermediate
	Maximum inclination	6%	15%
Route 8	Maximum curb height	0.06 m	0.03 m
Route 9	Maximum curb height	0.06 m	0.03 m
Route 15	Maximum curb height	0.06 m	0.03 m
Route 18	Maximum curb height	0.06 m	0.03 m
Route 24	Maximum curb height	0.06 m	0.03 m

Continued on the next page

Route Number	Parameter	Default Value	Applied Value
Route 25	Maximum inclination	6%	*No restriction*
Route 29	Route smoothness	Good	Intermediate

After creating the routes for all 30 origin-destination pairs for walking and wheelchair users using the ORS online tool, the routes were exported in JSON format and imported into R for further processing. Like the OSRM routes, these routes were already attributed with travel times and route lengths.

Dijkstra's Shortest Path Algorithm

The final routing step involved applying a shortest path routing algorithm to the footpath networks from District 1 in the City of Zurich, which had been enhanced with spatial accessibility features beforehand. Consequently, Dijkstra's Shortest Path algorithm was applied to the footpath networks (Dijkstra, 1959).

Since the algorithm operated on a footpath network sensitive to spatial accessibility, the approach presented in this thesis was named *Dijkstra's **S**hortest **P**ath **A**lgorithm for **A**ccessible **R**outing SPAAR.*

The *shortest_path* function from the *igraph* package was employed, which functions on *sfnetworks* networks (Csárdi et al., 2024). To generate 30 routes, one for each origin-destination pair, I iterated through the pairs. To ultimately account for accessibility in routing, the *Access Score* (at the footpath level) was used as a weight, representing the costs associated with footpath features affecting accessibility. However, as the *Access Score* yielded high values for accessible segments and low values for inaccessible segments (Li et al., 2022), it could not be directly employed as a weight for routing. Therefore, the *Access Score* was rescaled to generate high weights, i.e., high *Access Score* values, for inaccessible segments and vice versa. To alter the direction of the scale, a rescaling calculation, as demonstrated in Equation 4.4, was performed:

$$\text{Access Score}_{\text{rescaled}} = 1 - \text{Access Score}_{\text{original}} \tag{4.4}$$

Prior to applying the rescaling calculation, segments with an *Access Score* of 0.0 were removed from the network as they indicate inaccessible, and therefore unpassable, footpath segments. This action resulted from the method employed for the *Access Score* calculation (Section 4.3.2). In that section, inaccessible segments, namely those featuring spatial accessibility characteristics that completely obstruct the path, leading to a segment deemed unpassable (severity rating of 5), were allocated an *Access Score* value of 0.0. An alternative approach that introduces a value prompting the routing algorithm to disregard footpath segments with an *Access Score* of 0.0 may be more elegant. For instance, Beale et al. (2006) assigned negative weights to objects leading to inaccessible footpath segments, which caused the routing algorithm to reroute and overlook those segments. However, to employ Dijkstra's Shortest Path algorithm in the *shortest_ path* function, positive weights were required (Csárdi, 2024). Consequently, I decided to remove inaccessible segments from the footpath network. All resulting routes from SPAAR were manually analysed to ensure that the elimination of inaccessible edges did not result in incorrect routing outcomes or unconnected routes. This method was feasible due to the small study area of District 1 in Zurich.

As the raw output of the *shortest_path* function consisted of lists of visited vertices and edges for each route, the results required some post-processing steps to create continuous routes. These routes were subsequently stored as a DataFrame for further analysis.

SPAAR was executed on three distinct footpath networks: the network based on all obstacles, considered in *Access Score*$_{all}$, the network based on permanent obstacles only, *Access Score*$_{permanent}$, and the network that did not consider any obstacles. For all networks, routes were established for each of the 30 origin-destination pairs, resulting in 90 routes based on SPAAR.

4.4.3 Route Metrics

To compare the resulting routes, route lengths, travel times, and route complexities were assessed. The calculation of these three metrics is explained in the following sections.

Route Length

When applying Google Maps, OSRM, and ORS to the origin-destination pairs, routes were generated that were already attributed with the route lengths (Giraud, 2022; Google, 2024b; OpenRouteService, 2024b). To calculate the route length proposed by SPAAR, the lengths of all footpath segments of a route were summed, resulting in a length value for each of the 30 routes.

Travel Time

Similar to the route lengths, the routes created by Google Maps, OSRM, and ORS were already attributed with travel time information.

As Google Maps uses proprietary input data and algorithms, no further details about the underlying assumptions or the implementation of the routing algorithm are publicly available. Tannert and Schöning (2018) mentioned in their work that Google Maps assumes a general walking speed of 5 km/h to calculate travel time, a speed that seems reasonable when compared to studies investigating walking speeds (Montufar et al., 2007; Willis et al., 2004). However, Google Maps may also adjust travel speed based on a set of parameters, some of which potentially consider real-time data, such as pedestrian density, which can be a key influencing factor on pedestrian speed (Giannoulaki & Christoforou, 2024).

OSRM employs a base walking speed of 5 km/h. Depending on the surface type, the walking speed is reduced, which consequently increases the travel time on specific routes generated by OSRM. For example, on gravel surfaces and pebblestone, the walking speed decreases to 3.75 km/h, while mud and sand-covered surfaces can further reduce the walking speed to 2.5 km/h (Open Source Routing Machine, 2024a).

In ORS, the travel speed for walking is automatically set to 5 km/h on all permitted street types. If the trail difficulty greater than *hiking* on the *sac_scale*, a scale employed to classify the difficulty of hiking trails in mountainous areas, the travel speed is diminished to 2 km/h (OpenRouteService, 2024d; OpenStreetMap Wiki, 2024b). Since there are no segments classified with a trail difficulty greater than *hiking* within District 1 (OpenStreetMap contributors, 2024), a travel speed of 5 km/h is assumed. The base speed for wheelchair users in ORS is set at 4 km/h. This base speed is then modified based on a number of parameters. The actual speed on a route ranges from 3 to 10 km/h, depending on the type of path and the presence of sidewalks (OpenRouteService, 2024d).

In contrast to Google Maps, OSRM, and ORS, the travel times for the SPAAR routes were calculated manually. To determine the travel time for each route, Equation 4.5 was applied:

$$\text{travel time } t_{\text{travel}} = \frac{\text{Distance } s_{\text{route}}}{\text{travel speed } v_{\text{travel}}} \tag{4.5}$$

The walking travel speed used as input for Equation 4.5 was essential in determining the travel time for the routes created by SPAAR. As introduced in Section 2.2.3, travel speed varies greatly depending on numerous factors, such as pedestrian capacity and the characteristics of the walking environment (Giannoulaki & Christoforou, 2024). OSRM, ORS, and potentially Google Maps can adjust the travel speed based on a set of parameters defined by the walking environment (Open Source Routing Machine, 2024a; OpenRouteService, 2024d). For ORS, some parameters, such as maximum inclination or minimum surface type, are manually adjustable to a certain extent (Table 2.1). However, it is not possible to modify travel speed based on individual characteristics, such as unique pedestrian attributes, including individual travel speed for inclined surfaces influenced by mobility capabilities. The travel speed for SPAAR's travel time calculations, which consider the impacts on travel speed mentioned in Section 2.2.3, was determined based on the speed measurements provided by Aghabayk et al. (2021) for walking pedestrians.

As travel speed varies according to the parameters introduced in Section 2.2.3, the travel speeds from Aghabayk et al. (2021) for age groups ranging from 18 to 34 and 34 to 55 per inclination categories were averaged (Table 4.6). The group of older adults aged 55+ was not included in the average travel speed calculation. While not all older adults experience mobility impairments, they often encounter similar accessibility challenges, justifying the exclusion of this age group's travel speed values.

Table 4.6: Applied walking speeds for SPAAR, depending on inclines (Aghabayk et al., 2021)

Incline	**Incline Description**	**Travel Speed**
< -6 %	Steep downhill	1.525 m/s
-6 - -2 %	Gentle downhill	1.455 m/s
-2 - 2 %	Level	1.435 m/s
2 - 6 %	Gentle uphill	1.4 m/s
> 6 %	Steep uphill	1.33 m/s

For the mobility-impaired population, travel speeds based on the values provided by Boyce et al. (1999) were utilised, particularly the speeds for manual wheelchair users (Table 4.7). Since ORS returns routes for wheelchair users, only the speeds of manual wheelchair users were considered, rather than averaging the travel speeds of all mobility-impaired individuals mentioned in Boyce et al. (1999).

Table 4.7: Applied travel speeds for SPAAR for mobility-impaired individuals, depending on inclines (Boyce et al., 1999)

Incline	**Incline Description**	**Travel Speed**
< -7 %	Steep downhill	*inaccessible*
-7 - -2 %	Gentle downhill	1.05 m/s
-2 - 2 %	Level	0.69 m/s
2 - 7 %	Gentle uphill	0.7 m/s
> 7 %	Steep uphill	*inaccessible*

Following the definitions of travel speed, the incline of each footpath segment was calculated. With the travel direction now known, unlike the incline calculation presented in Section 4.3.1, inclines were assessed in relation to the direction, where positive inclines indicated travelling uphill and negative values signified travelling downhill. The incline per route segment was computed in accordance with the methodology introduced in Section 4.3.1, although the elevation difference was determined relative to the direction of travel. After calculating the incline, the travel speed for each segment was established using Equation 4.5. Ultimately, the travel speeds for each segment were summarised for the entire route, resulting in the final travel time per route.

Route Complexity

The overall number of turns on a route was examined to assess its complexity. This approach was used in the study conducted by Tannert and Schöning (2018), where the number of turns served to compare the complexity of various routes generated by different routing services, namely Google Maps, ORS, and Routino. Sevtsuk and Basu (2022) supported the assumption that a route's complexity can be estimated using the number of turns. Unlike route length and travel time, OSRM and ORS were not associated with the number of turns. The routes computed by Google Maps were attributed with different *steps* (Google, 2024b). Google (2024b) defined a step as follows:
"A step is the most atomic unit of a direction's route, containing a single step describing a specific, single instruction on the journey."

Based on this attribute, the number of turns in the routes computed by Google Maps could be determined by counting the number of *steps* (Johnson, 2017).

Despite the possibility of deriving the turn counts from the number of *steps*, this method was not utilised to evaluate the complexity of Google Maps routes. Instead, the same method applied to the OSRM, ORS, and SPAAR routes was used to analyse Google Maps routes, facilitating a meaningful comparison between routing services.

A definition of what constituted a turn was required to calculate the number of turns. Hereby, I assumed that a turn is defined as a 45-degree or greater change in direction, following the approach introduced by Sevtsuk and Basu (2022). The number of turns was determined by extracting the coordinates of the routes and computing the vectors representing each segment between consecutive points. Following the calculation of angles between these segments, the angles exceeding 45 degrees, indicative of significant turns in the path, were identified and counted. This count is then returned, providing insight into the complexity and navigational difficulty of the path.

This calculation was conducted for the routes resulting from Google Maps, OSRM, ORS, and SPAAR.

4.5 Statistical Analysis

To complete the analysis of this Master's thesis, the resulting metrics of route length, travel time, and route complexity were analysed for their statistical significance to identify differences between the routing algorithms of Google Maps, OSRM, ORS, and SPAAR. This section is divided into two parts: Firstly, the metrics were examined to determine whether any statistical significance regarding route length, travel time, and route complexity was evident in general. Following the first analysis, a pairwise comparison of routing services for route length, travel time, and route complexity was conducted.

4.5.1 Analysis of Variance ANOVA

The analysis of various metrics was conducted using an *Analysis of Variance (ANOVA)* (Kaufmann & Schering, 2014). Before performing the *ANOVA*, the *Shapiro-Wilk Test* (Shapiro & Wilk, 1965) was applied to ensure that the data was normally distributed. The *Shapiro-Wilk Test*, executed with the function *shapiro.test* from the *stats* package in R, evaluates whether a dataset originates from a normally distributed population (RDocumentation, 2024c). This is accomplished by examining the correlation between the data and the corresponding normal scores. A significant result indicates a departure from a normal distribution (Ghasemi & Zahediasl, 2012). This was followed by *Levene's Test* (Levene, 1960), carried out using the function *leveneTest* from the R package *car* (Fox & Ogle, 2024). It assesses whether multiple groups have equal variances, a crucial assumption of an *ANOVA*. The null hypothesis posits that all group variances are equal; a significant result suggests variance disparities among groups (STHDA, 2024a).

After analysing the variances of groups using the *Levene's Test*, an *ANOVA* was performed with the function *aov* from the package *stats* (RDocumentation, 2024a). This test assesses whether there are statistically significant differences between the means of independent groups. *ANOVA* assumes that the groups have equal variances (homogeneity of variance) and that the data is normally distributed. When these assumptions were met, the *aov* function was suitable for determining if at least one group mean differs from the others (STHDA, 2024b). However, when the assumption of equal variances was violated, as indicated by the *Levene's Test*, a *Welch's ANOVA* (Welch, 1951) was utilised via the *oneway.test* function from the *stats* package (RDocumentation, 2024b). *Welch's ANOVA* does not require equal variances and is therefore more robust in scenarios where this assumption is not fulfilled (Bobbitt, 2021). To conduct the analysis of variances, *aov* was applied to assess the number of turns, as the *Levene's Test* indicated that the variances between groups were homogeneous. In contrast, the *Levene's Test* suggested that the variances between groups for route length and travel time were heterogeneous, resulting in the application of the *Welch's ANOVA* for further analysis.

To analyse the significance of the conducted *ANOVAs*, either a *Tukey Honest Significance Difference Test* (Tukey, 1949) or a *Games-Howell post hoc Test* (Games & Howell, 1976) was conducted. The test for *Tukey Honest Significance Difference (TukeyHSD)* is a procedure for comparing pairs of means from different groups while controlling the family-wise error rate, i.e., the probability of making one or more Type I errors across all comparisons. The critical value is determined based on the studentised range distribution (Montgomery, 2017; Schlegel, 2016b). It assumes equal variances between groups (homogeneity of variances) (Schlegel, 2016a).

The *Games-Howell post hoc Test* is a non-parametric approach that facilitates the comparison of different groups. In contrast to the *TukeyHSD Test*, the *Games-Howell post hoc Test* does not assume equal variances between groups, meaning it can be employed when the assumption of homogeneity of variances is violated. It is structured based on *Welch's degrees of freedom correction* and utilises *Tukey's studentised range distribution* to compute p-values. The post hoc test provides confidence intervals for differences between group means and examines them for each pair. Consequently, it assesses whether differences between group means are statistically significant (Kassambara, 2023; Schlegel, 2016a).

These steps were applied to all analyses conducted. First, I evaluated whether there were significant differences in route length, travel time, and route complexity between routes suggested for wheelchair users and those recommended for individuals without mobility impairments. Additionally, an analysis was undertaken to determine whether the routes suggested by various routing services differed significantly in terms of route lengths, travel times, and route complexities.

4.5.2 Pairwise Comparison

A pairwise comparison of routing services was conducted to evaluate the length, travel time, and complexity, i.e., number of turns, of the generated routes.

Following the *ANOVA*, which indicated significant differences in the means of travel time, route length, and the number of turns per routing service, post hoc tests were employed to compare these metrics by routing service pair (Montgomery, 2017). Such post hoc tests are essential for gaining deeper insights into the patterns of specific groups, in this case, the various routing services applied and allow for a comparison of their means (Schlegel, 2016b). Depending on the outcome of the *Levene's Test* for homogeneity of variance across groups, a post hoc test with *Tukey Honest Significance Difference* or a *Games-Howell post hoc Test* were applied to determine whether the means of route length, travel time, and route complexity significantly differ between routing algorithms (Montgomery, 2017; Schlegel, 2016a).

If the *Levene's Test* indicated that the variances of route length, travel time, or the number of turns were homogeneous, the *TukeyHSD* test was conducted. In contrast, if the *Levene's Test* indicated that the variances across these variables were heterogeneous, the *Games-Howell post hoc Test* was performed. The applied *Levene's Test* demonstrated that the variances for route length and the number of turns across routing services were homogeneous, while for travel time, it indicated that the variances were heterogeneous. To compute the *TukeyHSD* for route length and the number of turns, the function *tukey_hsd* from the R *rstatix* package was used (Kassambara, 2023). Due to the heterogeneity of variances for the travel time values, the *Games-Howell post hoc Test* was applied. To compare the resulting travel times in R, the function *games_howell_test* from the package *rstatix* was employed (Kassambara, 2023).

A heatmap was created to visualise the results of the pairwise comparison, i.e. the outputs of the test for *TukeyHSD* and the *Games-Howell post hoc Test*. For a straightforward overview, the resulting p-values were classified. This classification is performed automatically for both the *Games-Howell post hoc Test* and the *TukeyHSD Test*. Even though Kassambara (2023) did not explicitly mention the thresholds for p-value significance classification in the *games_howell_test* function, the p-value thresholds for other functions within the same R package are known and consistent throughout the entire package (Table 4.8). Therefore, I assumed that the same p-value thresholds were used to classify the significance level. This assumption was confirmed when comparing the classifications to the p-values themselves.

Table 4.8: p-value and significance level classification (Kassambara, 2023)

p-value	**Significance Level**
$0.05 \leq p \leq 1$	ns (not significant)
$0.01 \leq p < 0.05$	*
$0.001 \leq p < 0.01$	**
$0.0001 \leq p < 0.001$	***
$0 \leq p < 0.0001$	****

5 Results

The results of the analysis are presented and detailed in the following sections. To localise spatial patterns, Figure 5.1 provides an overview of District 1, including neighbourhoods based on statistical zones (Stadt Zürich, 2024d), the rivers Schanzengraben and Limmat, and Lake Zurich (Kanton Zürich, 2024b).

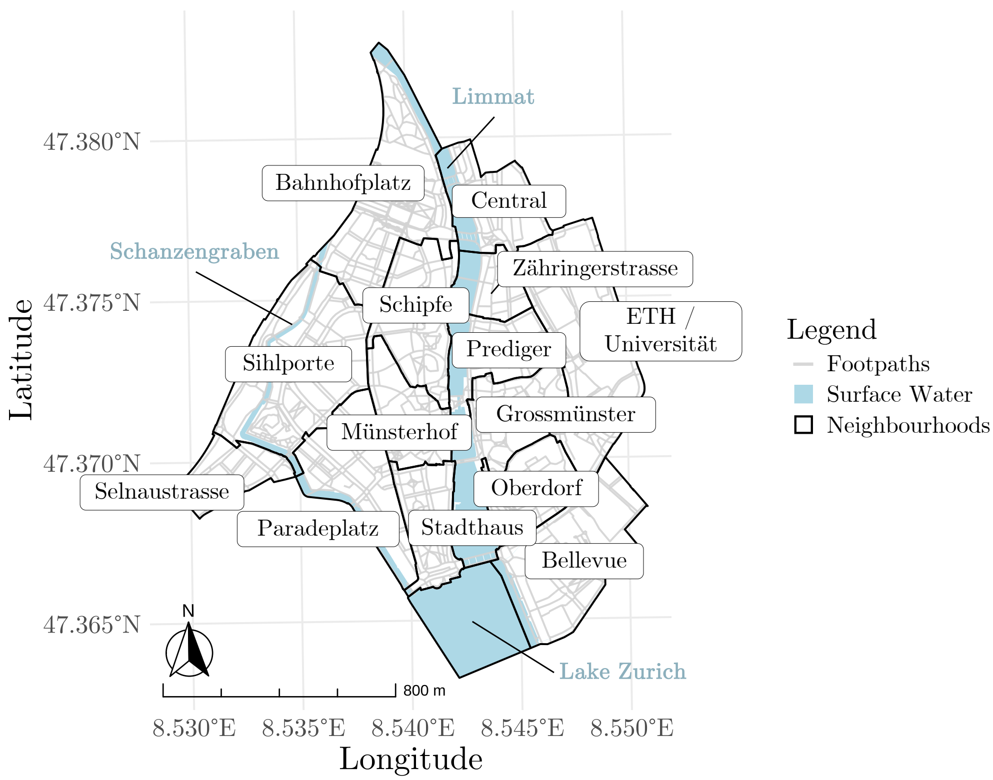

Figure 5.1: Overview of District 1

5.1 Clustering and Aggregation

Several preprocessing steps increased the number of spatial accessibility features from 8'909 raw data points to 13'850 data points. Subsequent data clustering and aggregation reduced this number to 4'841 spatial accessibility features (Section 4.2). These resulting features were ultimately used to enrich the footpath network of District 1 by allocating the features to the network (Section 4.3.1).

Figure 5.2 highlights substantial variability in the number of spatial accessibility features across categories, as also indicated in Table 5.1. Prior to clustering and aggregation, categories such as *curb* *ramp*, *surface problem*, and *rail/tram track* exhibited the highest feature counts, whereas categories like *missing curb ramp*, *no sidewalk*, and *shared space* (excluded from the final analysis) had comparatively fewer features.

Table 5.1 and Figure 5.2 illustrate the changes in feature count through clustering and aggregating spatial accessibility features representing the same object. The reduction was particularly pronounced in the categories *curb ramp*, *surface problem*, *surface material type*, *rail/tram track*, *crosswalk*, and *pedestrian signal*, where feature counts decreased by more than 50%. The most significant reduction occurred in the category *rail/tram track*, with a feature count declining from 4'824 to 999.

While the reduction for *obstacle* and *height difference* features was less dramatic, a clear decrease was still evident.

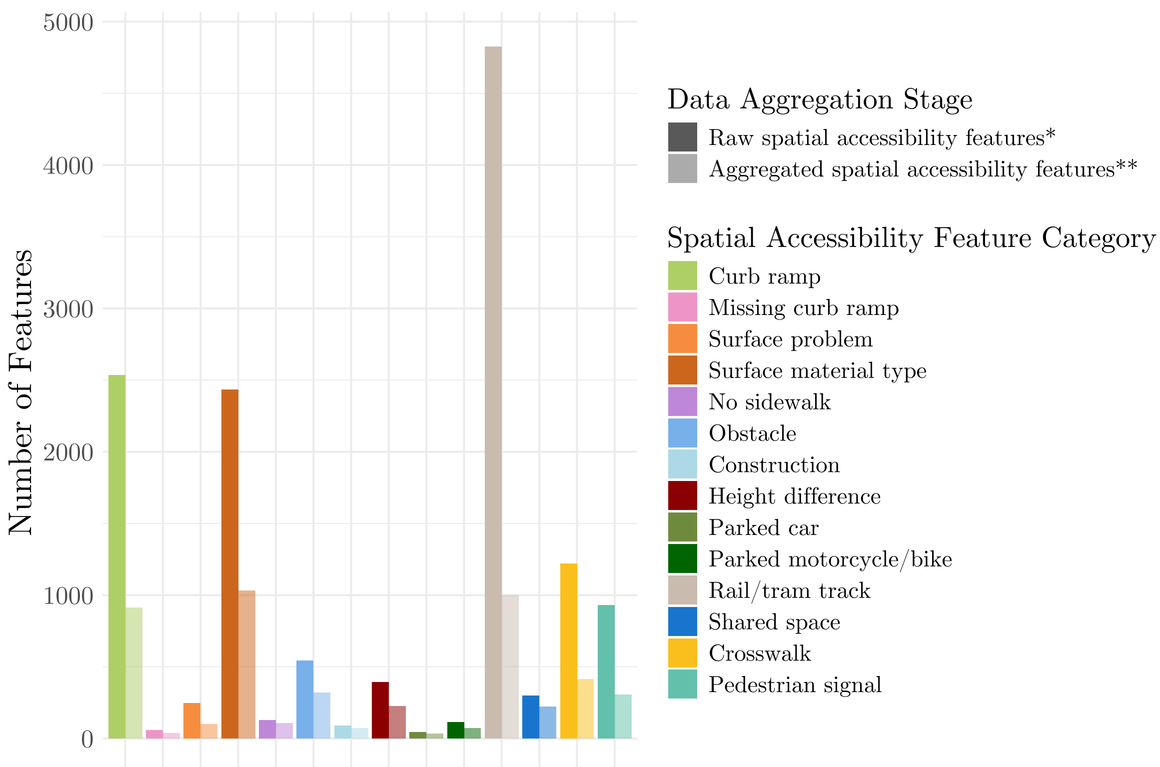

Figure 5.2: Spatial accessibility features before(*) and after(**) cluster generation and aggregation

In contrast, the categories *missing curb ramp*, *no sidewalk*, *construction*, *shared space*, *parked car*, and *parked motorcycle/bike* were less influenced by the clustering and aggregation process. Nevertheless, a modest reduction in feature counts was still evident for these categories.

The significant reduction in the feature categories *curb ramp*, *surface material type*, *crosswalk*, and *pedestrian signal* can be attributed to the initially high number of collected features within each category. This suggests that clustering and aggregation were most impactful for categories characterised by high spatial density or redundancy. Therefore, the marked feature reduction for these spatial accessibility categories through clustering and aggregation supports the conclusion that multiple data points existed and were used to identify the same object, particularly for the previously mentioned categories. In contrast, for categories with fewer initial features (e.g., *missing curb ramp* and *shared space*), the reduction is relatively modest, indicating less redundancy in these features.

Table 5.1: Reduction of spatial accessibility features through clustering and aggregation

Spatial Accessibility Feature Category	**Number of Raw Spatial Accessibility Features***	**Number of Aggregated Spatial Accessibility Features****
Curb ramp	2'534	911
Missing curb ramp	57	36
Surface problem	247	98
Surface material type	2'434	1'032
No sidewalk	126	105
Obstacle	544	320
Construction	89	71
Height difference	391	224
Parked car	43	32
Parked motorcycle/bike	115	72
Rail/tram track	4'824	999
Shared space	298	222
Crosswalk	1'220	415
Pedestrian signal	928	304

* before clustering and aggregation
** after clustering and aggregation

The spatial distribution of spatial accessibility feature points before and after the clustering and aggregation steps is presented in Figure 5.4 (before) and Figure 5.5 (after), respectively.

As the results illustrate, the number of *surface material type* features is among the highest counts per category, alongside *rail/tram track* and *curb ramp*. The significant number of *surface material type* points in District 1 (Figure 5.5) suggests that distinct footpath surfaces are present in the neighbourhoods of Schipfe and Grossmünster (Figure 5.1), with cobblestones being the most frequently recorded for *surface material type* features. In addition to cobblestones, the *surface material type* also includes gravel, sand, or grass surfaces. Nonetheless, the 939 *surface material type* points representing cobblestone surfaces considerably outnumber those of other materials. Only 93 points do not reflect cobblestone surfaces, which solely indicate sand/gravel surfaces, potentially combined with other surfaces (3 points). The 90 sand/gravel data points are primarily situated on Lindenhof, a square in the Schipfe neighbourhood, and Stadelhoferplatz in the Bellevue neighbourhood (Figure 5.3). Additional sand/gravel surface data points are found on the Sigi-Feigel-Terrasse, Platzspitz, and on the footpath located south of the Landesmuseum, all indicating unpaved surfaces (Figure 5.3).

Therefore, the clear pattern of the spatial accessibility feature category *surface material type* illustrated in Figure 5.5 almost exclusively indicates the presence of cobblestones in District 1, with the exception of squares such as Lindenhof and Stadelhoferplatz.
Furthermore, Figure 5.5 reveals that *crosswalk* points are situated at intersections, often accompanied

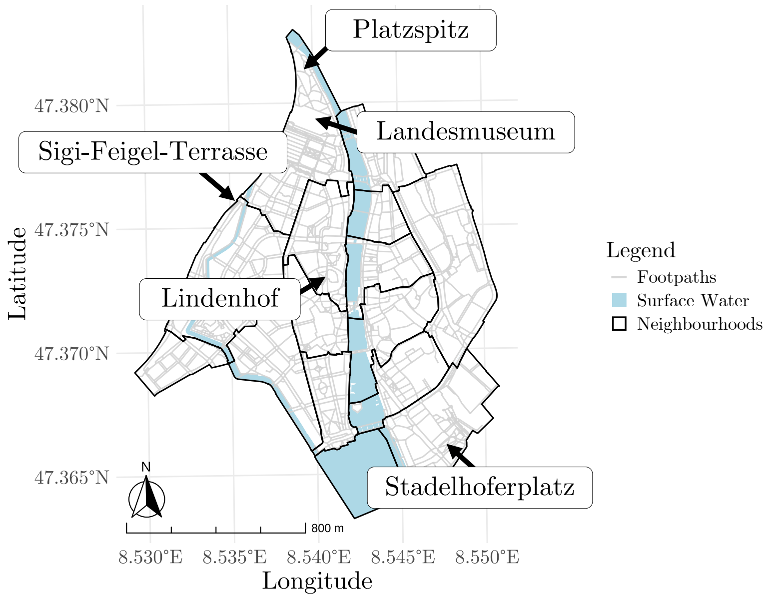

Figure 5.3: Locations of *surface material type* features indicating sand and gravel surfaces

by *pedestrian signal* features. Notably, the spatial distribution of *rail/tram track* features strikingly indicates where trams operate in District 1 (Figure 5.5).

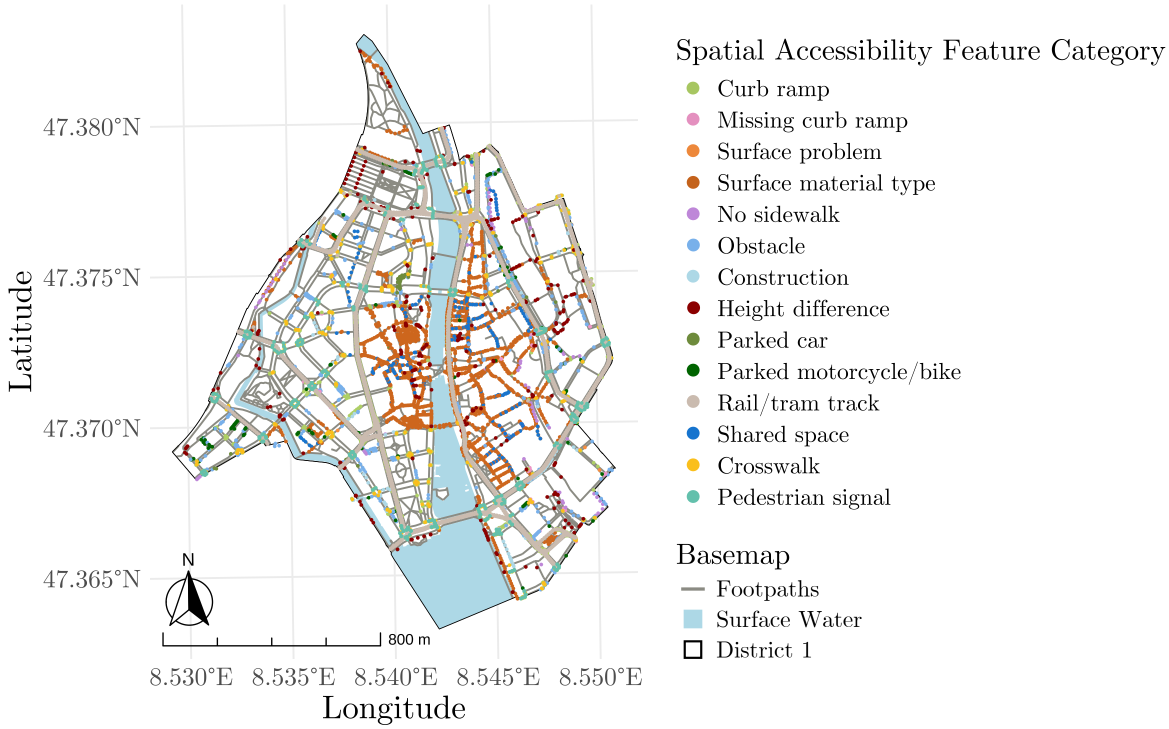

Figure 5.4: Results after revision of spatial accessibility feature categories

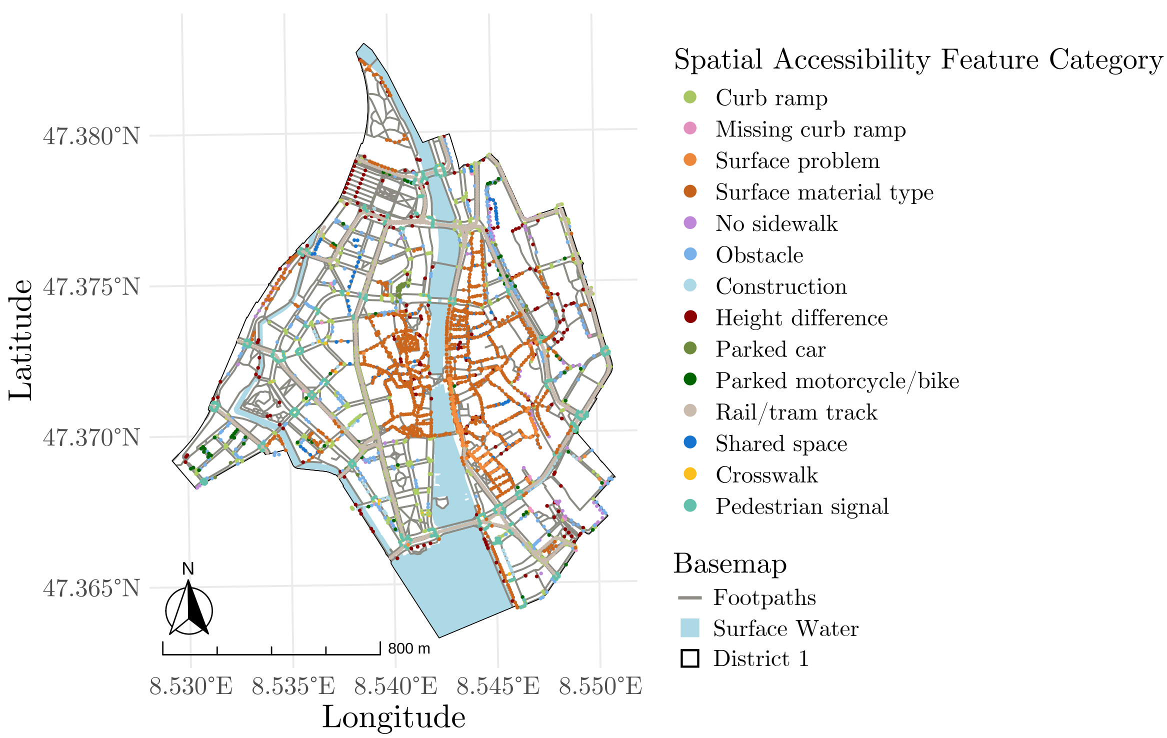

Figure 5.5: Results after cluster creation and aggregation of spatial accessibility features

5.2 Enriched Network

The *Access Scores*, based on the enriched footpaths, provided the foundation for routing by treating inaccessibility as a cost. This approach enables the identification of spatial (in)accessibility patterns within District 1 of the City of Zurich. The *Access Scores* for each footpath segment were calculated based on permanent spatial accessibility features ($Access\ Score_{permanent}$) and all spatial accessibility features ($Access\ Score_{all}$). The results are fully visualised in Figures 5.9 and 5.10.

Both figures highlight that accessibility in District 1 is generally high, with some notable exceptions in specific areas (locations indicated in Figure 5.6a). Reduced accessibility is observed in parts of the historic old town, such as the area between Central and Grossmünster on the east side of the river Limmat and the area around Lindenhof on the west side of the river Limmat. Additionally, regions around the Stadelhofen train station, Hohe Promenade, and the area west of Polyterrasse show increased inaccessibility. While most of District 1 on the west side of the Limmat demonstrates high accessibility, the Alter Botanischer Garten area stands out with a higher level of inaccessibility.

Footpath segments representing crosswalks and crossings display consistently high accessibility, attributed to the presence of spatial accessibility features such as *crosswalks*, *curb ramps*, and *pedestrian signals*. At intersections where all three features are present, their positive impact on accessibility is particularly pronounced (locations indicated in Figure 5.6b), exemplified by locations like the Sihlporte intersection and Pelikanplatz. Likewise, segments with lowered curbs, such as those on Bahnhofstrasse or Limmatquai, exhibit enhanced accessibility.

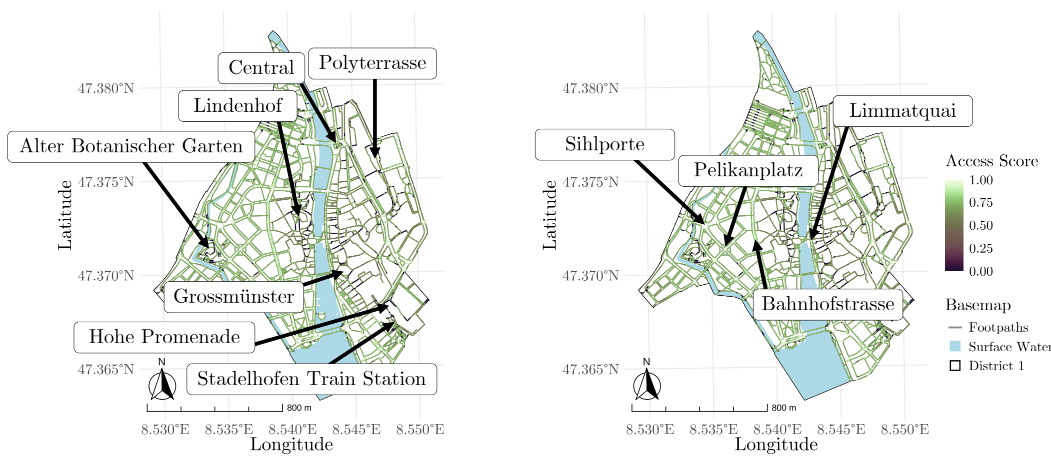

(a) Low accessibility locations

(b) High accessibility locations

Figure 5.6: Locations with particularly high and low accessibility

A comparison of $Access\ Score_{permanent}$ and $Access\ Score_{all}$ highlights the impact of temporary spatial accessibility features (locations indicated in Figure 5.7). For instance, the southern section of Talstrasse, situated in the neighbourhood of Paradeplatz, displays segments obstructed by temporary obstacles. Furthermore, footpaths on Bärengasse and Poststrasse experience reduced accessibility due to temporary spatial accessibility features. In the neighbourhoods of Bellevue and Bahnhofplatz, temporary features are distributed sporadically. Notably, none of the temporary spatial accessibility features were found to enhance the *Access Score*.

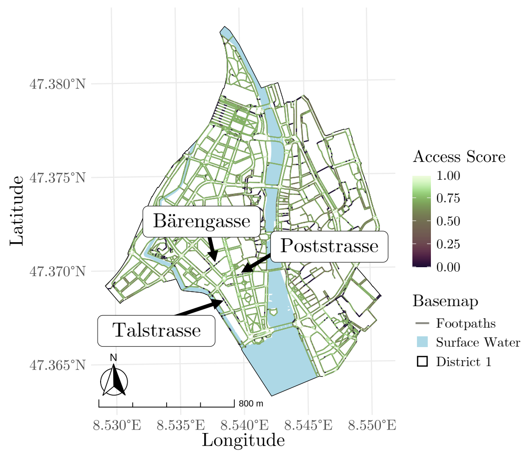

Figure 5.7: Locations with temporary obstacles

The distributions of $Access\ Score_{permanent}$ and $Access\ Score_{all}$ are illustrated in Figure 5.8. The average value for $Access\ Score_{permanent}$ is 0.672, which is slightly higher than the 0.667 average for $Access\ Score_{all}$. Both distributions show that most footpath segments achieve an *Access Score* greater than 0.5. Segments with an *Access Score* of 0.0, indicating complete inaccessibility, were automatically designated this value due to the existence of spatial accessibility features, such as steps or stairs, that completely obstruct movement for individuals with mobility impairments. Differences between the distributions are evident in the range from 0.6 to 0.75, with $Access\ Score_{permanent}$ exhibiting more segments in the upper part of this range, while $Access\ Score_{all}$ shows a greater concentration in the lower part.

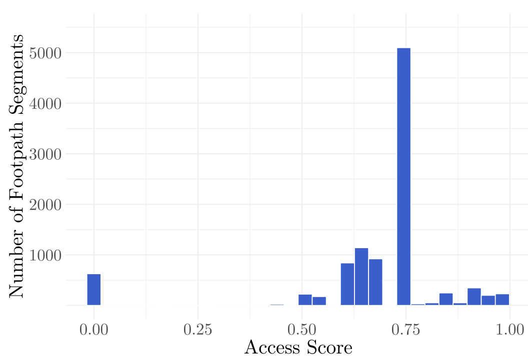

(a) $Access\ Score_{permanent}$

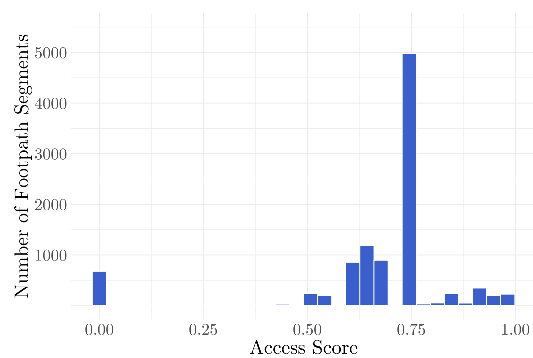

(b) $Access\ Score_{all}$

Figure 5.8: Distribution of footpath-level *Access Scores*

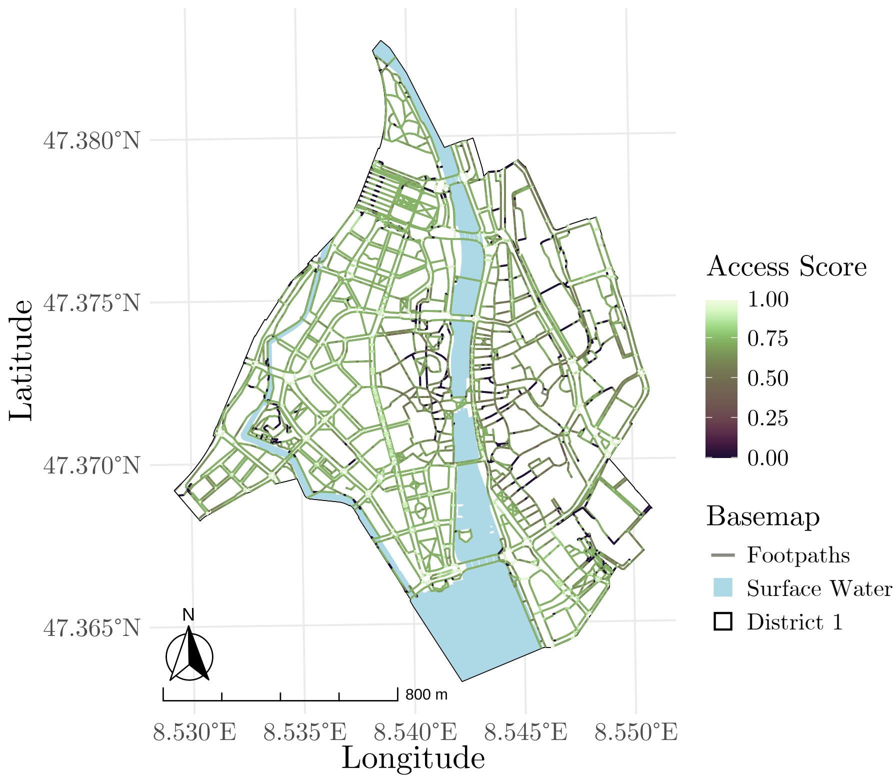

Figure 5.9: Footpath-level *Access Score* considering permanent spatial accessibility features only (*Access Score*$_{permanent}$); high values represent high accessibility

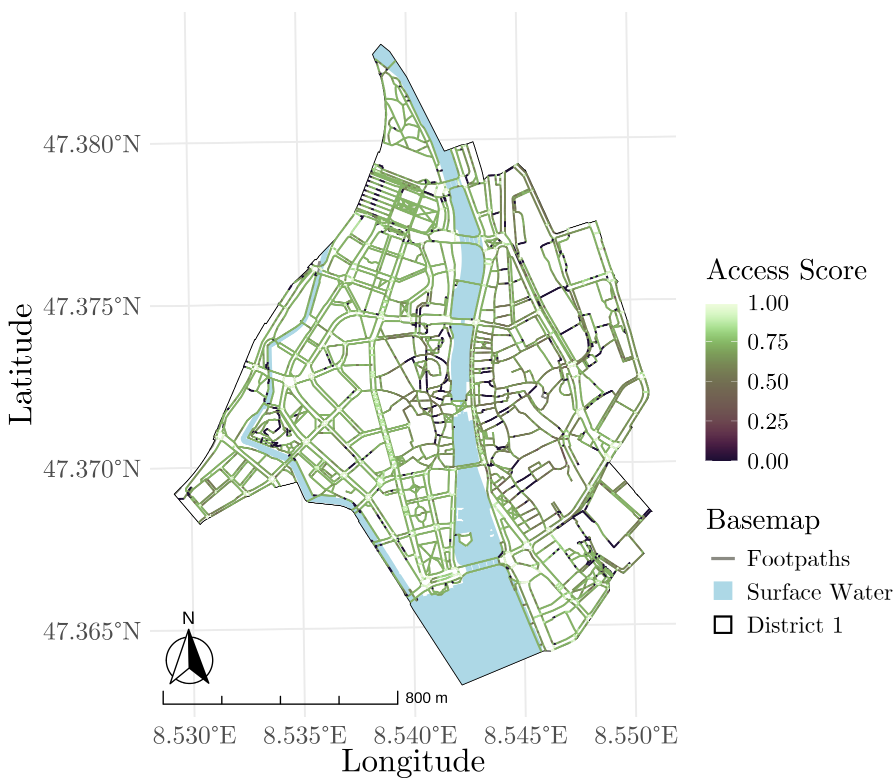

Figure 5.10: Footpath-level access score considering all spatial accessibility features (*Access Score*$_{all}$); high values represent high accessibility

From the footpath-level *Access Scores*, *Access Scores* at the neighbourhood level were computed and visualised in Figure 5.12 for *Neighbourhood Access Score*$_{permanent}$ and in Figure 5.13 for *Neighbourhood Access Score*$_{all}$. To better capture the differences between neighbourhoods and the two *Access Scores*, the colour gradient encompasses only the range in which *Access Score* values exist.

Generally, accessibility is higher on the west side of the river Limmat. The most significant *Access Score*$_{all}$ value at the neighbourhood level is 0.74, found in the Stadthaus neighbourhood. The neighbourhood of Schipfe is an exception on the Limmat's west side, with a relatively low *Access Score*$_{all}$ of 0.64. Similar values are observed for *Access Score*$_{permanent}$. On the east side of the Limmat, the lowest *Access Score*$_{all}$ value of 0.59 across all neighbourhoods can be found in Grossmünster. Aside from the neighbourhoods of Oberdorf (*Access Score*$_{permanent}$ of 0.61) and Zähringerstrasse (*Access Score*$_{permanent}$ of 0.68), the *Access Score*$_{permanent}$ ranges from 0.64 to 0.65 on the east side of the Limmat.

As depicted in Figures 5.12 and 5.13, the difference between *Neighbourhood Access Score*$_{permanent}$ and *Neighbourhood Access Score*$_{all}$ is minor. Only in the neighbourhood of Paradeplatz does a visual difference exist between the *Access Score* calculated based on permanent features and the *Access Score* that considers all features. Consequently, this difference arises from temporary spatial accessibility features. This area was previously identified in the footpath-level *Access Score* as being influenced by temporary spatial accessibility features. The most significant difference of 0.024 between *Neighbourhood Access Score*$_{permanent}$ and *Neighbourhood Access Score*$_{all}$ is found in Paradeplatz, while the differences in other neighbourhoods are minor. For Sihlporte, Selnaustrasse, Stadthaus, Bellevue, ETH/Universität, and Central, the differences between the two *Neighbourhood Access Scores* range from 0.005 to 0.010. These differences are even smaller for the neighbourhoods of Bahnhofplatz, Schipfe, Münsterhof, Oberdorf, Grossmünster, Prediger, and Zähringerstrasse, ranging from 0.000 to 0.005.

The distribution of *Neighbourhood Access Score*$_{permanent}$ and *Neighbourhood Access Score*$_{all}$ is illustrated in Figure 5.11. As *Neighbourhood Access Scores* typically range between 0.5 and 0.8, the figures are limited to this range for better visualisation. The average value for *Neighbourhood Access Score*$_{permanent}$ is 0.669, decreasing slightly to 0.664 for *Neighbourhood Access Score*$_{all}$. Figure 5.11 indicates that for *Neighbourhood Access Score*$_{all}$, the values are marginally lower than those of *Neighbourhood Access Score*$_{permanent}$. Particularly around the *Access Score* values of 0.65 and 0.70, neighbourhoods exhibit a shift to lower values from *Neighbourhood Access Score*$_{permanent}$ to *Neighbourhood Access Score*$_{all}$ when considering all spatial accessibility features.

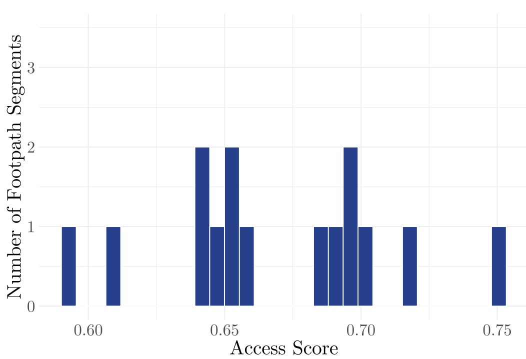

(a) *Neighbourhood Access Score*$_{permanent}$

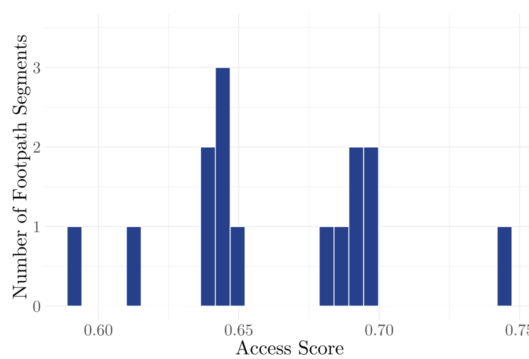

(b) *Neighbourhood Access Score*$_{all}$

Figure 5.11: Distribution of neighbourhood-level *Access Scores*

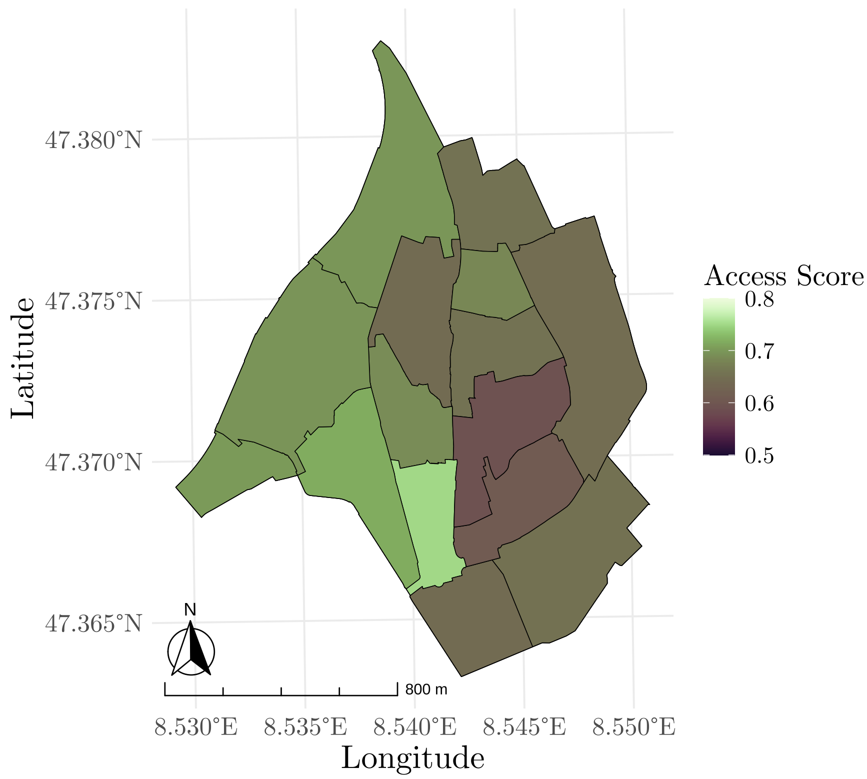

Figure 5.12: Neighbourhood-level *Access Score* considering permanent spatial accessibility features only (*Neighbourhood Access Score*$_{permanent}$); high values represent high accessibility

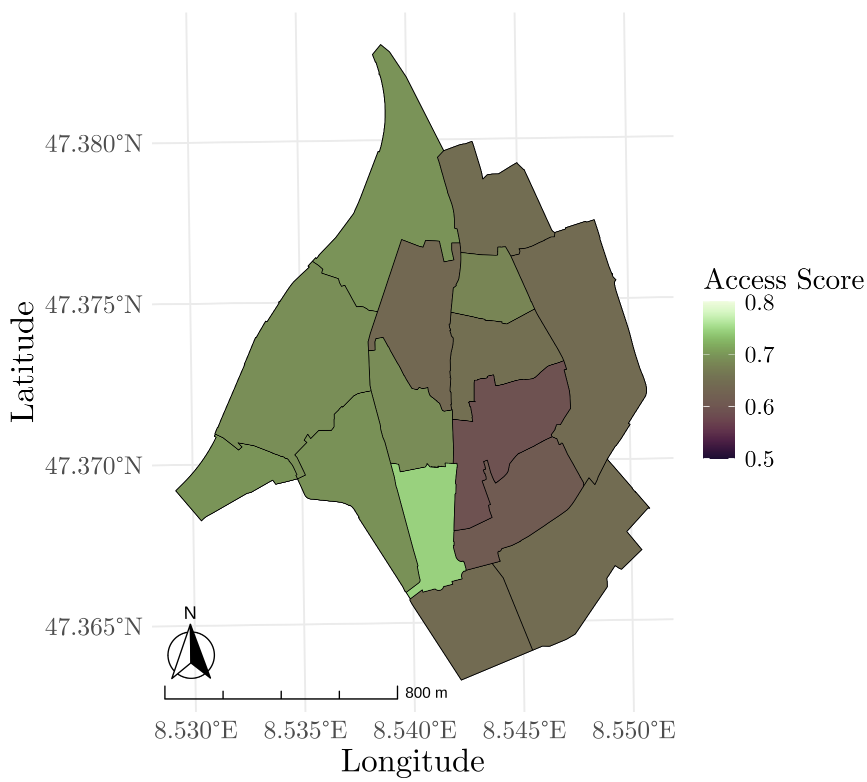

Figure 5.13: Neighbourhood-level *Access Score* considering all spatial accessibility features (*Neighbourhood Access Score*$_{all}$); high values represent high accessibility

5.3 Navigation and Routing

Based on 30 origin-destination pairs, routes for pedestrians were proposed by Google Maps, the Open Source Routing Machine (OSRM), OpenRouteService (ORS), and Dijkstra's Shortest Path Algorithm for Accessible Routing (SPAAR). Google Maps, i.e. Google's Directions API, and OSRM only suggested routes suitable for walking profiles, whereas ORS and SPAAR also provided wheelchair-accessible routes. Furthermore, SPAAR allowed temporary obstacles to be considered. Appendix A visualises all routes grouped by origin-destination pair. The number of resulting routes for each routing service across the 30 origin-destination pairs is summarised in Table 5.2, which includes the names used to distinguish the routing services and their suggested routes.

Table 5.2: Routing services and routes per service

Routing Services	**Name**	**Number of Routes**
Google Maps	Google Maps	30
Open Source Routing Machine (OSRM)	Open Source Routing Machine (OSRM)	30
OpenRouteService (ORS)	OpenRouteService (ORS), walking	30
	OpenRouteService (ORS), rolling	30
Dijkstra Shortest Path Algorithm for Accessible Routing (SPAAR)	SPAAR, walking	30
	SPAAR, rolling, all obstacles	30
	SPAAR, rolling, permanent obstacles	30

A total of 210 routes were generated from the 30 origin-destination pairs. The suggested routes can be grouped into two profiles: *walking* and *using a wheelchair (rolling).* Since only ORS and SPAAR provide wheelchair-accessible routes, 90 of the 210 routes (30 each for ORS, rolling; SPAAR, rolling, all obstacles; and SPAAR, rolling, permanent obstacles) consider accessibility. The remaining 120 routes (30 each for Google Maps; OSRM; ORS, walking; and SPAAR, walking) were proposed for walking profiles. Before analysing the impact of individual routing services, the influence of travel profiles, namely walking or using a wheelchair (rolling), was evaluated. Statistical analyses included a *Welch's ANOVA* for travel time and route length, as well as a standard *ANOVA* for the number of turns. The results indicate that the travel profile significantly affects route length, travel time, and route complexity, i.e., the number of turns. Post hoc tests revealed that wheelchair-accessible routes are, on average, 335.1 metres (m) longer and take 741.4 seconds (s) more. Additionally, walking between the origin and destinations involves, on average, 4.6 turns less than when using a wheelchair between the two locations.

The following sections summarise the resulting effects of routing services across three metrics: route length, travel time, and route complexity, commonly represented by the number of turns.

5.3.1 Routing Services Comparison

To compare the routes suggested by Google Maps, OSRM, ORS, and SPAAR, the routes were grouped according to length following the approach introduced by Tannert and Schöning (2018). For this purpose, the length of the shortest path, based on SPAAR walking, was determined for each origin-destination pair, in contrast to Tannert and Schöning (2018), who grouped routes based on straight-line distances between origin and destination locations. Depending on the resulting length, the origin-destination pairs were categorised into one of three groups: 0-600 m length, >600-1200 m length, and >1200-1800 m length. The routes were assigned as follows:

- **0-600 m:** Routes 10, 19, 25, 28
- **>600-1200 m:** Routes 1, 2, 3, 5, 7, 9, 12, 14, 16, 17, 18, 20, 21, 23, 24, 26, 27, 30
- **>1200-1800 m:** Routes 4, 6, 8, 11, 13, 15, 22, 29

The following sections compare routing services based on length, travel time, and complexity, i.e., number of turns, of the suggested routes.

Route Length

The lengths of the total 210 routes were grouped into the three previously introduced intervals. Figure 5.14 illustrates the distribution of route lengths proposed by various routing services, categorised into these three intervals.

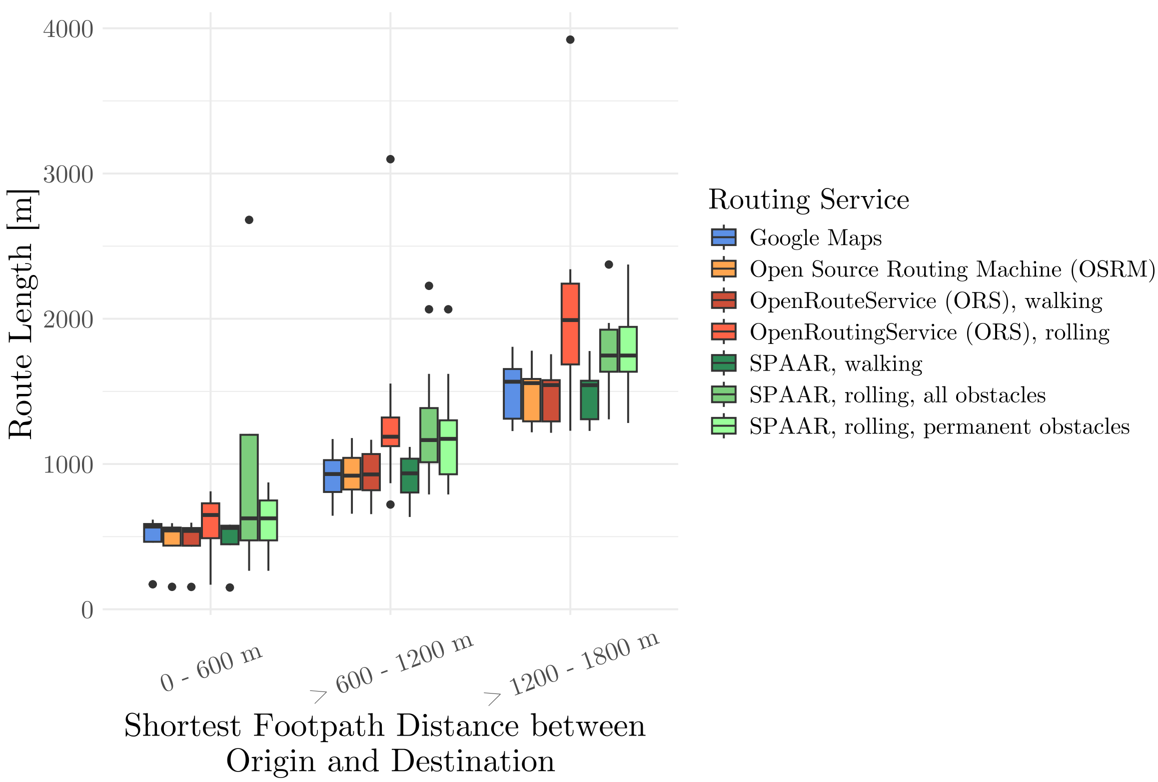

Figure 5.14: Route lengths resulting from all routing services

The results indicate distinct patterns in route lengths across the routing services and footpath distance categories. Most services generate relatively similar route lengths for shorter distances (0-600 m), although ORS rolling and SPAAR rolling routes occasionally suggest longer paths. As footpath distances increase, the variability in route lengths becomes more pronounced, particularly for the rolling profiles (ORS and SPAAR). This is particularly evident in the upper two length intervals >600-1200 m and >1200-1800 m categories, where rolling routes from ORS and SPAAR exhibit longer median lengths and greater variability compared to walking profiles.

Notably, ORS and SPAAR routes generated for wheelchair users (rolling) tend to be longer than walking routes, reflecting the additional constraints imposed for routing suggestions. This aligns with the findings of the statistical analysis assessing the impact of travel profiles on route length. In contrast, walking routes generated by Google Maps, OSRM, ORS, and SPAAR demonstrate similar outcomes in route length, even with increasing distance between origin and destination.

In summary, walking routes are generally shorter and less variable, while wheelchair-accessible routes are longer, exhibiting greater variability, particularly for SPAAR rolling profiles. These differences underscore the influence of accessibility considerations and routing algorithms on suggested route lengths.

Table 5.3: *ANOVA* results for route lengths and routing services

Source	**Df**	**Sum Sq**	**Mean Sq**	**F value**	**Pr(>F)**
Routing Services	6	6’110’176	1’018’363	4.333	0.000388
Residuals	203	47’714’734	235’048		

The results of the *ANOVA* examining the effect of routing services on the route length variable indicate a statistically significant relationship (Table 5.3). The factor routing service has 6 degrees of freedom, with a sum of squares of 6’110’176 and a mean square of 1’018’363. The F-value for this factor is

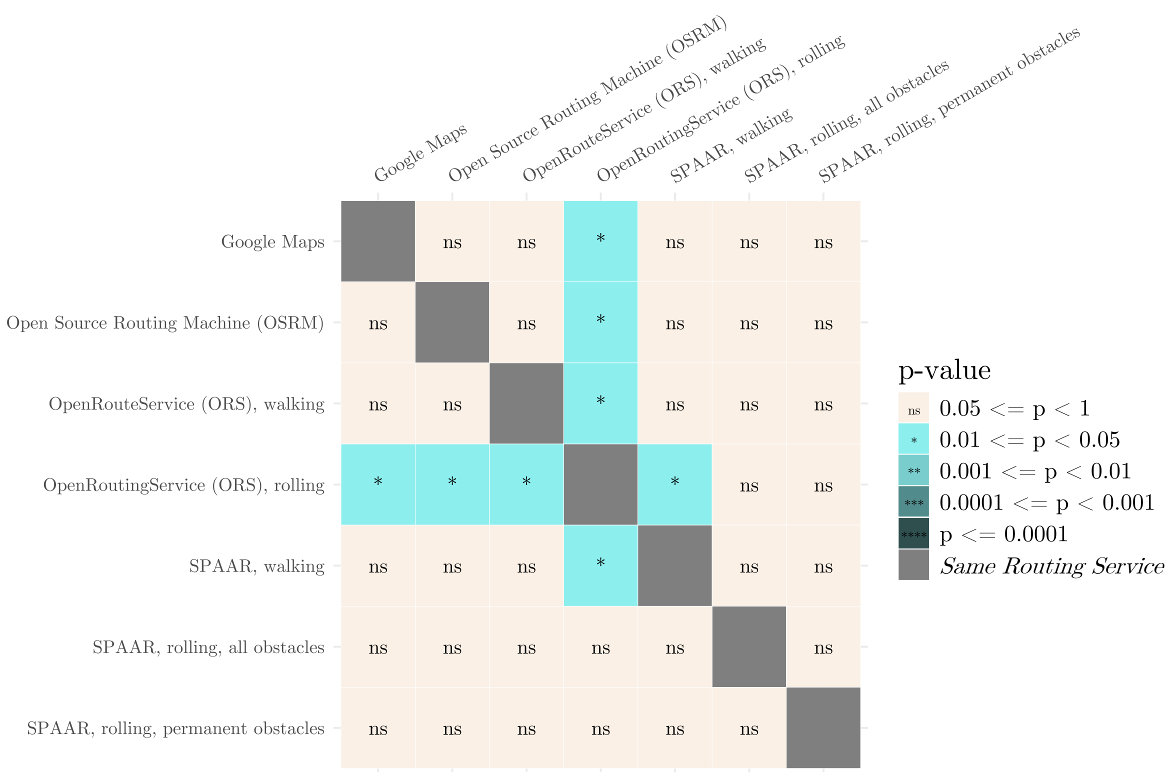

Figure 5.15: Pairwise comparison between routing services of resulting route lengths (*ns: not significant*)

4.333, and the associated p-value is 0.000388, which is much smaller than the commonly used 0.05 significance threshold. This strongly suggests that route length varies significantly across different routing services. The residuals, representing the unexplained variation, have 203 degrees of freedom with a sum of squares of 47'714'734 and a mean square of 235'048. This analysis provides strong evidence that the routing service employed significantly affects the length of the suggested routes.

Following the standard *ANOVA*, a *TukeyHSD post hoc Test* was applied to conduct a pairwise comparison between routing services and their impact on route length. The results are visualised in Figure 5.15. While most routing services generate routes of similar lengths, ORS rolling suggests significantly longer routes than nearly all routing services. Only the SPAAR rolling routes are not significantly different from ORS rolling. This aligns with previous findings that wheelchair-accessible routes are significantly different from walking routes suggested by all routing services. Notably, both SPAAR rolling routes, i.e., those with all obstacles and those with only permanent obstacles, do not differ statistically from other walking routes, despite considerable differences depicted in Figure 5.14.

Travel Time

Following the analysis of route lengths, the travel times of routes and the impact of routing services were assessed and visualised in Figure 5.16. The same route length intervals as mentioned earlier, based on the shortest paths in the footpath network and suggested by SPAAR, were applied for categorisation: 0-600 m, >600-1200 m, and >1200-1800 m.

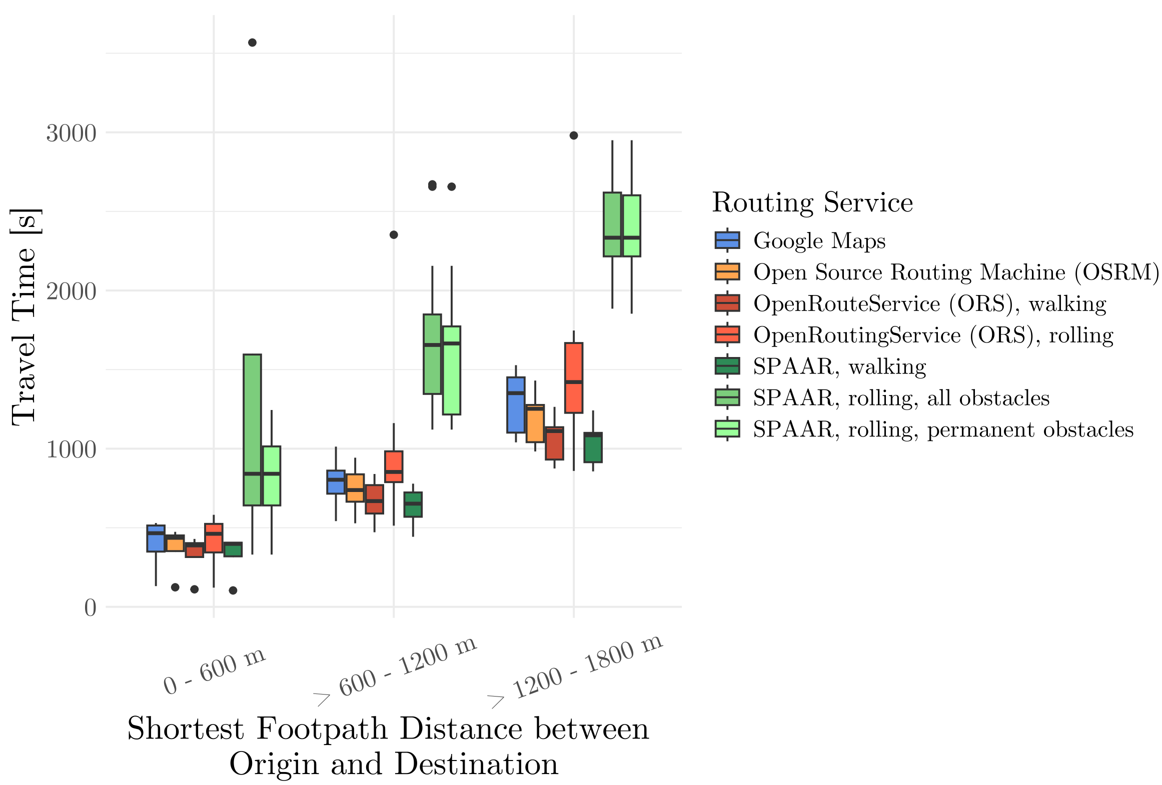

Figure 5.16: Travel times resulting from all routing services

The data reveal noticeable differences in travel times across routing services and distance categories. Travel times for short distances (0-600 m) are similar for most services, except for SPAAR rolling, which exhibits significantly longer travel times. As the distance of the shortest path increases, the variability in travel times becomes more pronounced, particularly for ORS and SPAAR rolling profiles.

In all three distance categories, wheelchair-accessible (rolling) routes tend to have the highest travel times, displaying higher medians than walking profiles. A comparison of suggested rolling routes from ORS and SPAAR indicates that SPAAR consistently shows higher travel times across all distance categories.

In contrast, walking profiles, including Google Maps, OSRM, ORS walking and SPAAR walking, generally suggest shorter and less variable travel times compared to their rolling counterparts. This trend remains consistent across all footpath distance categories, though variability in travel time increases with the length of the route intervals.

In summary, walking routes tend to be associated with shorter travel times and less variability, while wheelchair-accessible routes are linked to longer and more variable travel times, particularly for SPAAR rolling profiles. Statistical analysis of travel time per mode of transport supports these findings.

The results of the *Welch's ANOVA*, conducted to examine the effect of routing services on travel time, demonstrate a statistically significant difference in travel times across these services (Table 5.4). The *Welch's ANOVA* was selected as the *Levene's test* indicated that the assumption of equal variances across groups was violated. The F-statistic for the analysis is 21.596, with 6 numerator degrees of freedom (representing the different routing services) and approximately 89.209 denominator degrees of freedom (accounting for the residual variation). The associated p-value is exceedingly small at 1.607e-15, significantly less than the 0.05 significance level. This highlights that travel time varies significantly among the routing services.

Table 5.4: *ANOVA* results for travel times and routing services

Source	**Df**	**Sum Sq**	**Mean Sq**	**F value**	**Pr(>F)**
Routing Services	6	6'110'176	1'018'363	4.333	1.607e-15
Residuals	89.209				

The statistical analysis of the different impacts of the routing service on travel time was completed by conducting a *Games-Howell post hoc Test* for the pairwise comparison of routing services. The results of the *Games-Howell post hoc Test* are displayed in Figure 5.17. It prominently shows that the rolling routes suggested by SPAAR take significantly longer travel times than those suggested by any other routing services. This was already indicated in Figure 5.16 and is now supported by the statistical analysis. The statistical relationship between SPAAR rolling routes and the routes of other routing services is strongly significant, with p-values lower than 0.0001. The ORS rolling routes are an exception, as their significance level is slightly lower, with p-values between 0.001 and 0.0001.

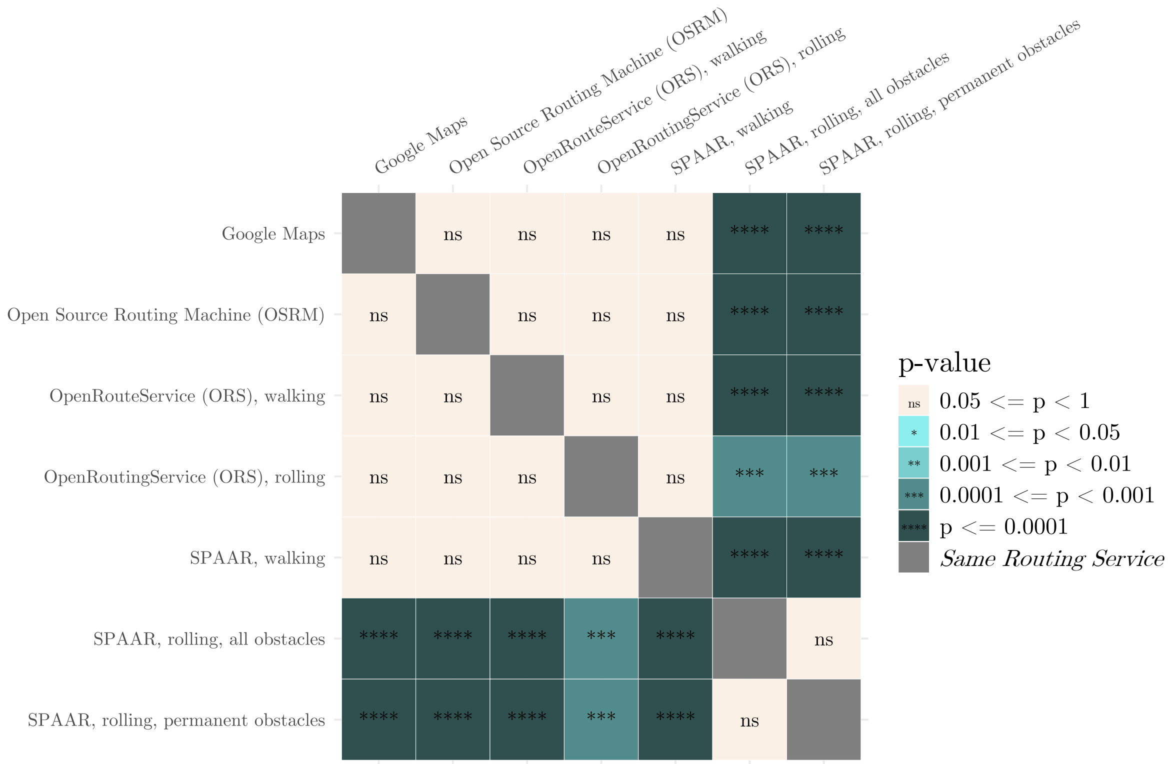

Figure 5.17: Pairwise comparison between routing services of resulting travel times (*ns: not significant*)

Route Complexity

Similarly to route length and travel time, route complexity, as indicated by the number of turns, is categorised into three shortest path distances between origin and destination locations: 0-600 m, >600-1200 m, and >1200-1800 m. The grouped number of turns per routing service is illustrated in Figure 5.18.

Across all distance categories, the number of turns generally increases with the shortest footpath distance, as expected due to the greater complexity associated with longer routes. For routes in the 0-600 m interval, the number of turns remains relatively low and consistent across services. However, some variation is evident, particularly for SPAAR rolling profiles, which exhibit wider variability in turn counts even for short distances.

For intermediate distances (>600-1200 m), Figure 5.18 reveals notable differences between routing services. Walking profiles from Google Maps, OSRM, and SPAAR walking tend to create routes with fewer turns and narrower interquartile ranges than rolling profiles. In contrast, wheelchair-accessible routes consistently show higher median turn counts and greater variability. Interestingly, ORS walking demonstrates a similar route complexity to ORS rolling for intermediate distances.

The distinction between walking and rolling profiles becomes more pronounced in the longest distance category (>1200-1800 m). While walking profiles maintain relatively lower turn counts, wheelchair-accessible profiles (ORS and SPAAR rolling) indicate more turns as well as increased variability across routes. ORS walking shows similar route complexity to other walking routes in this distance category, in contrast to the intermediate distance category.

As distance increases, it becomes increasingly clear that OSRM and SPAAR walking routes involve fewer turns than walking routes generated by other routing services.

Overall, ORS and SPAAR rolling routes require more turns than walking routes, with the differences becoming more pronounced as the shortest footpath distance increases. This is backed by the statistical analysis, which revealed significantly more turns for rolling than walking profiles.

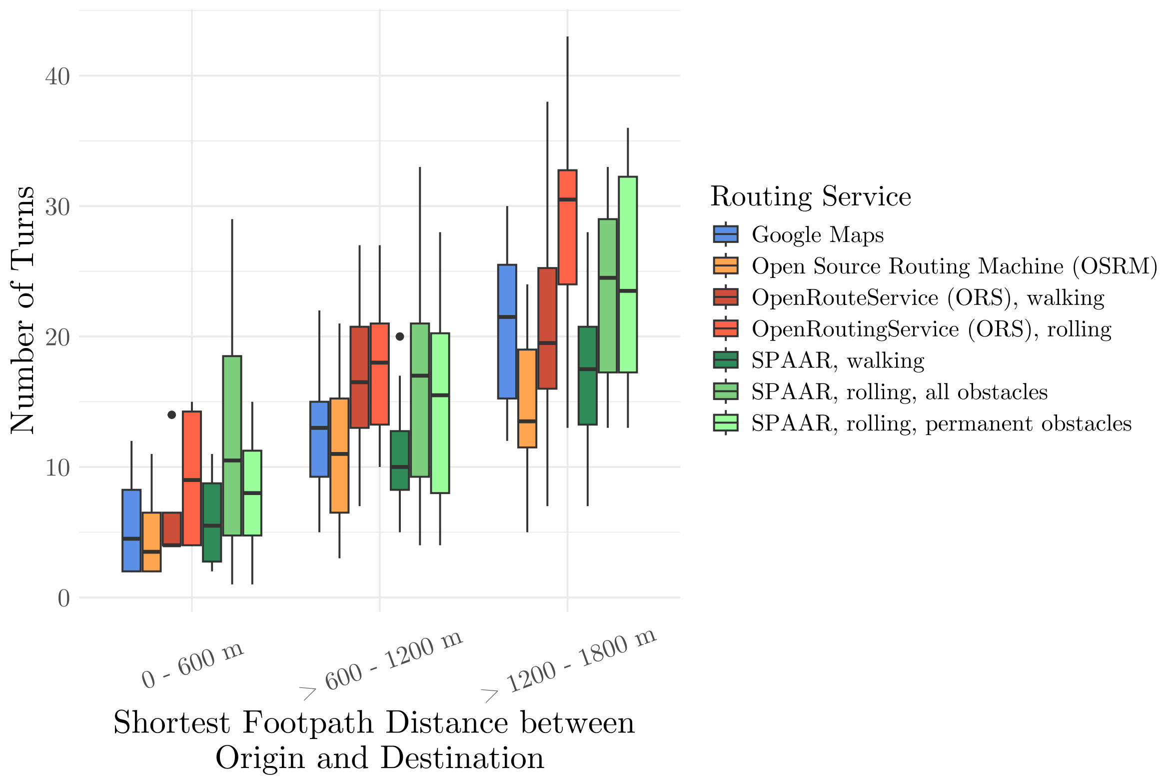

Figure 5.18: Number of turns resulting from all routing services

The results of the applied standard *ANOVA*, summarised in Table 5.5, indicate that the number of turns is significantly influenced by the routing service used. The analysis reveals that the routing services factor has 6 degrees of freedom, with a sum of squares of 1735 and a mean square of 289.15. The corresponding F-value is 4.873, associated with a very small p-value of 0.000113. This p-value is well below the commonly used significance level of 0.05, suggesting that the number of turns varies significantly across the different routing services. The residuals, which represent the variation unexplained by the model, have 203 degrees of freedom and a sum of squares of 12'046, with a mean square of 59.34. These results confirm that the routing service used is a crucial factor in determining the number of turns, with significant differences between the services.

Table 5.5: *ANOVA* results for the number of turns and routing services

Source	**Df**	**Sum Sq**	**Mean Sq**	**F value**	**Pr(>F)**
Routing Service	6	1'735	289.15	4.873	0.000113
Residuals	203	12'046	59.34		

Ultimately, a *TukeyHSD post hoc Test* for route complexity concluded the pairwise comparison of routing services. Route complexity exhibits fewer distinct patterns than the pairwise comparison for route length and travel time (Figure 5.19). Notably, ORS rolling routes demonstrate significantly more turns compared to OSRM, with p-values ranging from 0.001 to 0.0001, and significantly more turns than SPAAR walking routes, with p-values between 0.001 and 0.01. Similarly, SPAAR rolling routes, which account for all obstacles, are found to have significantly more turns than OSRM routes, with p-values ranging from 0.01 to 0.05. Additionally, SPAAR walking routes reveal significantly fewer turns than SPAAR rolling routes that account for all obstacles, highlighting the increased complexity of wheelchair-accessible routing.

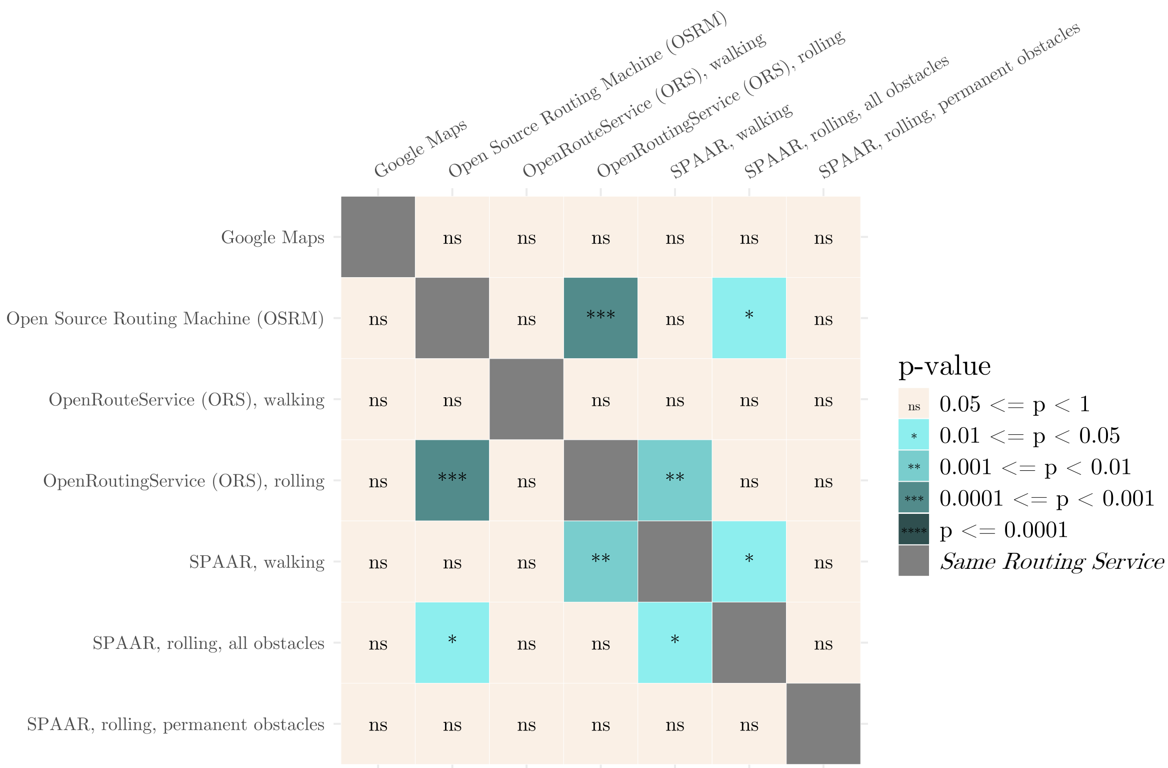

Figure 5.19: Pairwise comparison between routing services of resulting number of turns (*ns: not significant*)

5.3.2 Temporary Obstacles' Influence

To assess the impact of temporary obstacles on the generated routes, the two SPAAR rolling options were compared: one considering only permanent obstacles and the other including all obstacles. Standard *ANOVAs* were employed to test whether the route lengths, travel times, and route complexity of SPAAR rolling differed based on the obstacles considered.

The *ANOVA* results, summarised in Table 5.6, suggest that the presence of obstacles, all obstacles (temporary and permanent) or only temporary obstacles, does not have a statistically significant impact on SPAAR rolling route length, travel time, or route complexity, defined as the number of turns. In each of the three analyses, the p-values exceed the typical threshold of 0.05, indicating that the differences observed between the two groups are likely attributable to random variation rather than a systematic effect of the obstacles.

For route length, the F-value is 0.622 with a p-value of 0.433, indicating that the mean route lengths between the two obstacle groups do not differ significantly. Similarly, for travel time, the F-value is 0.546 with a p-value of 0.463, which again suggests no significant effect of obstacles on travel duration. Lastly, for the number of turns, the F-value is 0.554 with a p-value of 0.460, further corroborating the conclusion that the presence of obstacles does not meaningfully influence route complexity.

Overall, these results suggest that whether all obstacles or only temporary obstacles are considered, there is no significant impact on the analysed route characteristics.

Table 5.6: *ANOVA* results for route lengths, travel times, and number of turns across SPAAR rolling route options

Metric	**Source**	**Df**	**Sum Sq**	**Mean Sq**	**F value**	**Pr(>F)**
Route length	Obstacles	1	168’256	168’256	0.622	0.433
	Residuals	58	15’682’159	270’382		
Travel time	Obstacles	1	241’207	241’207	0.546	0.463
	Residuals	58	25’621’132	441’744		
Number of turns	Obstacles	1	43	43.35	0.554	0.46
	Residuals	58	4’542	78.30		

6 Discussion

6.1 Research Questions

The subsequent sections address the research questions presented in Section 1.3, situating this thesis within its spatial and scientific context. Furthermore, the limitations of this research are examined.

6.1.1 Research Question 1

How is the footpath network in Zurich's District 1 enhanced with spatial accessibility features?

The footpath network of District 1 in the City of Zurich was enhanced by allocating spatial accessibility features to the nearest footpath segment. Prior to the allocation of these features, the footpath segments were divided into smaller segments, similar to an approach presented by Rahaman et al. (2017). This allowed for a more precise allocation of spatial accessibility features, as the smaller footpath segments better represented the actual locations of the spatial accessibility features. The raw spatial accessibility features were preprocessed by clustering those describing the same object and aggregating them into a single data point.

As illustrated in Figure 5.2 and discussed in Section 5.1, the number of spatial accessibility features was considerably reduced due to the clustering and aggregation processes.

The most notable reduction of features occurred in the category *rail/tram track*, resulting from the methodology employed to enhance the spatial accessibility features with the Canton's dataset. By consistently segmenting the tram tracks in District 1 into 10 m segments, 4'453 points were created for District 1 alone. This number slightly increased to 4'824 by merging the Canton's dataset with the spatial accessibility features. The pattern in Figure 5.5 effectively illustrates where tram tracks are located in District 1 and the points at which footpaths cross them.

Likewise, the number of collected *crosswalk* points increased by augmenting the dataset with the City's crosswalk dataset. This dataset included 235 crosswalks for District 1, thus raising the total count of crosswalks to 1'455 (before removing *crosswalk* points through validation). Through clustering and aggregation, spatial accessibility features describing the same crosswalk were simplified into a single data point. Given that both ZuriACT participants and the City's dataset generally cover the same area, spatial overlaps existed. By applying data aggregation, the *crosswalk* data from both datasets, which potentially described the same objects, were merged into single *crosswalk* points per object, eliminating spatial overlaps and resulting in 415 crosswalks.

As a recently published study based on preliminary results analysed (Allahbakhshi & Ardüser, 2024), the high number of *surface material type* points in District 1 (1'032 after aggregation) results from the historic cobblestone pavements in the area, particularly in the neighbourhoods of Schipfe and Grossmünster. This is supported by the resulting spatial distribution of the category *surface material type*, depicted in Figure 5.5.

The number of *curb ramp* features (911 after aggregation) is slightly more than double that of the *crosswalk* features (415 after aggregation), suggesting that a curb ramp generally accompanies crosswalks at each end in District 1. Additional curb ramps can be found where crossing is possible, but no zebra crossing is present, such as along Bahnhofstrasse. Furthermore, the number of *pedestrian signal* features (304 after aggregation) is lower than that of the *crosswalk* features, clearly indicating a significant number of unsignalled crosswalks, considering that each *crosswalk* feature would typically be accompanied by two *pedestrian signal* features (one signal on each side of the street).

The aggregated spatial accessibility features were assigned to the footpath network of District 1 to assess spatial accessibility. Well-maintained, accessible, and safe footpaths enhance public health, promote social interaction, and support the mobility and independence of older adults and individuals with mobility impairments (Li et al., 2022). To measure whether District 1 of Zurich provides accessible footpaths, an *Access Score* was calculated. The average *Access Score*$_{permanent}$ of 0.672 and *Access Score*$_{all}$ of 0.667 at footpath level indicate that accessibility is generally high. However, areas with reduced accessibility are concentrated where footpath inclines exceed accessibility thresholds, leading to inaccessible segments. This supports the assertion of Rahaman et al. (2017) that inclines significantly affect accessibility. The impact of incline on accessibility is particularly pronounced in Zurich's historic old town on both sides of the river Limmat, with the east side being steeper overall, further diminishing accessibility. These conclusions are reinforced by *Access Scores* at both footpath and neighbourhood levels.

A comparison of the *Access Scores* presented in Figures 5.9 and 5.10 with the aggregated spatial accessibility features in Figure 5.5 underscores the influence of *surface material type* features. In the neighbourhoods of Schipfe, Münsterhof, Zähringerstrasse, Prediger, and Grossmünster, the *Access Scores* indicate reduced footpath accessibility, aligning with the spatial distribution of *surface material type* features. In contrast to the fully inaccessible segments in these neighbourhoods, caused by *height difference* features and steep footpath inclines, the moderate reduction in accessibility is attributed to cobblestone surfaces, included in the spatial accessibility feature *surface material type*.

Moreover, footpath-level *Access Scores* identify specific locations of inaccessible segments. This is particularly evident on footpaths along the river Schanzengraben. While these footpaths facilitate access to Schanzengraben, they are interspersed with stairs and steps, preventing mobility-impaired individuals from using them safely. Additionally, many of these footpaths are only accessible via stairs, resulting in low *Access Scores*. Such segments highlight significant barriers, leading to very low accessibility values. The *Access Scores* further pinpoint locations of height differences that cause completely inaccessible footpath segments. Striking examples include the stairs located on Sempersteig in the ETH/Universität neighbourhood. Furthermore, the stairs between the train platforms in the main station and the entrance stairs cause the footpath segments to be marked as inaccessible. While these stairs may not represent the most pertinent example regarding footpath accessibility due to the presence of accessible platforms and station entrances, they effectively illustrate the potential of the *Access Score* method in mapping spatial accessibility challenges.

The comparison of *Access Score*$_{permanent}$ and *Access Score*$_{all}$ revealed that differences exist in various areas of District 1. These differences arise from the inclusion of temporary spatial accessibility features considered in the computation of *Access Score*$_{all}$, such as *construction*, *parked car*, and *parked bike/motorcycle* features. The affected neighbourhoods include Paradeplatz, Sihlporte, Bahnhofplatz, and Bellevue. It is striking that spatial accessibility on footpaths in the old town was not affected by temporary obstacles. Furthermore, in the neighbourhoods of Schipfe, Münsterhof, Prediger, and Grossmünster, there are nearly no temporary spatial accessibility features impacting accessibility. In conclusion, while objects may still be present in these areas, they do not influence spatial accessibility, neither obstructing nor facilitating movement on the footpath. These conclusions are backed by the comparison of footpath-level *Access Scores* as well as by the neighbourhood-level *Access Scores*.

Analysing the relationship between *Access Score*$_{all}$ and temporary spatial accessibility features shows that *construction* features are responsible for the majority of entirely inaccessible segments. While parked vehicles, including *parked car* and *parked bike/motorcycle* features, may partially hinder movement, they typically do not result in entirely inaccessible segments.

The *Access Scores* at the footpath level effectively convey accessibility information in a score that can be utilised for accessibility-sensitive routing. Therefore, the allocation of spatial accessibility features to the footpath data in District 1 and the subsequent calculation of *Access Scores* has proven to be a suitable approach for enriching footpath information with spatial accessibility data.

6.1.2 Research Question 2

How well do existing routing services respond to the needs of mobility-restricted population groups?

As highlighted in various studies (Beale et al., 2006; Kasemsuppakorn & Karimi, 2009; Tannert & Schöning, 2018; Völkel & Weber, 2008), existing and commonly used routing services lack accessibility information to provide suitable routes for mobility-impaired population groups. This gap was further analysed for District 1 in the City of Zurich, and the potential of remotely collected spatial accessibility features in addressing this issue was assessed.

First, the **route length** results show that wheelchair-accessible routes generated by ORS rolling and both SPAAR rolling options, whether considering all obstacles or only temporary ones, are longer than walking routes from any other routing service. This underscores the inaccessibility of footpaths in District 1 of Zurich. Individual routes illustrate such inaccessibilities, as indicated by various datasets. For example, the routes between origin-destination pair 5, as shown in Figure A.2a, clearly visualise the differences among the underlying datasets. While the SPAAR rolling routes closely resemble the walking routes of all routing services, the ORS rolling route takes a markedly different path, likely due to an inaccessible feature within the ORS dataset, resulting in this detour. Moreover, differences in travel profiles increase as the distance between origin and destination locations grows. This suggests that the impact of less accessible footpaths accumulates with increasing distance, indicating that such inaccessibility persists throughout the entire route and is not merely the result of isolated objects obstructing the footpath.

Furthermore, routes generated for wheelchair profiles tend to avoid steep footpaths, which are associated with a high cost due to the *Access Scores*. This is evident in several routes generated for ORS rolling and both SPAAR rolling options. For instance, the routes between origin-destination pairs 3 (Figure A.1c), 4 (Figure A.1d), and 30 (Figure A.6b) illustrate how such steep segments result in detours for wheelchair profiles.

The route lengths suggested by Google Maps, OSRM, ORS walking, and SPAAR walking show no significant difference, with comparable route lengths across various distance categories between origin and destination locations. This indicates that, regardless of the origin and destination, routing services recommend similar routes or routes of similar length using alternative footpaths, such as route 10 (Figure A.2f), route 11 (Figure A.3a), route 21 (Figure A.4e), or route 26 (Figure A.5d).

Second, **travel times** of routing services concerning wheelchair profiles are significantly higher, particularly for SPAAR rolling routes. Although ORS rolling also exhibits increased travel times, the distinction between SPAAR rolling and ORS rolling remains notable. The reasons for these outcomes may differ from route to route. Generally, SPAAR rolling routes may take into account more spatial accessibility features (as discussed below), consequently causing detours and alternative routes. However, since Figure 5.15 does not reveal any significant differences in route length between ORS rolling and SPAAR rolling, the reason for the increased travel times for SPAAR rolling may lie in the travel speed assumptions outlined in Section 4.4.3. In comparison to the base travel speed of 4 km/h for the wheelchair profile, the travel speeds for wheelchair users on SPAAR routes are generally lower and range between 2.48 km/h and 3.78 km/h (Table 4.7). This implies that the travel speeds derived from the experiments conducted by Boyce et al. (1999) may represent rather conservative assumptions for wheelchair users, resulting in increased travel times for SPAAR rolling routes. Enhancing the travel speed to a more appropriate value could mitigate these differences between SPAAR rolling and ORS rolling. However, further assessments of wheelchair travel speeds are necessary to establish suitable travel speeds before merely adjusting them, as this could lead to unrealistic values.

The travel times of Google Maps, OSRM, ORS walking, and SPAAR walking are relatively similar; however, the differences increase with the growing distance between the origin and destination. ORS walking and SPAAR walking show similar travel times, generally lower than those of Google Maps and OSRM routes. As the route lengths between these routing services do not differ significantly, their varying travel times might stem from underlying assumptions about travel speed, as indicated in Section 4.4.3. As Google Maps (presumably), OSRM, and ORS walking apply a base travel speed of 5 km/h (Open Source Routing Machine, 2024a; OpenRouteService, 2024d; Tannert & Schöning, 2018), the differing travel times suggest that various parameters, such as incline or footpath surface, influence travel speeds and, consequently, travel times. Given that the travel times of SPAAR walking are comparable to those of ORS walking, a similar parameter, namely incline, could be considered, as SPAAR walking solely takes incline into account as a factor affecting travel speed. However, similar results between SPAAR and ORS walking might also arise from several parameters that affect the travel speed of ORS walking, not exclusively incline. This is more likely due to ORS's advanced routing algorithms.

Third, differences in **route complexity** indicate that routes generated for wheelchair profiles involve more turns, leading to more complex routes compared to walking routes. Furthermore, routes produced by OSRM and SPAAR walking exhibit fewer turns, a trend that becomes more apparent as the distance between the origin and destination increases. Unsurprisingly, route complexity grows with the increasing distance between origin and destination, concluding that longer routes are generally more complex. However, while this conclusion is corroborated by results found by Tannert and Schöning (2018), it significantly relies on the footpath design of a city. For instance, grid-like footpath layouts might provide alternative routes of similar length with more options to reduce the number of turns. In other cities, reducing the number of turns could result in a substantial increase in route length (Sevtsuk & Basu, 2022). Even in this small-scale study for District 1, the influence of footpath design on the number of turns in the generated routes could be analysed, given that the footpaths in the old town around Lindenhof (Schipfe neighbourhood) and Niederdorf (Zähringerstrasse and Prediger neighbourhoods) are more intricate than those in the Paradeplatz neighbourhood. This would require creating additional routes in these areas, strictly categorised by the underlying footpath design.

In contrast to Tannert and Schöning (2018), who observed that Google Maps diminishes the complexity of the generated routes by minimising turns, there is no significant difference in route complexity between Google Maps routes and those created by other routing services. This thesis does not confirm the higher number of turns associated with ORS walking compared to Google Maps routes, as noted in Tannert and Schöning (2018). Furthermore, ORS walking routes even show a lower median for the number of turns with increasing distance, contrary to findings by Tannert and Schöning (2018). This discrepancy may stem from the footpath design of the city, which could diverge from those examined by Tannert and Schöning (2018).

The differences in route length, travel time, and complexity among routing services underscore the significance of their underlying assumptions. While little is known about Google Maps' algorithms, both ORS and OSRM openly provide information about their routing methods. These services can adjust routes based on various parameters, such as travel speed, which is influenced by footpath surface, incline, or type as specified in OSM data (Open Source Routing Machine, 2024a; OpenRouteService, 2024d). ORS, in particular, offers an extensive range of adjustable parameters for wheelchair routing (Table 2.1), including considerations for surface type and route smoothness, enabling users to customise routes according to their needs.

In contrast, SPAAR routing incorporates a broader set of spatial accessibility features. While some ORS parameters align with SPAAR features (maximum curb height ↔ curb ramp/missing curb ramp; route smoothness ↔ surface problem; minimum surface type ↔ surface material type), others are not directly comparable. SPAAR's spatial accessibility feature categories, such as *no sidewalk*, *obstacle*, *construction*, *parked car*, *parked motorcycle/bike*, *rail/tram track*, *crosswalk*, and *pedestrian signal*, provide further insights into footpath accessibility. While ORS' parameters focus on the built environment of the footpaths, the spatial accessibility features included in SPAAR also take into account objects located on the footpaths, such as parked vehicles, obstacles, and construction sites. Moreover, SPAAR rolling routes consider temporary features that can significantly influence individual route results. Therefore, the spatial accessibility features included in the SPAAR route generation offer a considerable advantage over ORS parameters, as they provide more information for footpath accessibility assessments, enhancing the basis for accurate route generation that reflects real-world conditions.

As Tannert and Schöning (2018) concluded, the differences between routes suggested for wheelchair and walking profiles illustrate the failure to implement accessibility standards, resulting in longer and more complex wheelchair-accessible routes. While the city's underlying topography may contribute to inaccessibility, the footpath infrastructure further creates inaccessible segments, such as stairs or steps on footpaths.

The findings further indicate that existing routing services lack the potential to accommodate mobility-impaired individuals, as evidenced by the significant differences between accessibility-sensitive routing services and those that do not consider accessibility. This gap often stems from the unavailability of accessibility-relevant information necessary for such services (Froehlich et al., 2019). The disparities between walking and rolling routes also suggest that several barriers exist in District 1, primarily due to objects obstructing the footpath, the surface of the footpath itself, as well as steep footpaths, sometimes even incorporating steps and stairs, arising from Zurich's underlying topography.

Moreover, the results lead to the conclusion that SPAAR, based on the enhanced footpath network for District 1, performs well compared to the other routing services analysed. While differences between routing services are generally discernible, both SPAAR rolling options yield similar results concerning route length, travel time, and route complexity. In addition to the noted difference in travel times, SPAAR rolling routes resemble ORS rolling routes, demonstrating the efficacy of the accessibility-enhanced footpath network in routing for District 1. Furthermore, SPAAR routes generated for walking profiles rank among those with the shortest route lengths, travel times, and the fewest number of turns. Dijkstra's shortest path algorithm has performed admirably on the enhanced footpath network, underscoring the value of the spatial accessibility features dataset and the resulting advantage of SPAAR over other routing services by utilising such a practical dataset.

The 30 origin-destination pairs were generated without specific conditions, except that both origin and destination points were not located on water surfaces. These points were matched randomly. When comparing routes within the same shortest path distance categories, two distinct groups emerge: one comprising routes that cross the river Limmat, and the other consisting of routes that do not (i.e., both origin and destination points are on the same side of the river). These comparisons reveal significant differences between the groups.

Of the 30 pairs, 19 comprised origins and destinations situated on opposite sides of the river Limmat, necessitating pedestrians to cross the river during their journey. Among these 19 pairs, only 1 shortest path was shorter than 600 m. 10 shortest paths fell into the >600–1200 m category, while 8 were classified as >1200–1800 m.

For the remaining 11 origin-destination pairs, where origin and destination points were on the same side of the Limmat, only 3 shortest paths were shorter than 600 m. The other 8 shortest paths ranged from 600 to 1200 m in length. Notably, no shortest paths connecting origin-destination pairs without crossing the Limmat exceeded 1200 m.

The informative value for the category containing origin-destination pairs located less than 600 m apart is limited, as only four origin-destination pairs have shortest paths less than 600 m. Of these, 3 pairs do not cross the Limmat, highlighting the rarity of very short routes crossing the river. All origin-destination pairs in the category >1200–1800 m involve crossing the Limmat, underscoring the connection between longer routes and the necessity of crossing the river. The category encompassing routes of intermediate length (>600-1200 m) offers the most insight into Zurich's District 1. The majority of routes within this range are approximately 1000 m long, irrespective of whether they cross the Limmat. However, routes crossing the Limmat tend to show more variability, with some longer outliers (e.g., Route 3, Figure A.1c; Route 29, Figure A.6a). This trend is particularly pronounced for wheelchair-accessible routes (SPAAR and ORS rolling routes). While previous results have demonstrated that rolling routes are significantly longer than walking routes, these findings suggest that this issue is particularly acute when origin and destination locations are positioned on opposite sides of the Limmat.

No clear patterns were observed between the travel times of routes crossing the Limmat and those that do not.

A distinct difference in complexity emerges between crossing and non-crossing routes. Routes that cross the river tend to incorporate more turns, whereas routes on the same side of the Limmat involve fewer turns. Unlike route length, route complexity does not show a significant difference between rolling and walking routes of both crossing and non-crossing varieties.

An additional analysis comparing routes on the east and west sides of the Limmat did not yield further insights. Both sides are characterised by diverse topography, and no discernible topographical effect on route characteristics was observed. Future research should focus on incorporating additional origin-destination pairs that are more clearly distinguishable by their specific locations.

6.1.3 Research Question 3

Do temporary obstacles significantly impact routing outcomes for mobility-impaired individuals?

According to the results summarised in Section 5.3.2, the impact of temporary obstacles is negligible when analysing all routes.

Temporary features present in District 1 mainly consisted of parked vehicles, including 32 *parked car* and 72 *parked motorcycle/bike* features, and construction sites indicated by 71 *construction* features. Considering only the features completely blocking the footpath, i.e., features with a severity rating of 5, and thereby preventing movement on them for mobility-impaired individuals, these numbers were further reduced. 35 *construction* features, 8 *parked motorcycle/bike* features and 5 *parked car* features were considered to completely blocking footpaths.

Temporary obstacles can influence individual routes, such as those created between the origin-destination pairs 24 (Figure A.5b) and 25 (Figure A.5c), prompting mobility-impaired individuals, such as wheelchair users, to opt for alternative routes. Furthermore, as shown in Section 6.1.1, the temporary obstacles that completely obstruct footpaths are predominantly construction sites, as indicated by the aforementioned numbers. By providing current information on these construction sites in commonly used routing services, the development of routes passing through such inaccessible construction areas could be minimised.

In addition to up-to-date information on relevant temporary obstacles, particularly construction sites, the significance of data regarding spatial accessibility on footpaths is once again highlighted. By incorporating such information into commonly used routing services, routes for mobility-impaired individuals can be recommended that reflect real-world conditions.

6.2 Limitations

As this analysis greatly depended on the spatial accessibility features collected remotely from Street View Imagery (SVI), certain limitations must be considered. Firstly, data is only provided in areas with SVI coverage, leading to unassessed regions lacking such coverage. Although footpath segments without SVI coverage are very limited in District 1 of Zurich, they do still exist. For instance, SVI in the infra3D tool does not cover Ankengasse and Schoffelgasse, located in the Grossmünster neighbourhood. This introduces uncertainty in the *Access Scores* and consequently in the routing results from SPAAR. Such uncertainty is also present in cases where the view of footpaths is obstructed by objects, as indicated by the data point *occlusion* in the spatial accessibility feature dataset. In-situ data collection is required to complete these obstructed footpath segments as well as the footpath segments lacking SVI coverage, thereby ensuring complete and valid data for spatial accessibility assessments (Allahbakhshi, 2023).

Further limitations arise in connection with these introduced uncertainties. While remote data collection using SVI offers several advantages, such as cost and time efficiency (Steinmetz-Wood et al., 2019), it is always based on images taken at a single moment in time, providing merely a snapshot of the footpath condition. For ongoing spatial accessibility assessments and real-world routing applications, maintaining an up-to-date database of spatial accessibility features is crucial (Allahbakhshi, 2023).

As demonstrated in Section 6.1.3, the temporary spatial accessibility feature *construction* renders footpath segments completely inaccessible. While these features were collected for individuals with reduced mobility capabilities within ZuriACT, various features are also relevant for those without mobility restrictions. For instance, certain objects that completely block a footpath and, therefore, prevent movement along this segment act as barriers for all individuals regardless of whether these individuals suffer mobility restrictions. However, the spatial accessibility features do not provide this information, meaning that this cannot be derived from a spatial accessibility feature, whether it affects the movement of all individuals or the movement of mobility-restricted individuals.

The Dijkstra's Shortest Path algorithm has limitations when applied to large graphs due to the considerable computational effort required. In contrast, other shortest path algorithms, such as Contraction Hierarchies and A* (Luxen & Vetter, 2011; Mehta et al., 2019), can effectively handle larger graphs. However, as noted by Neis (2015), wheelchair route lengths are typically shorter than 10 km, which justifies the use of Dijkstra's Shortest Path algorithm in this thesis.

Although Google introduced wheelchair-accessible routing on Google Maps (https://maps.google.com/) several years ago (Akasaka, 2018), the Google Directions API is currently limited to routing for the travel profiles walking, cycling, driving, and transit (using public transportation) (Google, 2024b). However, I opted for Google's Directions API, although Google Maps could provide wheelchair-accessible routing. This decision was made with regard to the statistical analysis. The exact routes, lengths, and travel times were obtained through the Directions API. These values would have only been approximated through Google Maps. Therefore, I preferred the Directions API as it delivered precise values for later comparison with other routing services.

Lastly, this work is based on spatial accessibility features gathered for a broad group of mobility-impaired individuals, including older adults, those with situational mobility restrictions, and people with disabilities affecting mobility. Without further differentiation of the varying mobility requirements for spatial accessibility features, as summarised in the work of Georgescu et al. (2024), these features were employed to enhance the accessibility of footpaths. This step was succeeded by the application of a shortest path routing algorithm, whose resulting route metrics were determined using the speed of manual wheelchair users. Various studies (e.g., Beale et al. (2006), Völkel and Weber (2008), and Kasemsuppakorn and Karimi (2009)) have highlighted that route preferences and requirements in terms of accessibility vary greatly among different population groups and individuals with mobility restrictions. Hence, future work on routing, using the spatial accessibility features as a foundation, should incorporate these perspectives and provide a rating of these features based on their (relative) importance. This would facilitate the generation of more realistic routing results tailored to individuals' needs.

Since the study is confined to District 1, edge effects may influence the results. Even though District 1 is relatively compact, there may be shorter and more accessible routes between the used origin-destination pairs that could exist using footpaths outside District 1. However, such routes were not evaluated due to the spatial limitations of this study.

7 Conclusion

7.1 Contributions

By applying Dijkstra's Shortest Path algorithm to the footpath network of District 1, which was enhanced with spatial accessibility features primarily gathered through the citizen science project ZuriACT, this thesis generated routes catering to both walking and wheelchair profiles. The spatial accessibility features were clustered and consolidated into points representing the same real-world object. These clustering and aggregation processes were subsequently linked to the footpath network, demonstrating a suitable approach for enriching the network with accessibility-relevant information. This provides a robust foundation for routing tailored to the broad spectrum of mobility-impaired individuals.

A total of 210 routes were analysed: 30 routes each were generated by Google Maps and the Open Source Routing Machine (OSRM) for walking profiles, while OpenRouteService (ORS) produced 30 routes for both walking and wheelchair profiles. Dijkstra's shortest path algorithm for accessible routing (SPAAR) yielded 90 routes: 30 for walking profiles and 60 for wheelchair profiles (with 30 routes considering all obstacles and 30 considering only permanent obstacles). Pairwise comparisons revealed significant differences in the routing results.

7.2 Insights

The results demonstrated that routes generated for wheelchair profiles are significantly longer, require more time, and are more complex, incorporating a higher number of turns. Furthermore, obstacles along the way significantly impact the shortest paths between origin and destination pairs, forcing individuals with mobility impairments to take substantial detours. These deviations, particularly evident in ORS wheelchair and SPAAR wheelchair routes, indicate accessibility limitations within District 1 of Zurich. While some barriers arise from the city's topography, others are caused by physical obstructions such as construction sites or cobblestones, which restrict or prevent movement on footpaths. In conclusion, routing services that solely suggest routes for walking profiles, such as Google Maps, through the Directions API, and OSRM, do not adequately serve mobility-impaired individuals, as they fail to provide appropriate routes.

While temporary obstacles do not significantly affect the results of summarised routes, they may still influence individual routes, such as the routes from the origin-destination pairs 24 (Figure A.5b) and 25 (Figure A.5c). Temporary obstacles that entirely block footpaths and thus prevent movement on them are most commonly construction sites. By incorporating the location of construction sites on footpaths into common routing services, the impact of temporary obstacles on routing could be mitigated, allowing for better planning security for mobility-impaired individuals and fostering greater inclusivity in urban mobility.

Addressing accessibility challenges is crucial to creating inclusive urban environments in light of projected urbanisation and a growing population. As cities expand, the integration of spatial accessibility data into routing systems becomes increasingly important. This would enable routing services to reflect real-world conditions and cater to the diverse range of individual mobility needs. The findings of this thesis emphasise the necessity of accessible infrastructure and routing services to ensure equitable participation in urban life for all population groups.

7.3 Outlook

Based on the analysis conducted in this thesis, several further studies can be undertaken. For example, personalised routing for individuals with varying mobility impairments and restrictions could be developed, offering reliable routing services tailored to the diverse mobility needs of individuals, as indicated by Beale et al. (2006). The spatial accessibility features provide an excellent data foundation, as data collection was carried out by individuals with different mobility restrictions and impairments, including their perspectives on accessibility (Allahbakhshi, 2023).

Moreover, an approach that introduces uncertainty in accessibility-sensitive routing would be particularly interesting, similar to the stochastic model for travel time presented by Gendreau et al. (2015). The work conducted by Gendreau et al. (2015) distinguished between two models for determining travel time: deterministic and stochastic models. While deterministic models resulted in fixed travel times based on historical data, stochastic models considered the variability and uncertainty in travel times due to the dynamic nature of real-world conditions (Gendreau et al., 2015). Employing a stochastic model would result in a range of travel times, each associated with a particular probability and uncertainty regarding travel conditions. This methodology could be applied to accessibility assessments that take uncertainty into account by incorporating an additional value alongside the introduced metrics of route length, travel time, route complexity, and an accessibility rating, indicating the reliability of the accessibility assessments for the route (segments). A stochastic model could suggest multiple routes, each with a probability value reflecting the certainty of the route's accessibility assessment. Consequently, mobility-impaired individuals would be able to determine whether they wish to risk taking a particular route, such as a shorter route, but with higher uncertainty regarding the accessibility assessments.

As vehicles are only permitted in pedestrian areas in District 1 at specific times (Stadt Zürich, 2021b), with some exceptions, spatio-temporal components could be taken into account. For instance, accessibility in pedestrian areas could be rated more favourably during times when vehicles are barred from entering these areas. This would lead to improved accessibility ratings and, therefore, a reduction in the costs associated with travelling through such footpath segments. In conclusion, routes traversing pedestrian areas would be preferred at certain times of the day.

Additional data sources could be explored, such as information provided by OpenStreetMap (OSM). Incorporating such information may offer significant potential for accessibility-sensitive routing (Neis, 2015). Furthermore, combining existing datasets with OSM data would enhance the results, better reflecting real-world conditions. Similarly, line features collected within the ZuriACT project could be utilised to enrich the footpath data for the City of Zurich.

Overall, accessibility-sensitive routing presents considerable potential for future research, aiming for applicable routing services for mobility-impaired populations. This would contribute to a more inclusive city, enabling all individuals to engage in the communities of cities.

Bibliography

Achuthan, K., Titheridge, H., & Mackett, R. L. (2010). Mapping accessibility differences for the whole journey and for socially excluded groups of people. *Journal of Maps*, *6*(1), 220–229. https://doi.org/10.4113/jom.2010.1077

Aghabayk, K., Parishad, N., & Shiwakoti, N. (2021). Investigation on the impact of walkways slope and pedestrians physical characteristics on pedestrians normal walking and jogging speeds. *Safety Science*, *133*, 105012. https://doi.org/10.1016/j.ssci.2020.105012

Akasaka, R. (2018). *Introducing "wheelchair accessible" routes in transit navigation* [Google]. Retrieved January 12, 2025, from https://blog.google/products/maps/introducing-wheelchair-accessible-routes-transit-navigation/

Allahbakhshi, H. (n.d.). Assessing open street map spatial accessibility data quality at different geographical scales (working title, in preparation).

Allahbakhshi, H. (2023). Towards an inclusive urban environment: A participatory approach for collecting spatial accessibility data in zurich, 6 pages, 413856 bytes. https://doi.org/10.4230/LIPICS.GISCIENCE.2023.13

Allahbakhshi, H., & Ardüser, A. (2024). Navigation challenges in urban areas for persons with mobility restrictions. *LIPIcs, Volume 315, COSIT 2024*, *315*, 22:1–22:8. https://doi.org/10.4230/LIPICS.COSIT.2024.22

Allahbakhshi, H., Senn, J., Maiani, N., & Georgescu, A. (2023). Spatial accessibility assessment of homecare workers to the older population in the city of zurich. *AGILE: GIScience Series*, *4*, 1–7. https://doi.org/10.5194/agile-giss-4-17-2023

Arora, S., & Deshpande, A. (2021). Inclusive design—designing barrier-free public spaces [Series Title: Smart Innovation, Systems and Technologies]. In A. Chakrabarti, R. Poovaiah, P. Bokil, & V. Kant (Eds.), *Design for tomorrow—volume 1* (pp. 133–146, Vol. 221). Springer Singapore. https://doi.org/10.1007/978-981-16-0041-8_12

Beale, L., Field, K., Briggs, D., Picton, P., & Matthews, H. (2006). Mapping for wheelchair users: Route navigation in urban spaces. *The Cartographic Journal*, *43*(1), 68–81. https://doi.org/10.1179/000870406X93517

Bobbitt, Z. (2021). *How to perform welch's ANOVA in r (step-by-step)* [Statology]. Retrieved December 23, 2024, from https://www.statology.org/welchs-anova-in-r/

Boles, W. E., & Hayward, S. C. (1978). Effects of urban noise and sidewalk density upon pedestrian cooperation and tempo. *The Journal of Social Psychology*, *104*(1), 29–35. https://doi.org/10.1080/00224545.1978.9924035

Boyce, K. E., Shields, T. J., & Silcock, G. W. H. (1999). Toward the characterization of building occupancies for fire safety engineering: Capabilities of disabled people moving horizontally and on an incline. *Fire Technology*, *35*(1), 51–67. https://doi.org/10.1023/A:1015339216366

Bundesamt für Landestopographie swisstopo. (2024). swissALTI3d. Retrieved December 13, 2024, from https://www.swisstopo.admin.ch/de/hoehenmodell-swissalti3d#Das-hochpr%C3%A4zise-digitale-H%C3%B6henmodell-der-Schweiz

Bundesamt für Statistik BFS. (2023). Statistik der bevölkerung und der haushalte (STATPOP) ab 2010. https://www.bfs.admin.ch/bfs/de/home/dienstleistungen/geostat/geodaten-bundesstatistik/gebaeude-wohnungen-haushalte-personen/bevoelkerung-haushalte-ab-2010.html

Cadkin, J. (2002). Understanding dynamic segmentation: Working with events in ArcGIS 8.2. *ArcUser October-December*. www.esri.com

Caputcu, M., Sengoz, B., Ozuysal, M., Tanyel, S., Kaplan, S., & Karabayir, A. (2016). Use of laser measurements and video images to investigate pedestrian movement along non-uniform sidewalks. https://doi.org/10.11159/icte16.105

Cass, N., Shove, E., & Urry, J. (2005). Social exclusion, mobility and access. *The Sociological Review*, *53*(3), 539–555. https://doi.org/10.1111/j.1467-954X.2005.00565.x

Cooley, D., Barcelos, P., & Muir, C. (2024). *googlePolylines: Encoding coordinates into 'google' polylines* [Institution: Comprehensive R Archive Network Pages: 0.8.5]. Retrieved December 23, 2024, from https://CRAN.R-project.org/package=googlePolylines

Csárdi, G. (2024). *Shortest (directed or undirected) paths between vertices*. Retrieved December 23, 2024, from https://r.igraph.org/reference/distances.html#arguments

Csárdi, G., Nepusz, T., Traag, V., Horvát, S., Zanini, F., Noom, D., Müller, K., Salmon, M., Antonov, M., & Zuckerberg, C. (2024). Igraph: Network analysis and visualization [Institution: Comprehensive R Archive Network Pages: 2.1.2]. https://doi.org/10.32614/CRAN.package.igraph

Cushley, L. N., Galway, N., Curran, K., & Peto, T. (2022). Navigating the unseen city: Town planners, architects, ophthalmic professionals, and charity opinions on navigating of the built environment with a visual impairment. *International Journal of Environmental Research and Public Health*, *19*(12), 7299. https://doi.org/10.3390/ijerph19127299

Delamater, P. L. (2013). Spatial accessibility in suboptimally configured health care systems: A modified two-step floating catchment area (m2sfca) metric. *Health & Place*, *24*, 30–43. https://doi.org/10.1016/j.healthplace.2013.07.012

Dijkstra, E. W. (1959). A note on two problems in connexion with graphs. *Numerische Mathematik*, *1*(1), 269–271. https://doi.org/10.1007/BF01386390

Drake, C., Nagy, D., Nguyen, T., Kraemer, K. L., Mair, C., Wallace, D., & Donohue, J. (2021). A comparison of methods for measuring spatial access to health care. *Health Services Research*, *56*(5), 777–787. https://doi.org/10.1111/1475-6773.13700

Foody, G., See, L., Fritz, S., Mooney, P., Olteanu-Raimond, A.-M., Fonte, C. C., & Antoniou, V. (Eds.). (2017). *Mapping and the citizen sensor*. Ubiquity Press. https://doi.org/10.5334/bbf

Fox, J., & Ogle, D. (2024). *leveneTest: Levene's test* [RDocumentation]. Retrieved December 23, 2024, from https://www.rdocumentation.org/packages/car/versions/3.1-3/topics/leveneTest

Froehlich, J. E., Brock, A. M., Caspi, A., Guerreiro, J., Hara, K., Kirkham, R., Schöning, J., & Tannert, B. (2019). Grand challenges in accessible maps. *Interactions*, *26*(2), 78–81. https://doi.org/10.1145/3301657

Games, P. A., & Howell, J. F. (1976). Pairwise multiple comparison procedures with unequal n's and/or variances: A monte carlo study. *Journal of Educational Statistics*, *1*(2), 113–125. https://doi.org/10.3102/10769986001002113

Geetha, S. (2022). *Hierarchical clustering - types of linkages* [Sai's data website]. Retrieved December 18, 2024, from https://www.saigeetha.in/post/hierarchical-clustering-types-of-linkages

Geisberger, R., Sanders, P., Schultes, D., & Delling, D. (2008). Contraction hierarchies: Faster and simpler hierarchical routing in road networks [Series Title: Lecture Notes in Computer Science]. In C. C. McGeoch (Ed.), *Experimental algorithms* (pp. 319–333, Vol. 5038). Springer Berlin Heidelberg. https://doi.org/10.1007/978-3-540-68552-4_24

Gendreau, M., Ghiani, G., & Guerriero, E. (2015). Time-dependent routing problems: A review. *Computers & Operations Research*, *64*, 189–197. https://doi.org/10.1016/j.cor.2015.06.001

Georgescu, A.-I., Allahbakhshi, H., & Weibel, R. (2024). The impact of microscale street elements on active transport of mobility-restricted individuals: A systematic review. *Journal of Transport & Health*, *38*, 101842. https://doi.org/10.1016/j.jth.2024.101842

Ghasemi, A., & Zahediasl, S. (2012). Normality tests for statistical analysis: A guide for non-statisticians. *International Journal of Endocrinology and Metabolism*, *10*(2), 486–489. https://doi.org/10.5812/ijem.3505

Giannoulaki, M., & Christoforou, Z. (2024). Pedestrian walking speed analysis: A systematic review. *Sustainability*, *16*(11), 4813. https://doi.org/10.3390/su16114813

Giraud, T. (2022). Osrm: Interface between r and the OpenStreetMap-BasedRouting service OSRM. *Journal of Open Source Software*, *7*(78), 4574. https://doi.org/10.21105/joss.04574

Goodchild, M. F. (2007). Citizens as sensors: The world of volunteered geography. *GeoJournal*, *69*(4), 211–221. https://doi.org/10.1007/s10708-007-9111-y

Goodwin, M. (2024). *What is an API (application programming interface)?* [IBM]. Retrieved January 21, 2025, from https://www.ibm.com/think/topics/api

Google. (2024a). *About google maps: Explore and navigate your world*. Retrieved December 22, 2024, from https://www.google.com/intl/ALL_ALL/maps/about/#!/

Google. (2024b). *Directions API - google maps platform documentation* [Google for developers]. Retrieved November 7, 2024, from https://developers.google.com/maps/documentation/directions

Google. (2024c). *Google maps* [Google maps]. Retrieved December 22, 2024, from https://www.google.com/maps/

Guagliardo, M. F. (2004). Spatial accessibility of primary care: Concepts, methods and challenges. *International Journal of Health Geographics*, *3*(1), 3. https://doi.org/10.1186/1476-072X-3-3

Guptill, S. C. (1975). The spatial availability of physicians. *Proceedings of the association of American Geographers*, *7*, 80–84.

Hambleton, R. (2015). *Leading the inclusive city: Place-based innovation for a bounded planet*. Policy Press.

Hammel, J., Magasi, S., Heinemann, A., Gray, D. B., Stark, S., Kisala, P., Carlozzi, N. E., Tulsky, D., Garcia, S. F., & Hahn, E. A. (2015). Environmental barriers and supports to everyday participation: A qualitative insider perspective from people with disabilities. *Archives of Physical Medicine and Rehabilitation*, *96*(4), 578–588. https://doi.org/10.1016/j.apmr.2014.12.008

Han, S. R., Yoon, S., & Cho, S. (2020). Smart accessibility: Design process of integrated geospatial data models to present user-customized universal design information. *Frontiers in Psychology*, *10*, 2951. https://doi.org/10.3389/fpsyg.2019.02951

Hansen, W. G. (1959). How accessibility shapes land use. *Journal of the American Institute of Planners*, *25*(2), 73–76. https://doi.org/10.1080/01944365908978307

Hara, K. (2016). *Scalable methods to collect and visualize sidewalk accessibility data for people with mobility impairments* [Doctoral dissertation, Digital Repository at the University of Maryland]. https://doi.org/10.13016/M2RZ4N

Harris, F., Yang, H.-Y., & Sanford, J. (2015). Physical environmental barriers to community mobility in older and younger wheelchair users. *Topics in Geriatric Rehabilitation*, *31*(1), 42–51. https://doi.org/10.1097/TGR.0000000000000043

Hijmans, R. J. (2020). *Terra*. https://www.rdocumentation.org/packages/terra/versions/0.5-2

Hijmans, R. J., Karney, C., Williams, E., & Vennes, C. (2024, October 4). *Geosphere: Spherical trigonometry* [Institution: Comprehensive R Archive Network Pages: 1.5-20]. Retrieved December 18, 2024, from https://CRAN.R-project.org/package=geosphere

Hosseini, A., Farhadi, E., Hussaini, F., Pourahmad, A., & Seraj Akbari, N. (2022). Analysis of spatial (in)equality of urban facilities in tehran: An integration of spatial accessibility. *Environment, Development and Sustainability*, *24*(5), 6527–6555. https://doi.org/10.1007/s10668-021-01715-3

Iburg, K. M., Charalampous, P., Allebeck, P., Stenberg, E. J., O'Caoimh, R., Monasta, L., Peñalvo, J. L., Pereira, D. M., Wyper, G. M. A., Niranjan, V., Devleesschauwer, B., & Haagsma, J. (2023). Burden of disease among older adults in europe—trends in mortality and disability, 1990–2019. *European Journal of Public Health*, *33*(1), 121–126. https://doi.org/10.1093/eurpub/ckac160

iNovitas AG. (2024). *Infra3d*. Retrieved September 12, 2024, from https://www.infra3d.ch/latest/

Jamtsho, S., Corner, R., & Dewan, A. (2015). Spatio-temporal analysis of spatial accessibility to primary health care in bhutan. *ISPRS International Journal of Geo-Information*, *4*(3), 1584–1604. https://doi.org/10.3390/ijgi4031584

Johnson, I. (2017). *GitHub: Route-externalities/routelevel_externalities*. Retrieved November 8, 2024, from https://github.com/joh12041/route-externalities/blob/master/routelevel_externalities/routelevel_externalities.ipynb

Jokar Arsanjani, J., Mooney, P., Zipf, A., & Schauss, A. (2015). Quality assessment of the contributed land use information from OpenStreetMap versus authoritative datasets [Series Title: Lecture Notes in Geoinformation and Cartography]. In J. Jokar Arsanjani, A. Zipf, P. Mooney, & M. Helbich (Eds.), *OpenStreetMap in GIScience* (pp. 37–58). Springer International Publishing. https://doi.org/10.1007/978-3-319-14280-7_3

Jörg, R., Lenz, N., Wetz, S., & Widmer, M. (2019). *Ein Modell zur Analyse der Versorgungsdichte: Herleitung eines Index zur räumlichen Zugänglichkeit mithilfe von GIS und Fallstudie zur ambulaten Grundversorung in der Schweiz* (No. 01/2019). Schweizerisches Gesundheitsobservatorium. Neuchâtel.

Kanton Zürich. (2020). Orthofoto. https://doi.org/https://data.stadt-zuerich.ch/dataset/geo_orthofoto_2020_kanton_zuerich___sommer___inkl-_infrarot___1m

Kanton Zürich. (2024a). Linien des öffentlichen Verkehrs. Retrieved December 16, 2024, from https://geo.zh.ch/data/maps/00e5983e-7689-4edd-b488-ac602f080331

Kanton Zürich. (2024b). Öffentliche Oberflächengewässer (OGD). Retrieved April 9, 2024, from https://data.stadt-zuerich.ch/dataset/ktzh_oeffentliche_oberflaechengewaesser__ogd_

Kasemsuppakorn, P., & Karimi, H. A. (2009). Personalised routing for wheelchair navigation. *Journal of Location Based Services*, *3*(1), 24–54. https://doi.org/10.1080/17489720902837936

Kassambara, A. (2023, February 1). Rstatix: Pipe-friendly framework for basic statistical tests [Institution: Comprehensive R Archive Network Pages: 0.7.2]. https://doi.org/10.32614/CRAN.package.rstatix

Kaufmann, J., & Schering, A. (2014, September 29). Analysis of variance ANOVA. In R. S. Kenett, N. T. Longford, W. W. Piegorsch, & F. Ruggeri (Eds.), *Wiley StatsRef: Statistics reference online* (1st ed.). Wiley. https://doi.org/10.1002/9781118445112.stat06938

Kenyon, S. (2011). Transport and social exclusion: Access to higher education in the UK policy context. *Journal of Transport Geography*, *19*(4), 763–771. https://doi.org/10.1016/j.jtrangeo.2010.09.005

Kenyon, S., Lyons, G., & Rafferty, J. (2002). Transport and social exclusion: Investigating the possibility of promoting inclusion through virtual mobility. *Journal of Transport Geography*, *10*(3), 207–219. https://doi.org/10.1016/S0966-6923(02)00012-1

Lanza, G., Pucci, P., & Carboni, L. (2023). Measuring accessibility by proximity for an inclusive city. *Cities*, *143*, 104581. https://doi.org/10.1016/j.cities.2023.104581

Lättman, K., Friman, M., & Olsson, L. E. (2016). Perceived accessibility of public transport as a potential indicator of social inclusion. *Social Inclusion*, *4*(3), 36–45. https://doi.org/10.17645/si.v4i3.481

Levene, H. (1960). Robust tests for equality of variances (E. Olkin, Ed.). *Contributions to Probability and Statistics: Essays in Honor of Harold Hotelling. Stanford University Press*, 278–292.

Li, C., Orii, L., Saugstad, M., Mooney, S. J., Eisenberg, Y., Labbé, D., Hammel, J., & Froehlich, J. E. (2022). A pilot study of sidewalk equity in seattle using crowdsourced sidewalk assessment data [Version Number: 1]. https://doi.org/10.48550/ARXIV.2211.11545

Lid, I. M., & Solvang, P. K. (2016). (dis)ability and the experience of accessibility in the urban environment. *Alter*, *10*(2), 181–194. https://doi.org/10.1016/j.alter.2015.11.003

Lopes, H. S., Ribeiro, V., & Remoaldo, P. C. (2019). Spatial accessibility and social inclusion: The impact of portugal's last health reform. *GeoHealth*, *3*(11), 356–368. https://doi.org/10.1029/2018GH000165

Lovelace, R., & Ellison, R. (2019). Stplanr: A package for transport planning. *The R Journal*, *10*(2), 7. https://doi.org/10.32614/RJ-2018-053

Luo, W., & Wang, F. (2003). Measures of spatial accessibility to health care in a GIS environment: Synthesis and a case study in the chicago region. *Environment and Planning B: Planning and Design*, *30*(6), 865–884. https://doi.org/10.1068/b29120

Luxen, D., & Vetter, C. (2011). Real-time routing with OpenStreetMap data. *Proceedings of the 19th ACM SIGSPATIAL International Conference on Advances in Geographic Information Systems*, 513–516. https://doi.org/10.1145/2093973.2094062

McGrail, M. R., & Humphreys, J. S. (2009). Measuring spatial accessibility to primary care in rural areas: Improving the effectiveness of the two-step floating catchment area method. *Applied Geography*, *29*(4), 533–541. https://doi.org/10.1016/j.apgeog.2008.12.003

Mehta, H., Kanani, P., & Lande, P. (2019). Google maps. *International Journal of Computer Applications*, *178*(8), 41–46. https://doi.org/10.5120/ijca2019918791

Mohamad Ali, M. F., Abustan, M. S., & Abu Talib, S. H. (2019). A case study of malaysian pedestrian walking speed at shopping malls in kuala lumpur, malaysia using human behaviour simulator

(HBS). *International Journal of Integrated Engineering*, *11*(4). https://doi.org/10.30880/ijie.2019.11.04.025

Mohammed Alhassan, H., & Mashros, N. (2015). Modelling of pedestrian speed-density and volume-density relationships in outdoor walkways. *Jurnal Teknologi*, *73*(4). https://doi.org/10.11113/jt.v73.4295

Montgomery, D. C. (2017). *Design and analysis of experiments* (Ninth edition). John Wiley & Sons, Inc.

Montufar, J., Arango, J., Porter, M., & Nakagawa, S. (2007). Pedestrians' normal walking speed and speed when crossing a street. *Transportation Research Record: Journal of the Transportation Research Board*, *2002*(1), 90–97. https://doi.org/10.3141/2002-12

Mooney, P., & Minghini, M. (2017). A review of OpenStreetMap data. In G. Foody, L. See, S. Fritz, P. Mooney, A.-M. Olteanu-Raimond, C. C. Fonte, & V. Antoniou (Eds.), *Mapping and the citizen sensor* (pp. 37–59). Ubiquity Press. https://doi.org/10.5334/bbf.c

Mueller, N., Rojas-Rueda, D., Cole-Hunter, T., De Nazelle, A., Dons, E., Gerike, R., Götschi, T., Int Panis, L., Kahlmeier, S., & Nieuwenhuijsen, M. (2015). Health impact assessment of active transportation: A systematic review. *Preventive Medicine*, *76*, 103–114. https://doi.org/10.1016/j.ypmed.2015.04.010

Murtagh, F. (2024). *Hclust: Hierarchical clustering*. https://search.r-project.org/R/refmans/stats/html/hclust.html

Neis, P. (2015). Measuring the reliability of wheelchair user route planning based on volunteered geographic information. *Transactions in GIS*, *19*(2), 188–201. https://doi.org/10.1111/tgis.12087

Neis, P., & Zipf, A. (2008). OpenRouteService.org is three times "open": Combining OpenSource, OpenLS and OpenStreetMaps, 248–251.

Open Source Routing Machine. (2024a). *GitHub: Open source routing machine (OSRM): Project OSRM: Osrm-backend*. Retrieved November 7, 2024, from https://github.com/Project-OSRM/osrm-backend

Open Source Routing Machine. (2024b). *Open source routing machine*. Retrieved December 22, 2024, from https://map.project-osrm.org/

OpenRouteService. (2023). *ORS forum: Routing algorithm* [Openrouteservice] [Section: openrouteservice]. Retrieved December 22, 2024, from https://ask.openrouteservice.org/t/what-is-the-algorithm-used-by-ors-api-for-qgis/2476

OpenRouteService. (2024a). *API OpenRouteService*. Retrieved December 23, 2024, from https://openrouteservice.org/dev/#/api-docs

OpenRouteService. (2024b). *OpenRouteService maps*. Retrieved December 22, 2024, from https://maps.openrouteservice.org/

OpenRouteService. (2024c). *ORS backend documentation*. Retrieved December 22, 2024, from https://giscience.github.io/openrouteservice/

OpenRouteService. (2024d). *ORS backend documentation: Travel speeds* [OpenRouteService]. Retrieved November 5, 2024, from https://giscience.github.io/openrouteservice/technical-details/travel-speeds/#travel-speeds

Openshaw, S. (1984). *The modifiable areal unit problem*. Geo.

OpenStreetMap contributors. (2024). OpenStreetMap: Points of interest. Retrieved October 3, 2024, from https://www.openstreetmap.org

OpenStreetMap contributors. (2025). *OpenStreetMap* [OpenStreetMap]. Retrieved January 7, 2025, from https://www.openstreetmap.org/

OpenStreetMap Wiki. (2024a). *About OpenStreetMap* [OpenStreetMap wiki]. Retrieved December 13, 2024, from https://wiki.openstreetmap.org/wiki/About_OpenStreetMap

OpenStreetMap Wiki. (2024b). *Key: Sac_scale* [OpenStreetMap wiki]. Retrieved November 5, 2024, from https://wiki.openstreetmap.org/wiki/Key:sac_scale

OpenStreetMap Wiki. (2024c). *OpenStreetMap wiki* [OpenStreetMap wiki]. Retrieved December 13, 2024, from https://wiki.openstreetmap.org/

Ortega, E., Martín, B., López-Lambas, M. E., & Soria-Lara, J. A. (2021). Evaluating the impact of urban design scenarios on walking accessibility: The case of the madrid 'centro' district. *Sustainable Cities and Society*, *74*, 103156. https://doi.org/10.1016/j.scs.2021.103156

Ottoni, C. A., Sims-Gould, J., Winters, M., Heijnen, M., & McKay, H. A. (2016). “benches become like porches”: Built and social environment influences on older adults’ experiences of mobility and well-being. *Social Science & Medicine*, *169*, 33–41. https://doi.org/10.1016/j.socscimed.2016.08.044

Pebesma, E. (2016). Sf: Simple features for r [Institution: Comprehensive R Archive Network Pages: 1.0-17]. https://doi.org/10.32614/CRAN.package.sf

Pot, F. J., Heinen, E., & Tillema, T. (2024). Sufficient access? activity participation, perceived accessibility and transport-related social exclusion across spatial contexts. *Transportation*. https://doi.org/10.1007/s11116-024-10470-z

Prandi, F., Soave, M., Devigili, F., Amicis, R. D., & Astyakopoulos, A. (2014). Collaboratively collected geodata to support routing service for disabled people [Publisher: Unpublished]. https://doi.org/10.13140/2.1.2937.1203

Pude, Y. (2022). *An automated approach to enrich OpenStreetMap data on footways* [Master’s Thesis]. University of Zurich.

Rahaman, M. S., Mei, Y., Hamilton, M., & Salim, F. D. (2017). CAPRA: A contour-based accessible path routing algorithm. *Information Sciences*, *385-386*, 157–173. https://doi.org/10.1016/j.ins.2016.12.041

RDocumentation. (2024a). *Aov: Fit an analysis of variance model* [RDocumentation]. Retrieved December 23, 2024, from https://www.rdocumentation.org/packages/stats/versions/3.6.2/topics/aov

RDocumentation. (2024b). *Oneway.test: Test for equal means in a one-way layout* [RDocumentation]. Retrieved December 23, 2024, from https://www.rdocumentation.org/packages/stats/versions/3.6.2/topics/oneway.test

RDocumentation. (2024c). *Shapiro.test: Shapiro-wilk normality test*. https://www.rdocumentation.org/packages/stats/versions/3.6.2/topics/shapiro.test

Rekha, R. S., Radhakrishnan, N., & Mathew, S. (2020). Spatial accessibility analysis of schools using geospatial techniques. *Spatial Information Research*, *28*(6), 699–708. https://doi.org/10.1007/s41324-020-00326-w

Rhoads, D., Rames, C., Solé-Ribalta, A., González, M. C., Szell, M., & Borge-Holthoefer, J. (2023). Sidewalk networks: Review and outlook. *Computers, Environment and Urban Systems*, *106*, 102031. https://doi.org/10.1016/j.compenvurbsys.2023.102031

Roche, S., Propeck-Zimmermann, E., & Mericskay, B. (2013). GeoWeb and crisis management: Issues and perspectives of volunteered geographic information. *GeoJournal*, *78*(1), 21–40. https://doi.org/10.1007/s10708-011-9423-9

Rosenberg, D. E., Huang, D. L., Simonovich, S. D., & Belza, B. (2013). Outdoor built environment barriers and facilitators to activity among midlife and older adults with mobility disabilities. *The Gerontologist*, *53*(2), 268–279. https://doi.org/10.1093/geront/gns119

Saha, M., Saugstad, M., Maddali, H. T., Zeng, A., Holland, R., Bower, S., Dash, A., Chen, S., Li, A., Hara, K., & Froehlich, J. (2019). Project sidewalk: A web-based crowdsourcing tool for collecting sidewalk accessibility data at scale. *Proceedings of the 2019 CHI Conference on Human Factors in Computing Systems*, 1–14. https://doi.org/10.1145/3290605.3300292

Schlegel, A. (2016a). *Games-howell post-hoc test*. Retrieved December 2, 2024, from https://rpubs.com/aaronsc32/games-howell-test

Schlegel, A. (2016b). *RPubs - post-hoc analysis with tukey’s test*. Retrieved December 4, 2024, from https://rpubs.com/aaronsc32/post-hoc-analysis-tukey

Schmidt, E., & Manser, J. A. (2024). Strassen — Wege — Plätze. Richtlinien ”Behindertengerechte Fusswegnetze”. www.hindernisfreie-architketur.ch

Schonfeld, H. K., Heston, J. F., & Falk, I. S. (1972). Numbers of physicians required for primary medical care. *New England Journal of Medicine*, *286*(11), 571–576. https://doi.org/10.1056/NEJM197203162861104

Schweizerischer Verband der Strassen- und Verkehrsfachleute VSS. (2014). Fussgängerverkehr: Hindernisfreier Verkehrsraum. SN 640 075.

Seekins, T., Traci, M. A., & Hicks, E. C. (2022). Exploring environmental measures in disability: Using google earth and street view to conduct remote assessments of access and participation in urban and rural communities. *Frontiers in Rehabilitation Sciences*, *3*, 879193. https://doi.org/10.3389/fresc.2022.879193

Sevtsuk, A., & Basu, R. (2022). The role of turns in pedestrian route choice: A clarification. *Journal of Transport Geography*, *102*, 103392. https://doi.org/10.1016/j.jtrangeo.2022.103392

Shapiro, S. S., & Wilk, M. B. (1965). An analysis of variance test for normality (complete samples). *Biometrika*, *52*(3), 591–611. https://doi.org/10.1093/biomet/52.3-4.591

Stadt Zürich. (2021a). Fussgängerübergänge.

Stadt Zürich. (2021b). Permanente Verkehrsvorschriften, Kreis 1. *12 Verkehrsvorschriften*, (2021).

Stadt Zürich. (2023). Signalisierte geschwindigkeiten. Retrieved December 20, 2024, from https://data.stadt-zuerich.ch/dataset/geo_signalisierte_geschwindigkeiten

Stadt Zürich. (2024a). Amtliche vermessungsdaten stadt zürich jahresendstand 2023. Retrieved December 12, 2024, from https://data.stadt-zuerich.ch/dataset/geo_amtliche_vermessungsdaten_stadt_zuerich_jahresendstand_2023

Stadt Zürich. (2024b). Fuss- und velowegnetz. Retrieved January 26, 2024, from https://data.stadt-zuerich.ch/dataset/geo_fuss__und_velowegnetz

Stadt Zürich. (2024c). Stadtkreise. Retrieved December 12, 2024, from https://data.stadt-zuerich.ch/dataset/geo_stadtkreise

Stadt Zürich. (2024d). Statistische zonen. https://www.stadt-zuerich.ch/geodaten/download/Statistische_Zonen

Stefanidis, R.-M., & Bartzokas-Tsiompras, A. (2024). Pedestrian accessibility analysis of sidewalk-specific networks: Insights from three latin american central squares. *Sustainability*, *16*(21), 9294. https://doi.org/10.3390/su16219294

Steinmetz-Wood, M., Velauthapillai, K., O'Brien, G., & Ross, N. A. (2019). Assessing the micro-scale environment using google street view: The virtual systematic tool for evaluating pedestrian streetscapes (virtual-STEPS). *BMC Public Health*, *19*(1), 1246. https://doi.org/10.1186/s12889-019-7460-3

STHDA. (2024a). *Compare multiple sample variances in r* [Statistical tools for high-throughput data analysis]. Retrieved December 23, 2024, from https://www.sthda.com/english/wiki/compare-multiple-sample-variances-in-r?utm_source=chatgpt.com

STHDA. (2024b). *One-way ANOVA test in r* [Statistical tools for high-throughput data analysis]. Retrieved December 23, 2024, from https://www.sthda.com/english/wiki/one-way-anova-test-in-r?utm_source=chatgpt.com

Tannert, B., & Schöning, J. (2018). Disabled, but at what cost?: An examination of wheelchair routing algorithms. *Proceedings of the 20th International Conference on Human-Computer Interaction with Mobile Devices and Services*, 1–7. https://doi.org/10.1145/3229434.3229458

Tukey, J. W. (1949). Comparing individual means in the analysis of variance. *Biometrics*, *5*(2), 99. https://doi.org/10.2307/3001913

United Nations. (2018). *Inclusive cities: Trends and new initiatives*. Department for Economic, Social Affairs, Division for Social Policy, and Development.

United Nations. (2019). *World urbanization prospects: The 2018 revision (ST/ESA/SER.a/420)*. United Nations, Department of Economic and Social Affairs, Population Division. New York.

United Nations. (2022). *World population prospects 2022: Summary of results*.

United Nations. (2024a). *11 make cities and human settlements inclusive, safe, resilient and sustainable*. Retrieved November 26, 2024, from https://sdgs.un.org/goals/goal11#targets_and_indicators

United Nations. (2024b). *The 17 sustainable development goals*. Retrieved November 26, 2024, from https://sdgs.un.org/goals

United Nations. (2024c). *Population. global issue.* [United nations] [Publisher: United Nations]. Retrieved November 26, 2024, from https://www.un.org/en/global-issues/population

University of Washington, Makeability Lab. (2024a). *APIs - project sidewalk*. Retrieved December 12, 2024, from https://sidewalk-zurich.cs.washington.edu/api

University of Washington, Makeability Lab. (2024b). *Labeling guide - project sidewalk*. Retrieved December 11, 2024, from https://sidewalk-zurich.cs.washington.edu/labelingGuide

University of Washington, Makeability Lab. (2024c). *Project sidewalk*. Retrieved September 12, 2024, from https://sidewalk-zurich.cs.washington.edu/

University of Zurich. (2024a). Project sidewalk: Labelling guide.

University of Zurich. (2024b). Spatial accessibility features.

University of Zurich. (2024c). *ZuriACT: Zurich accessible CiTy*. Retrieved December 9, 2024, from https://www.geo.uzh.ch/en/units/gis/research/ZuriACT.html

van der Meer, L., Abad, L., Gilardi, A., & Lovelace, R. (2024). *Sfnetworks: Tidy geospatial networks* (Version 0.6.5). Retrieved December 21, 2024, from https://cran.r-project.org/web/packages/sfnetworks/index.html

Völkel, T., & Weber, G. (2008). RouteCheckr: Personalized multicriteria routing for mobility impaired pedestrians. *Proceedings of the 10th international ACM SIGACCESS conference on Computers and accessibility*, 185–192. https://doi.org/10.1145/1414471.1414506

Wang, F., & Luo, W. (2005). Assessing spatial and nonspatial factors for healthcare access: Towards an integrated approach to defining health professional shortage areas. *Health & Place*, *11*(2), 131–146. https://doi.org/10.1016/j.healthplace.2004.02.003

Warren, S., Hohmann, M., Auerswald, K., & Mitasova, H. (2004). An evaluation of methods to determine slope using digital elevation data. *CATENA*, *58*(3), 215–233. https://doi.org/10.1016/j.catena.2004.05.001

Welch, B. L. (1951). On the comparison of several mean values: An alternative approach. *Biometrika*, *38*(3), 330–336. https://doi.org/10.1093/biomet/38.3-4.330

Wickham, H., François, R., Henry, L., Müller, K., & Vaughan, D. (2024). *Dplyr*. Retrieved December 18, 2024, from https://dplyr.tidyverse.org

Wiggins, A., Newman, G., Stevenson, R. D., & Crowston, K. (2011). Mechanisms for data quality and validation in citizen science. *2011 IEEE Seventh International Conference on e-Science Workshops*, 14–19. https://doi.org/10.1109/eScienceW.2011.27

Willis, A., Gjersoe, N., Havard, C., Kerridge, J., & Kukla, R. (2004). Human movement behaviour in urban spaces: Implications for the design and modelling of effective pedestrian environments. *Environment and Planning B: Planning and Design*, *31*(6), 805–828. https://doi.org/10.1068/b3060

Wolff, M., Mascarenhas, A., Haase, A., Haase, D., Andersson, E., Borgström, S. T., Kronenberg, J., Łaszkiewicz, E., & Biernacka, M. (2022). Conceptualizing multidimensional barriers: A framework for assessing constraints in realizing recreational benefits of urban green spaces. *Ecology and Society*, *27*(2), art17. https://doi.org/10.5751/ES-13180-270217

World Health Organization. (2022). *Global report on health equity for persons with disabilities* [OCLC: 1410743033].

Zürich Tourismus. (2025). *Kreis 1: Altstadt*. Retrieved January 20, 2025, from https://www.zuerich.com/de/neighborhood

A Routing Results

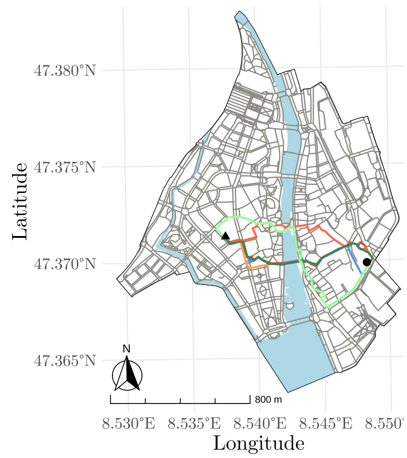

(a) Routes 1

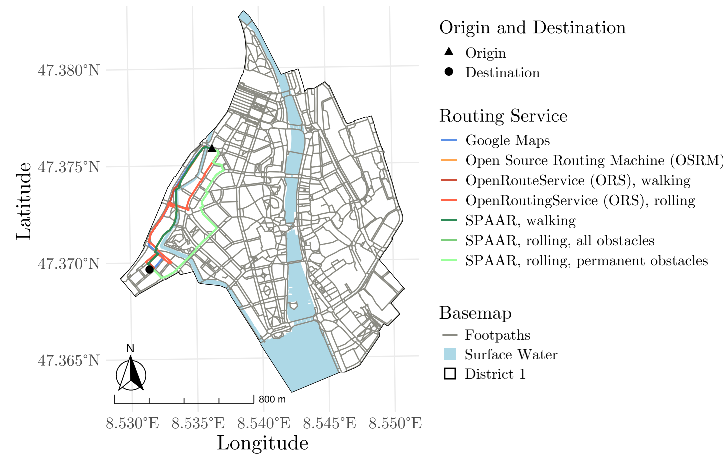

(b) Routes 2

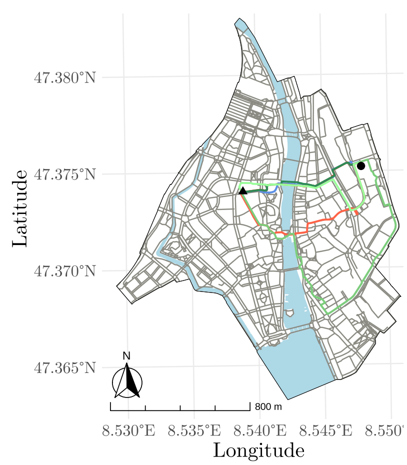

(c) Routes 3

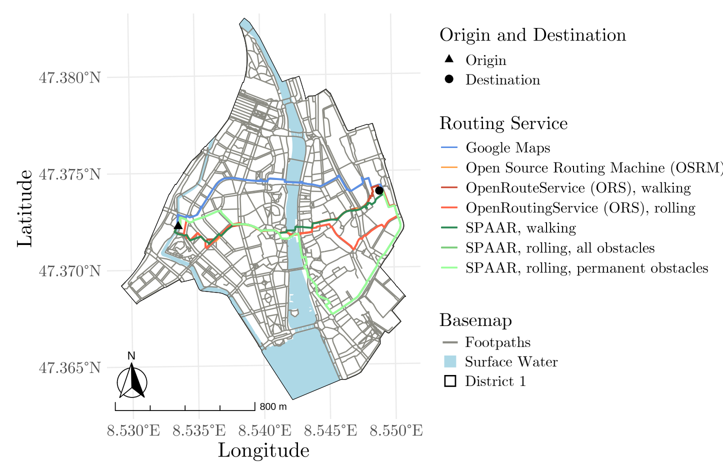

(d) Routes 4

Figure A.1: Resulting routes for the origin-destination pairs 1 to 4

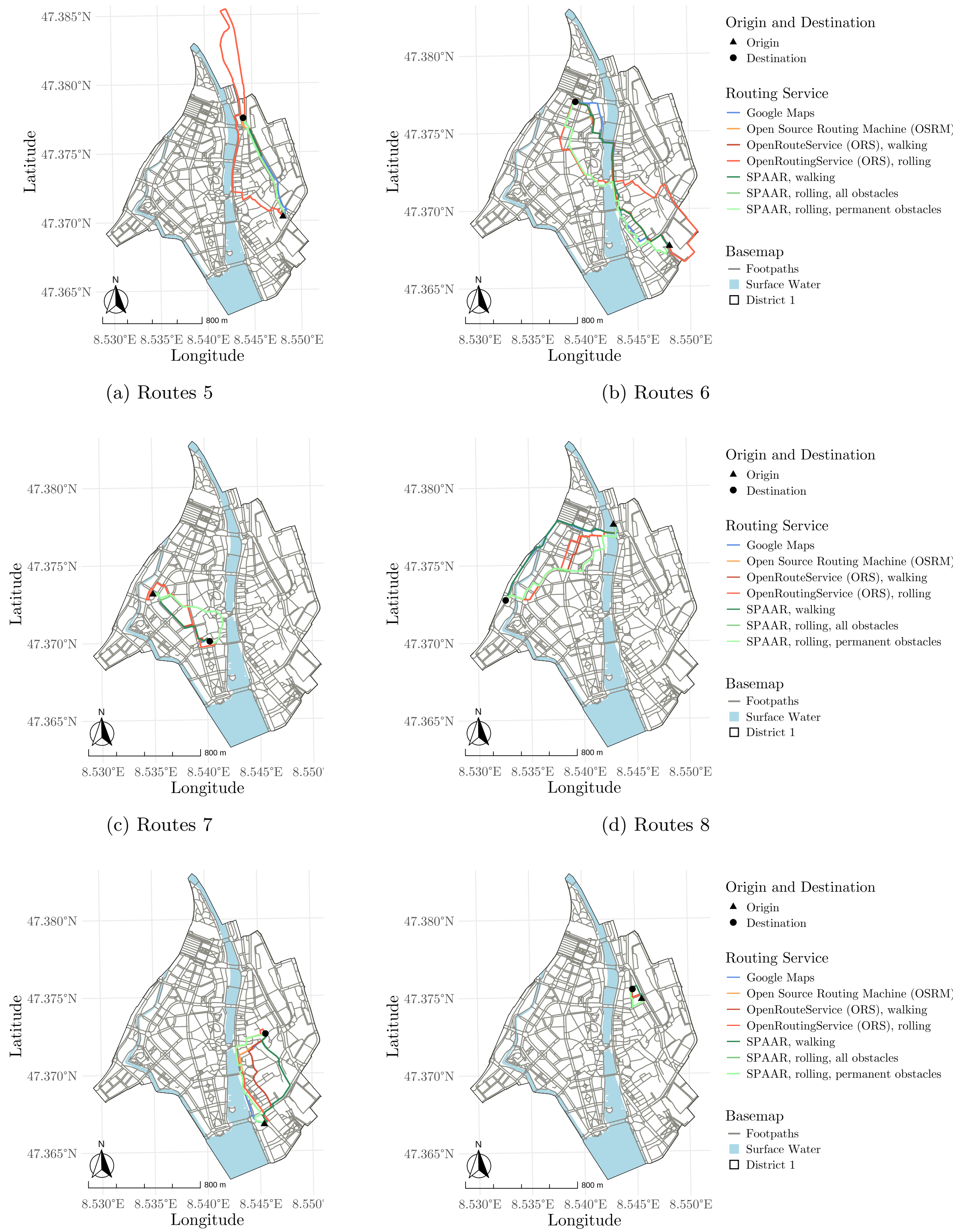

(a) Routes 5

(b) Routes 6

(c) Routes 7

(d) Routes 8

(e) Routes 9

(f) Routes 10

Figure A.2: Resulting routes for the origin-destination pairs 5 to 10

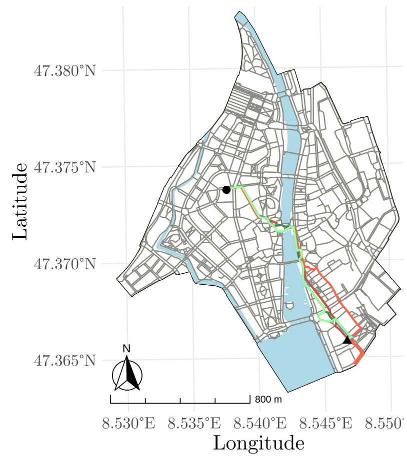

(a) Routes 11

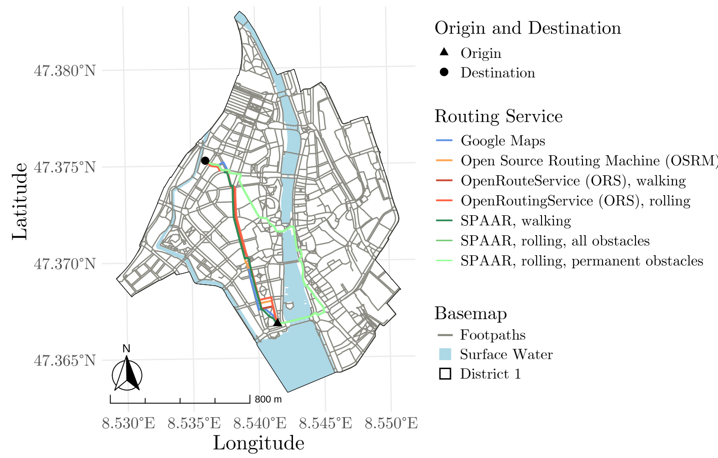

(b) Routes 12

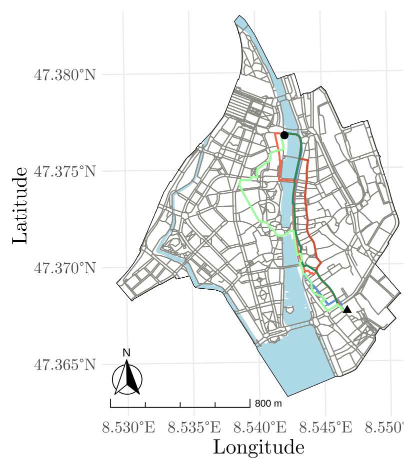

(c) Routes 13

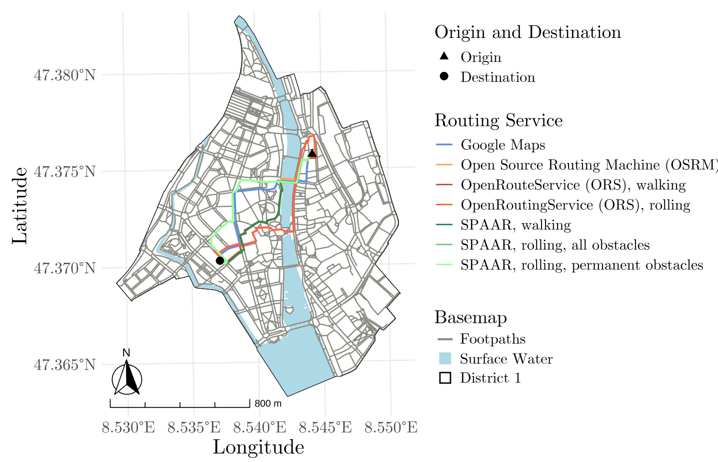

(d) Routes 14

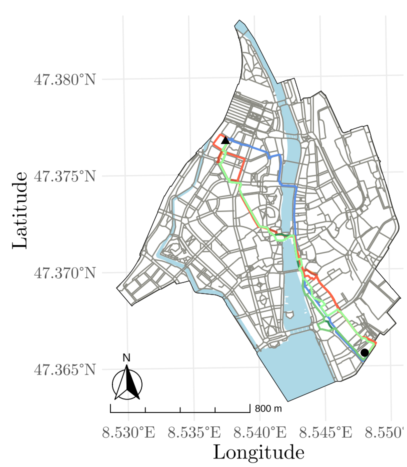

(e) Routes 15

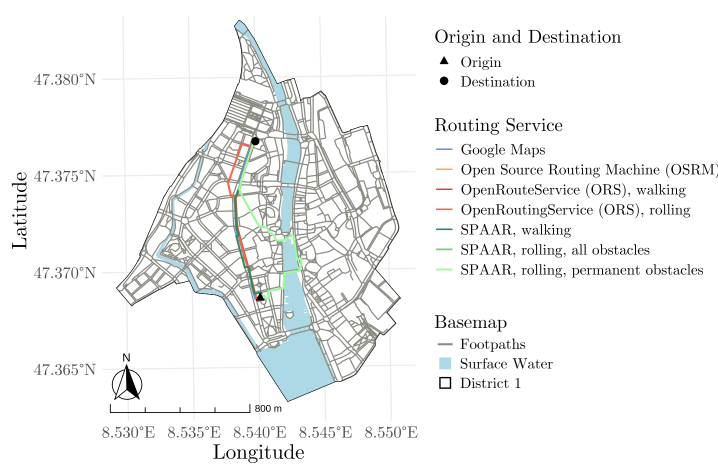

(f) Routes 16

Figure A.3: Resulting routes for the origin-destination pairs 11 to 16

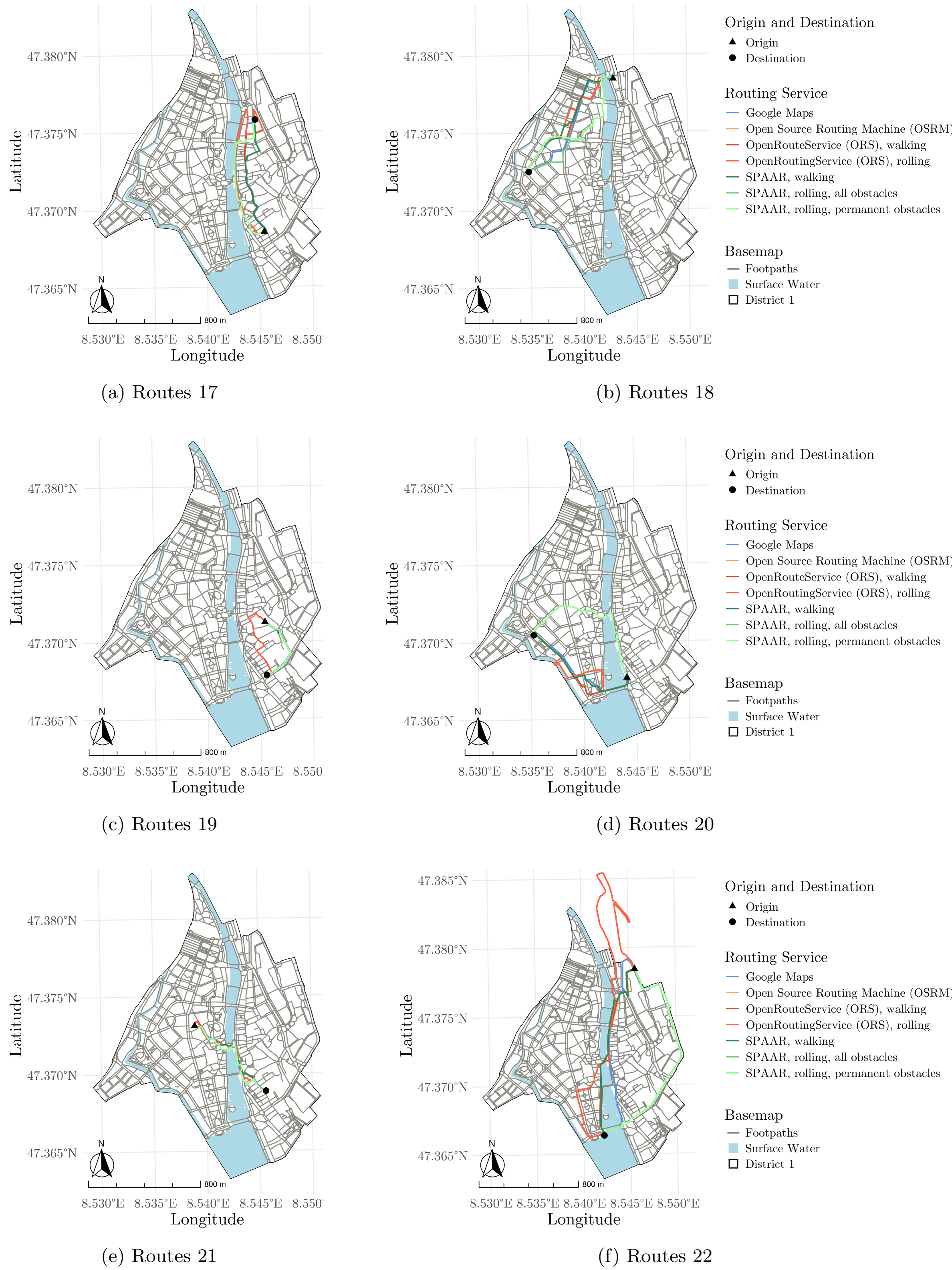

(a) Routes 17

(b) Routes 18

(c) Routes 19

(d) Routes 20

(e) Routes 21

(f) Routes 22

Figure A.4: Resulting routes for the origin-destination pairs 17 to 22

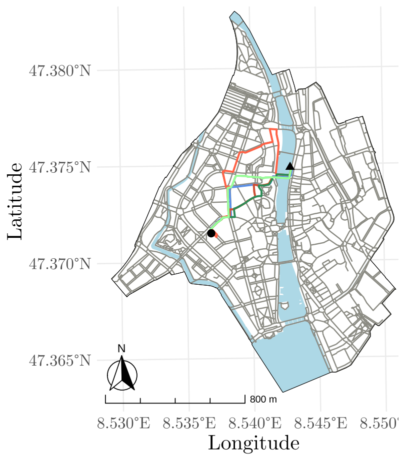

(a) Routes 23

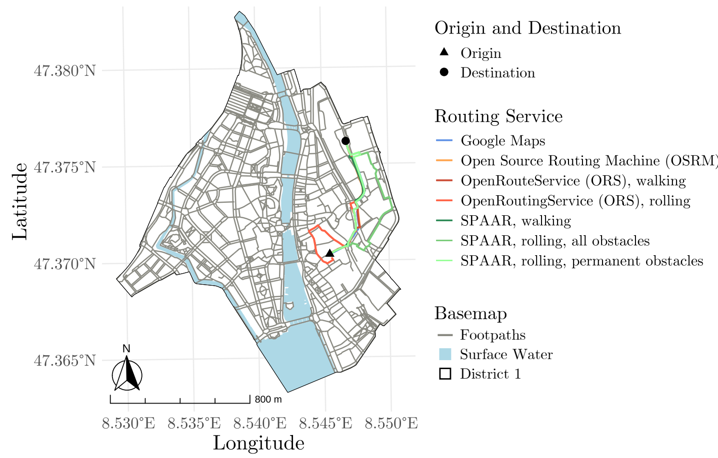

(b) Routes 24

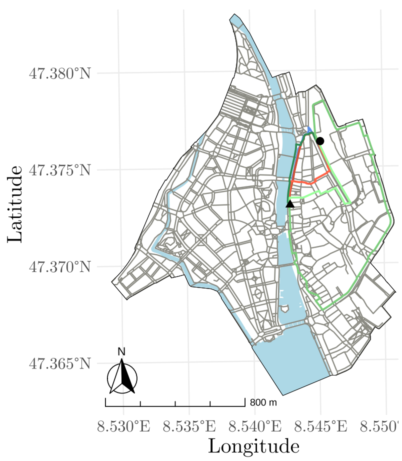

(c) Routes 25

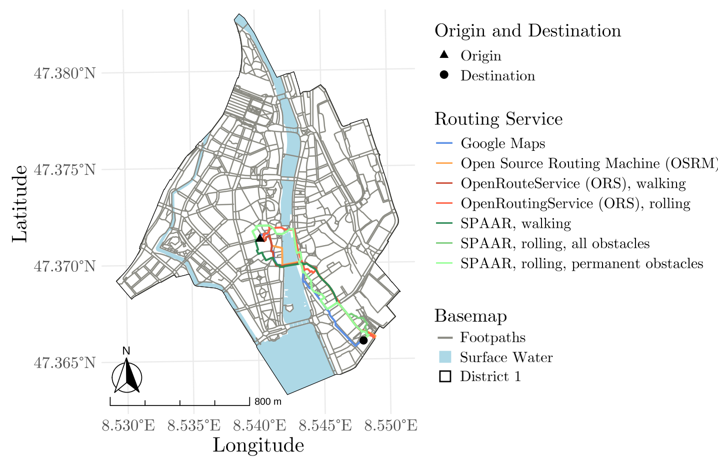

(d) Routes 26

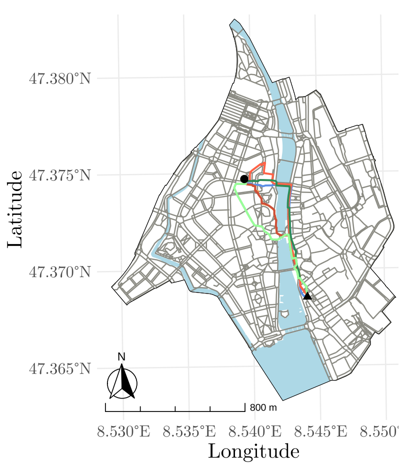

(e) Routes 27

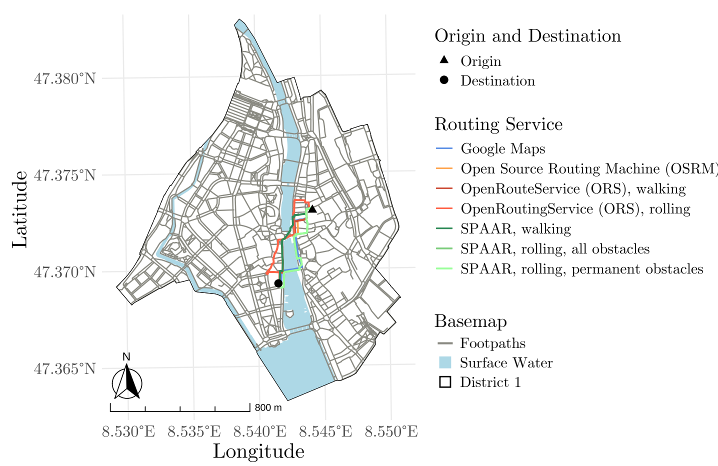

(f) Routes 28

Figure A.5: Resulting routes for the origin-destination pairs 23 to 28

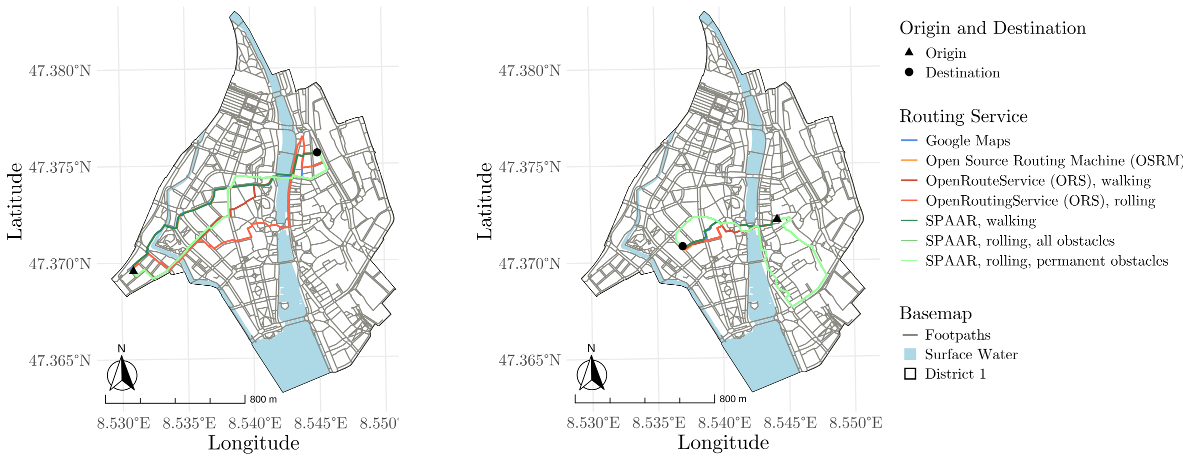

(a) Routes 29

(b) Routes 30

Figure A.6: Resulting routes for the origin-destination pairs 29 and 30

B Personal Declaration

I hereby declare that the submitted thesis is the result of my own independent work. All external sources are explicitly acknowledged in the thesis.

I used AI tools, namely ChatGPT[1] and Grammarly[2], for English proofreading and sentence refinement.

Annina Ardüser Chur, 28 January 2025

[1]OpenAI. (2025). ChatGPT (Version 2) [large language model]. https://chatopenai.com
[2]Grammarly. (2025). Grammarly [Writing assistant software]. https://www.grammarly.com